TÉCNICO LISBOA

Synthesis of Titanium and Vanadium Diamine Bis(Phenolate) Complexes. Application of Ti Catalysts to the Pinacol Coupling Reaction

Ana Margarida Martins Neto Coelho

Dissertação para obtenção do Grau de Mestre em

Química

Júri

Presidente: Prof.ª Maria Matilde Duarte Marques

Orientador: Prof.ª Ana Margarida Sousa Dias Martins

Co-orientador: Dr.ª Sónia Duarte Barroso

Vogal: Prof. Fabio Marchetti

Novembro 2013

To Bárbara,
always dare to dream

Acknowledgments

First and foremost, I want to thank my thesis coordinator, Professor Ana Margarida Martins, for all her help and support in the last year, for everything she has taught me and for her invaluable insights and guidance throughout this work.

I would also like to thank my co-coordinator, Dr. Sónia Barroso, for taking the time to teach me the basics in the laboratory and pass her knowhow, for all her ideas and constructive criticisms, and for her precious help with the X-Ray characterizations.

To all my colleagues in the laboratory throughout the year, thank you for making me feel welcome, for teaching and helping me whenever I needed, and for the amazing work environment.

A special thanks to Dr. Pedro Adão, for always being available and willing to help me although he had no requirement to do so, for all his great suggestions which often helped me find my direction, and for allowing me the use of his lab for the low temperature experiments.

Finally, I want to thank my friends and family for their loving support, for forgiving my absences and for believing in me even when I didn't. To TFIST, for being my safe haven and for giving me the wings to fly, for being my home away from home, for all that I've learned and all that I've grown with you, I will always be thankful. And last but not least, to Pedro, thank you for everything you do and for everything you are.

Abstract

Diamine bis(phenolate) ligand precursors 6,6'-(2-(dimethylamino)ethylazanediyl) bis(methylene)bis(2,4-di-tert-butylphenol) (**H_2L^1**, **1**) and (*S*)-6,6'-((1-ethylpyrrolidin-2-yl) methylazanediyl)bis(methylene)-bis(2,4-di-tert-butylphenol) (**H_2L^2**, **2**) were used to prepare titanium and vanadium complexes. The compounds, with formulas $[VOL^2(O^iPr)]$ (**3**), $[TiL^1Cl(THF)]$ (**4**), $[TiL^1Cl]_2(\mu\text{-}O)$ (**5**), $[TiL^1(O^iPr)_2]$ (**6**) and $[TiL^1Cl_2]$ (**7**) were characterized by NMR and elemental analysis, and the molecular structures of **3** and **7** were obtained by single crystal X-ray diffraction.

The reactivity of the titanium complexes $[TiL^1Cl_2]$ and $[TiL^1Cl]_2(\mu\text{-}O)$ towards the pinacol coupling of benzaldehyde was tested and optimized in relation to the following parameters: i) catalyst precursor ii) metallic reductant (Mg, Sn, Zn, Mn), iii) catalyst to benzaldehyde proportion (from 1% to 20%), iv) reaction temperature (between 0ºC and 55ºC) and v) solvent (THF and toluene). It was found that the best results were obtained using $[TiL^1Cl_2]$ and Mn/TMSCl in THF at 55ºC. This system gave complete conversion of benzaldehyde to its pinacol product PhCH(OH)CH(OH)Ph with a diastereomeric excess of 71%, when the ratio [Ti]:benzaldehyde is 15%, and of 67 % when it is 7,5%.

Resumo

Os ligandos diamina bis(fenolato) 6-6'-(2-(dimetilamino)etilazanedil)bis(metileno) bis(2,4-di-ter-butilfenol) (**H^2L1, 1**) e (S)-6,6'-((1-etilpirrolidin-2-il)bis(2,4-di-ter-butilfenol) (**H^2L2, 2**) foram utilizados para preparar complexos de titânio e vanádio. Estes compostos, com as fórmulas $[VOL^2(O^iPr)]$ (**3**), $[TiL^1Cl(THF)]$ (**4**), $[TiL^1Cl]_2(\mu\text{-}O)$ (**5**), $[TiL^1(O^iPr)_2]$ (**6**) e $[TiL^1Cl_2]$ (**7**) foram caracterizados por NMR e análise elementar, e as estruturas moleculares dos complexos **3** e **7** foram obtidas por Difração de Raio-X.

A reactividade dos complexos de titânio $[TiL^1Cl_2]$ e $[TiL^1Cl]_2(\mu\text{-}O)$ no acoplamento pinacol do benzaldeído foi testada e optimizada tendo em conta os seguintes parâmetros: i) precursor catalítico ii) redutor metálico (Mg, Sn, Zn, Mn), iii) proporção catalisador:benzaldeído (de 1% a 20%), iv) temperatura (entre 0ºC e 55ºC) e v) solvente (THF e Tolueno). Os melhores resultados foram conseguidos com $[TiL^1Cl_2]$ e Mn/TMSCl em THF a 55ºC. Este sistema deu uma conversão completa do benzaldeído ao seu produto pinacol, PhCH(OH)CH(OH)Ph, com um excesso diasteriomérico de 71% quando a razão [Ti]:benzaldeído é 15% e de 67% quando esta razão é de 7,5%.

Table of Contents

Symbols and Abbreviations

δ	Chemical shift
μ	Bridging ligand
η^n	Ligand hapticity
^{1}H NMR	Proton nuclear magnetic resonance spectroscopy
13C NMR	Carbon-13 nuclear magnetic resonance spectroscopy
acac	Acetylacetonate
AX	Spin system between nucleus A appearing at the lowest field and nucleus B appearing at much higher field
Cp	Cyclopentadienyl (η^5-C_5H_5)
EPR	Electron Paramagnetic Resonance
NMR	Nuclear Magnetic Resonance
d. e.	Diastereomeric excess
d,l-	Diastereomer with two chiral centers of the same configuration (S,S or R,R), resulting in a chiral molecule
H_2L^1	6,6'-(2-(dimethylamino)ethylazanediyl)bis(methylene)bis(2,4-di-tert-butylphenol)
H_2L^2	(*S*)-6,6'-((1-ethylpyrrolidin-2-yl)methylazanediyl)bis(methylene)- bis(2,4-di-tert-butylphenol)
meso-	Diastereomer with two chiral centers of opposite configuration (S,R), resulting in an achiral molecule
R	Absolute configuration *R* at a chiral atom
S	Absolute configuration *S* at a chiral atom

Index of Figures

Index of Tables

1. Introduction

Few topics in Chemistry are as important and extensively explored as the formation of carbon-carbon bonds that are the cornerstone of organic chemistry and a fundamental tool to the synthesis of complex organic molecules from readily available and cheap precursors. Of course that, along this path, joining two carbon atoms is only the starting point. In order to have a useful synthetic tool it is necessary that such joining occurs in a specific mode that leads to the desired product. It is therefore of no surprise that, aiming at a definite compound, so many solutions exist, each with its own particularities, and that the pharmaceutical industry spends millions every year doing basic research that intends to achieve new and more efficient processes. However, while the particulars of each C-C bond formation can vary, the basic premise is always the same: to find a specific functional group that upon activation reacts selectively with another molecule to give a specific product in the most efficient way.

The role of catalysis as a key methodology in synthetic chemistry revolutionized both laboratory and industrial processes. Reactions that would have been impossible by conventional organic means, as the Nobel-winning Heck reaction or the ubiquitous Grignard reaction are two of the many examples that establish the search for metal-based processes as a long, but productive, approach in syntheses.

The C-C bond formation can be achieved by several means as, for example, polar reactions (such as nucleophilic attacks), pericyclic additions, and free-radical reactions. The later are by far the least explored as, for a long time, it was assumed that radical reactions are difficult to control, have none-to-low selectivity and their mechanisms are hard to understand since they rely on elusive paramagnetic species. In the last decades, however, a large amount of work has been done to take down these myths and show radical reactions as valuable synthetic processes.[1,2] In this work paramagnetic titanium complexes were used as catalysts for the pinacol coupling, which leads to the formation of diols from the reductive coupling of two ketones with concomitant formation of a C-C bond between the carbonyl carbons of the substrates.

1.1 Titanium catalysts in organic syntheses

While several radical reactions that use iron and copper as catalysts are well known, early-transition metals, and particularly titanium, have been major targets for research within this type of reactions.[3] Several advantages are associated with the use of titanium, which is widely used in asymmetric catalysis research.[4] Indeed, titanium is a cheap metal with low-toxicity hydrolysis products, it is very acidic and oxophilic and, in low oxidation states, it forms readily accessible paramagnetic species. It is also a very versatile metallic center that has a rich coordination chemistry, the reactivity of which may readily be tuned by different ligands.

Indeed, low-valence titanium species have a long and prolific history in electron-transfer reactions, both in catalytic and stoichiometric processes. As can be seen in Figure 1, titanium species have been employed to promote the reductive ring opening of epoxides to alkenes (a) and alcohols

(b), the reduction of alkyl and aryl halides (c), the reductive deoxygenation of alcohols (d), the opening of strained rings (e) and the reductive coupling of carbonyl compounds to alkenes (g) and dialcohols (h).[3–13]

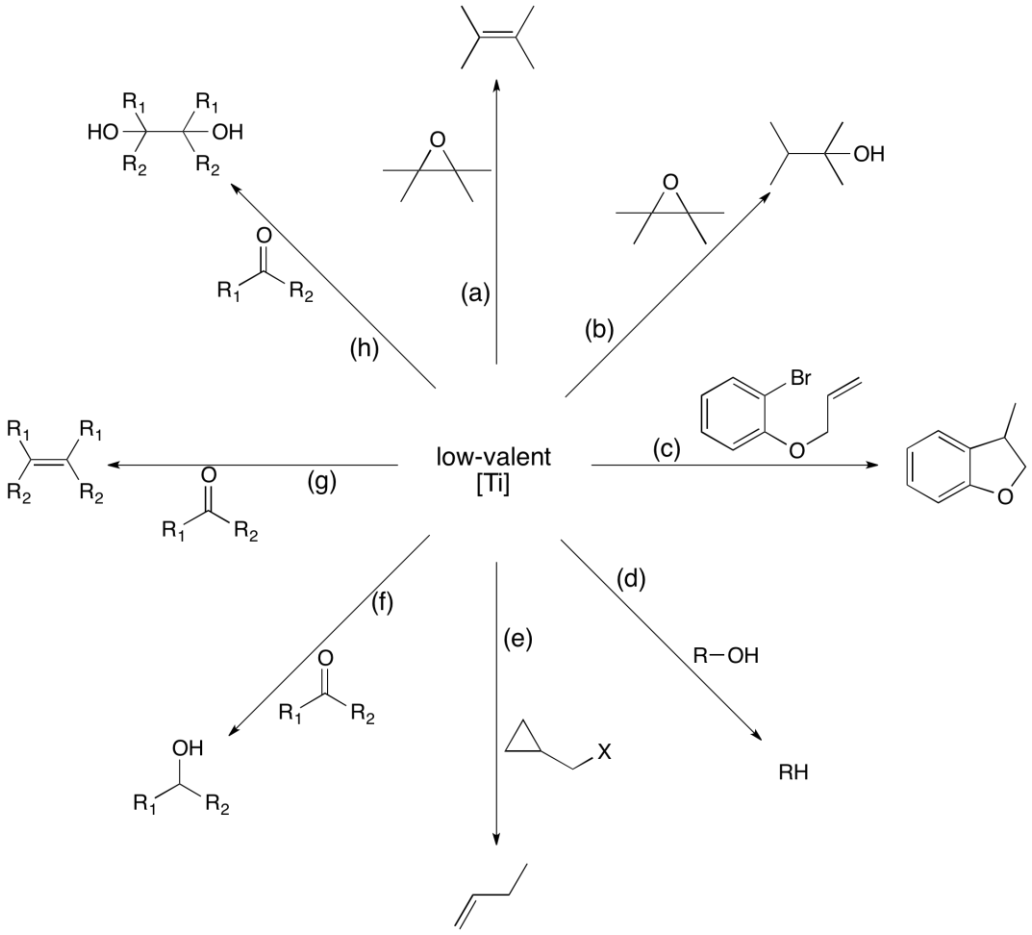

Figure 1: Electron-transfer processes mediated by low-valent Ti species

Low-valent titanium has also been successfully used in a vast array of asymmetric reactions, as illustrated by Ramon and Yus statement "In the Arena of Enantioselective Synthesis, Titanium Complexes Wear the Laurel Wreath".[4] Examples of these reactions are, for instance, Sharpless epoxidations, enantioselective allylations and alkylations and even enantioselective cycloadditions. In general these catalytic systems were prepared in situ by addition of titanium salts and chiral ligand precursors such as tartarate derivatives.[3,4]

1.2 The McMurry and Pinacol-Coupling Reactions

The most powerful tools in titanium catalyzed C-C bond formation are undoubtedly the McMurry and the pinacol coupling reactions, in which two carbonyl groups from ketone or aldehyde molecules

are coupled to give an alkene or diol, respectively (Figure 2). The catalysts are low-valent titanium species usually obtained *in situ* using a reducing agent.

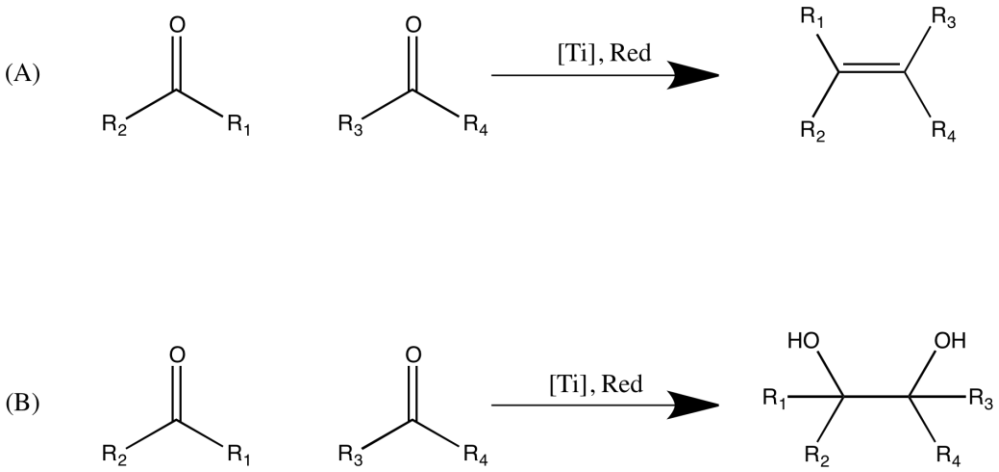

Figure 2: The McMurry (A) and Pinacol Coupling (B) reactions

The first mechanism for these reactions, proposed by McMurry, considered that Ti(0) particles, formed *in situ* by reduction of Ti(III) or Ti(IV) precursors, would bind to the carbonyl oxygen of the substrates originating radical pinacolate intermediates which could then either suffer hydrolysis to give the pinacol or, if heating was provided, originate a carbon-carbon double bond.[14] This effectively meant that the McMurry and the Pinacol Coupling reactions occurred through the same mechanism, differing only in the last steps, as shown in Figure 3.

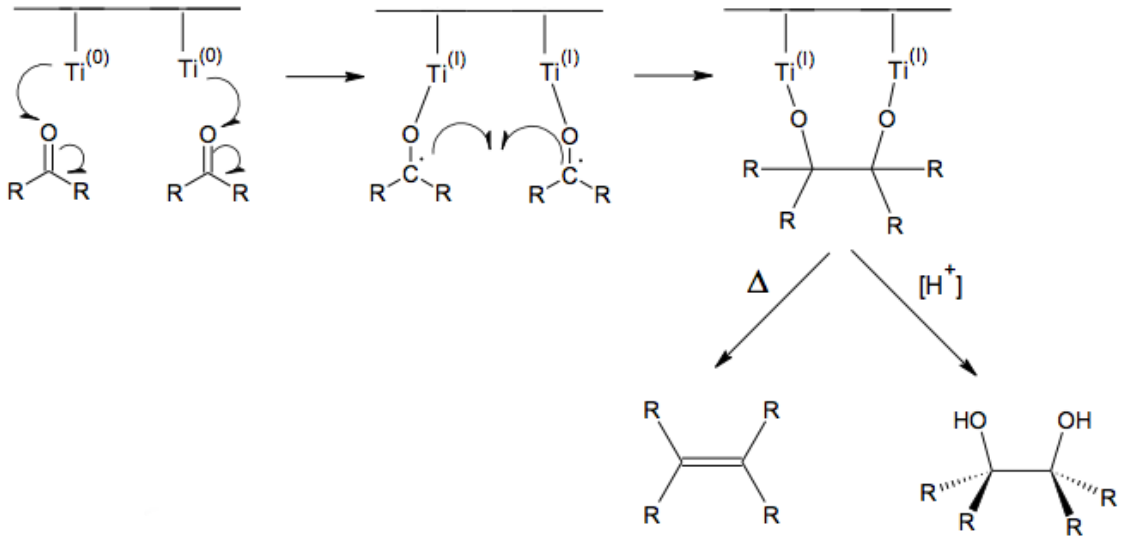

Figure 3: Mechanism of the Ti(0) mediated McMurry and Pinacol Coupling Reactions

The McMurry method quickly widespread in the scientific community, but it wasn't free of complications: it was plagued by poor reproducibility and very dependent on the solvent and reaction conditions. Several different systems were developed using different reducing agents, and in 1989 McMurry proposed an optimized version of the reaction using $TiCl_3$/Zn-Cu as reagents.[13] The reaction was successfully used for the synthesis of strained olefins, complex organic molecules and natural products, using a wide range of substrates; however, the high reducing power of the catalyst was incompatible with several common functional groups and the scope of the reaction was restricted by this constraint.

Over the years, more data became available and shed light on the mechanism of the transformation. In 1999, Michel Ephritikhine published "A new look at the McMurry reaction" and proposed that McMurry and pinacol reactions might follow different mechanisms.[15] Based on the evidence accumulated for carbonyl coupling reactions catalyzed by tungsten or molybdenum complexes, which were known to involve carbenoid intermediates through a 2+2 cyclisation path similar to alkene metathesis, Ephritikhine suggested the mechanism represented in Figure 4. This implied, first of all, that the alkene and pinacolate products weren't different byproducts of the same reaction, but rather arose from different transformations altogether.

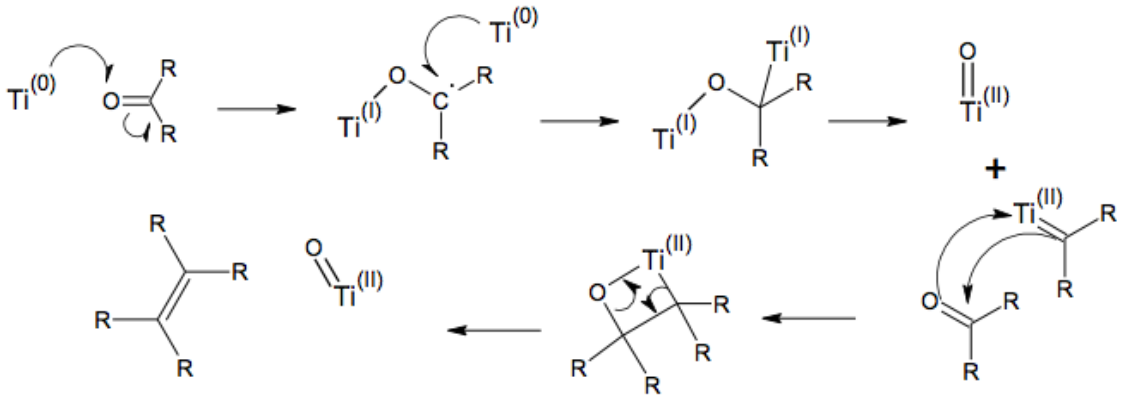

Figure 4: Alternative mechanism proposal for the McMurry reaction via Schrock-type carbenoids

The mechanism of the pinacol coupling reaction was further studied by the same author and, using Uranium catalysts, it was possible to characterize the intermediate metallopinacol species formed upon radical transfer from the metal, as shown in Figure 5**.**

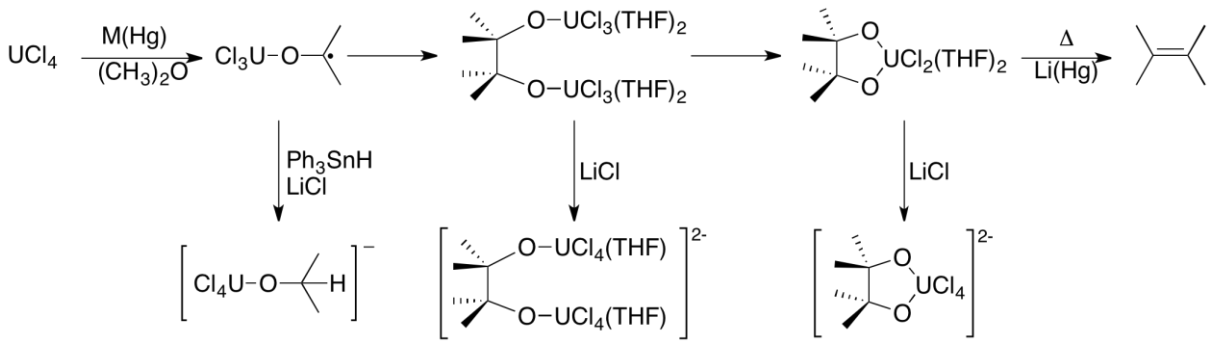

Figure 5: Metallopinacols isolated from the reductive coupling of acetone with the UCl_4-M(Hg) systems (M = Li or Na)

Ephritikhine also found that the path followed by the reactions strongly depended on the bulkiness of the reagents and on the strength of the reducing agents. Accordingly, McMurry products are favored by strong reducing agents and bulky substrates (R = ^{i}Pr, ^{t}Bu) and must involve Ti(II) catalysts (route (b) in Figure 6) while the pinacol coupling reaction occurs preferentially when milder reducing agents and less hindered substrates (R = H, Me, Et) are used. The catalysts are, in the latter case, Ti(III) species.[15]

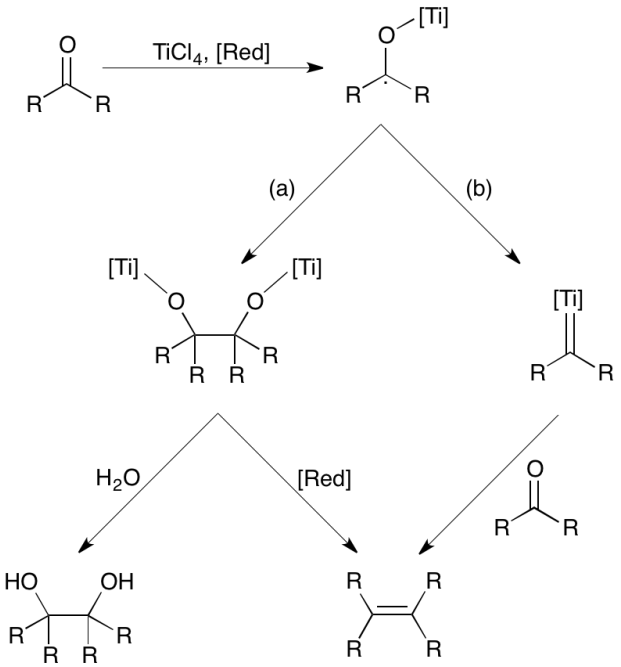

Figure 6: Mechanisms of pinacol coupling (path a) and McMurry (path b) reactions.

More recently, new catalytic versions of the pinacol coupling reaction have been developed. Dunlap and Nicholas showed that using Cp_2TiCl_2 as the catalyst precursor and either Mn or Mg as reducing agents, it is possible to obtain pinacol products in good yield and diastereomer selectivity.

[16,17] In this case, the active species are Ti-M-Ti aggregates that force the orientation of the intermediate pinacolates to minimize steric effects and thereby decide the stereochemistry of the product (Figure 7).

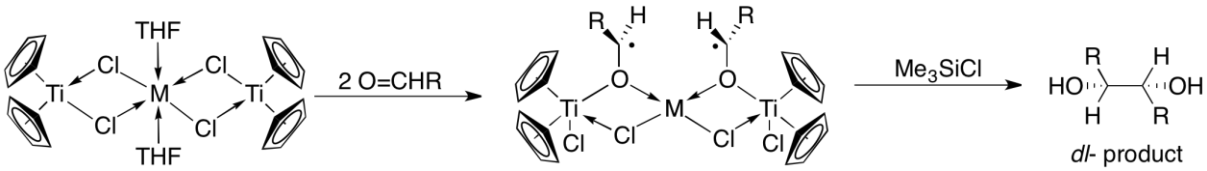

Figure 7: Structure of the active aggregate species with Cp_2TiCl_2 - M systems (M= Mn, Mg).

Reactions of stoichiometric amounts of Cp_2TiCl with the benzaldehyde confirmed that the oxidation state of titanium is Ti(III). Furthermore, the stereoselectivity of the reaction depends on the form of the titanocene chloride present in solution: the monomeric form of the catalyst gives preferably the meso- product while the dimeric form gives the dl- product (Figure 8).[17]

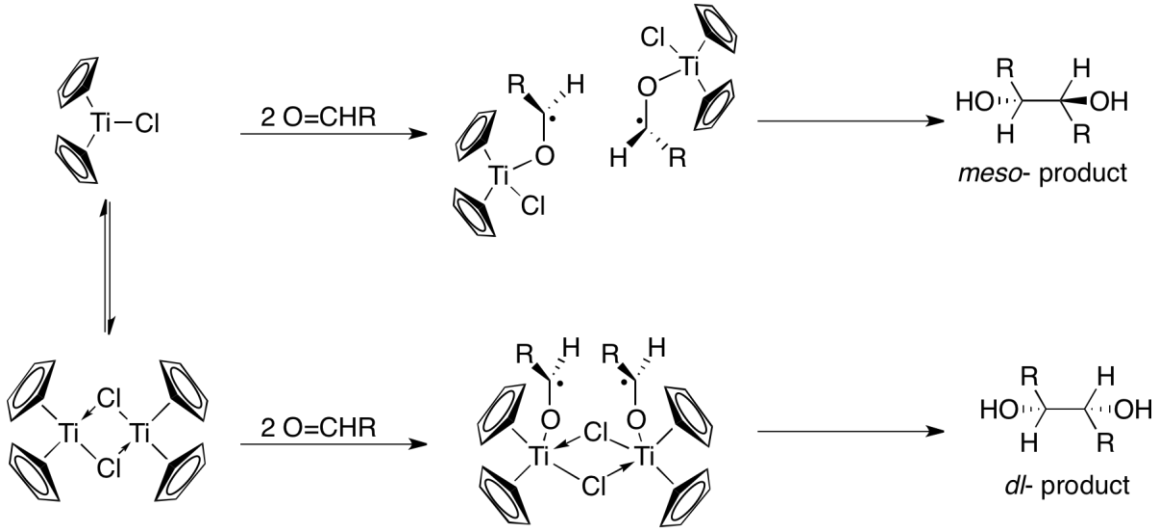

Figure 8: Different products obtained from the monomeric and dimeric forms of the Cp_2TiCl catalyst, with the steric effects shown.

Other organometallic complexes of Titanium, displaying chiral ligands, have also been applied in the pinacol coupling reaction with the purpose of obtaining enantiopure products. Very few studies have so far been published and only a few types of ligands have been tested, some of which are shown in Figure 9.[12,18–22] Several groups have used titanium complexes, including the SALEN ligand (a) and other chiral Schiff bases (b) in both stoichiometric and catalytic conditions and reported the most active co-catalyst system to be the Mn/TMSCl mixture at 0ºC. Complexes of tartaric acid

derivatives, such as TADDOL, (c), and chiral ethers, (d), have also been found to give good results with a Zn/TMSCl system both with aromatic and aliphatic aldehydes.[21–23]

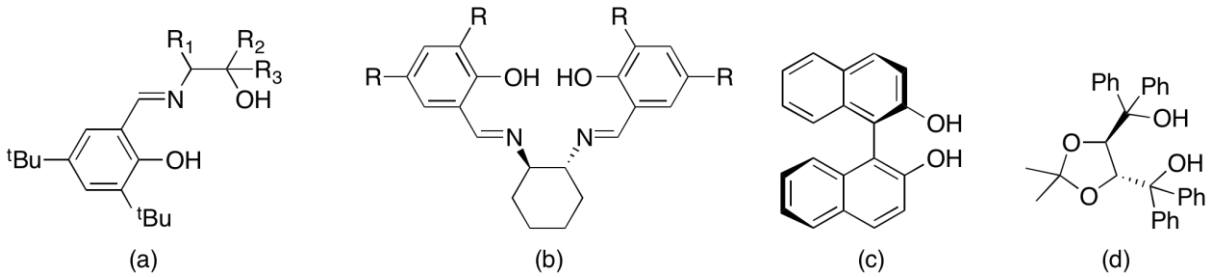

Figure 9: Examples of chiral ligands used in enantioselective pinacol coupling reactions.

In addition to the steric hindrance created by the ligands, the nature of the substrates was found to be a decisive factor. Aliphatic aldehydes did not react, aromatic aldehydes gave high yields and stereoselectivity, and the presence of electron-donating groups such as $–CH_3$ and $–OCH_3$ in para-position of the aromatic rings increased both the yield and the stereoselectivity of the reactions.[12,23,24] Table 1 summarizes the best results from literature.

Table 1: Selected data for Ti catalysed pinacol coupling Reactions

Catalyst[a]	%	T(ºC)	Reductant	Yield	Diastereomeric excess
Cp_2TiCl_2,[16]	10%	25ºC	Mn/TMSCl	73.0%	86%
TiL(a)Cl_2,[21]	10%	-10ºC	Zn/TMSCl	94.0%	96%
TiL(b)Cl_2,[20]	15%	0ºC	Mn/TMSCl	95.0%	86%
TiL(c)Cl_2,[23]	10%	25ºC	Zn/TMSCl	99.0%	66%

[a] *Ligands (a) to (d) shown in Figure 9*

1.3 Ti and V Diamine bis(phenolate) Complexes

Anionic polydentate ligands containing oxygen and/or nitrogen donors have proven particularly well suited for early-transition metals,[25–29] which are usually acidic and oxophylic. The hard nature of the N and O donors gives thermodynamic stability to the complexes and the ligand topologies provide kinetic stabilization, well-defined coordination geometries and strong steric protection of the metallic centers.

Diamine bis(phenol) ligand precursors are easily synthesized from readily available starting materials, namely a diamine of the type H_2N-spacer-NR_2, formaldehyde, and substituted phenols, through a single-step Mannich condensation reaction (Figure 10).

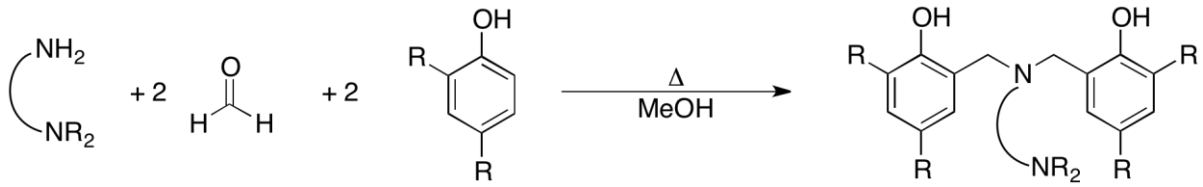

Figure 10: General synthesys of diamine bis(phenol) ligand precursors *via* a Mannich reaction

Diamine bis(phenolate) ligands have long been used in coordination chemistry with late transition metals[30–32] and more recently in complexes of early transition metals[33–35] of Group 3 (Sc, Y), Group 4 (Ti, Zr, Hf) and Group 5 (V, Ta). Several of these complexes have been applied in catalysis, particularly olefin and cyclic esters polymerizations, [36–39] epoxidations,[40,41] and sulfoxidations[42–44].

The chemistry of diamine bis(phenolate) ligands to Titanium, Vanadium and Zirconium was largely developed in recent years.[40,44–48] The complexes obtained have, in general, octahedral geometry, sometimes coordinating a solvent molecule, and can support different oxidation states (Figure 11).

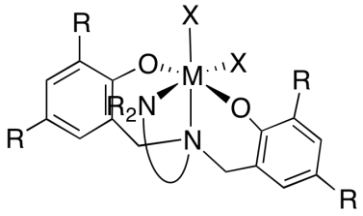

Figure 11: Octahedral Structure of diamine bis(phenolate) organometallic complexes (X represents either an anionic or neutral ligand).

Diamine bis(phenolate) ligands were first introduced in Group 4 transition metals chemistry by Kol, Goldschmidt and co-workers in 1999.[26,27] They synthesized various types of titanium and zirconium isopropoxide complexes (Figure 12) and evaluated steric effects resulting from different substitution of the phenol rings and variations of the amine substituent. Several of these complexes were found to be effective catalysts in the ring-opening polymerisation (ROP) of lactides, and others have cytotoxic activity against colon and ovarian cancer cells.[49,50]

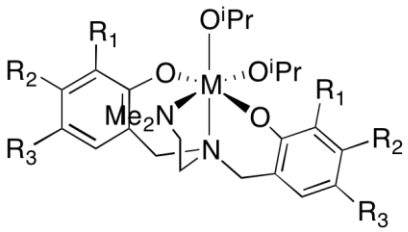

L1: M = Ti, R_1 = H, R_2 = R_3 = Me
L2: M = Ti, R_1 = R_3 = ^{t}Bu, R_2 = H
L3: M = Ti, R_1 = R_3 = Me, R_2 = H
L4: M = Ti, R_1 = R_3 = Cl, R_2 = H
L5: M = Zr, R_1 = R_3 = ^{t}Bu, R_2 = H
L6: M = Zr, R_1 = R_3 = Cl, R_2 = H

Figure 12: Titanium and zirconium diamine bis(phenolate) complexes described by Kol , Goldschmidt et al.

The same group also reported the first titanium(IV) aminebisphenolate alkyls that were found to be very reactive towards 1-hexene polymerisation (Figure 13).[27,51] The catalytic activity of these complexes showed a great dependence on steric and electronic effects of the ligand. Complex L9, with Cl groups in the *para* and *ortho* positions of the phenolate ring, afforded particularly good results yielding a polymer with remarkably high molecular weight (Mw>4 000 000) in less than 1h at room temperature.

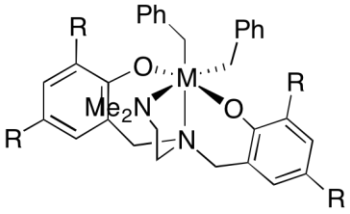

L7: M = Ti, R = ^{t}Bu
L8: M = Ti, R = Me
L9: M = Ti, R = Cl
L10: M = Zr, R = ^{t}Bu
L11: M = Zr, R = Me

Figure 13: Titanium (IV) diamine bis(phenolate) alkyl complexes prepared by Kol, Goldschmidt *et al.*

Mountford and co-workers described the syntheses and solution dynamics of zirconium and titanium complexes supported by the pyridine-based diamine bis(phenolate) ligand that is presented in Figure 14.[52] Attempts to generate catalytically active systems for the polymerisation of ethylene were unsuccessful and only trace amounts of polymer were obtained.

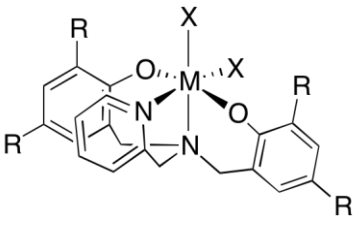

M = Ti, Zr
X = NMe_2, Me, CH_2SiMe_3, CH_2CMe_3, CH_2Ph, η^3-C_3H_5, S-4-C_6H_4Me
R = Me, ^{t}Bu

Figure 14: Titanium and zirconium diamine bis(phenolate) complexes described by Mountford *et al.*

Choukroun and co-workers introduced diamine bis(phenolate) ligands of Group 5 metals.[53] They described several vanadium(II–V) diamine bis(phenolate) complexes with octahedral geometry (Figure 15). All complexes were shown to be active catalysts for ethylene-α-olefin copolymerisation, producing both poly(ethylene-co-1-hexene) and poly(ethylene-co-norborene) with high α-olefin content. The vanadium(III) complex **L12** was found to be a particularly efficient catalyst.[54]

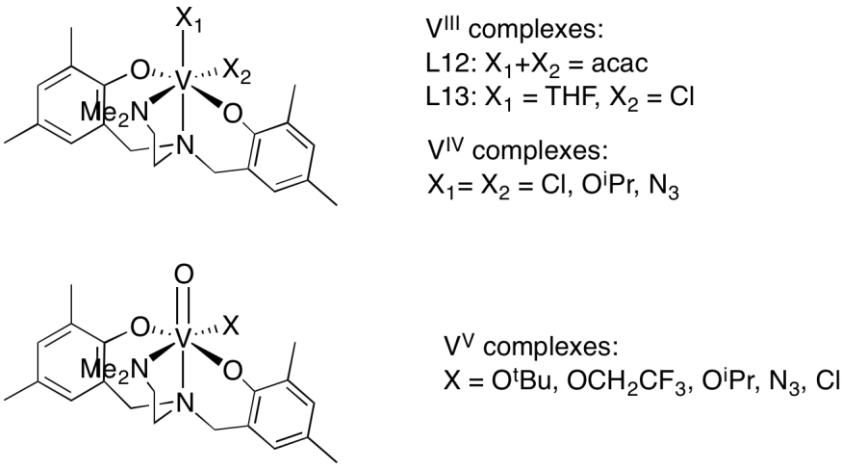

Figure 15: Vanadium diamine bis(phenolate) complexes described by Choukroun et al.

Martins and co-workers reported in recent years the synthesis, reactivity and catalytic aplications of several new diamine bis(phenolate) complexes of Ti, Zr, V, Mo and W, using both achiral (**A**) and chiral (**B** and **C**) ligand precursors (Figure 16).[44,46,47,55,56]

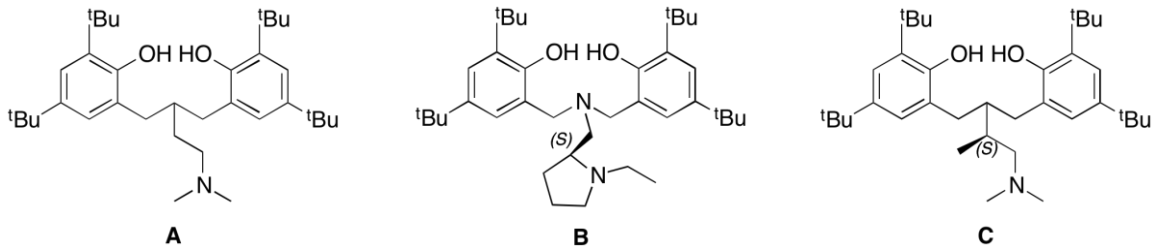

Figure 16: Ligand precursors used by Martins *et al.* for diamine bis(phenolate) complexes of Group 4, 5 and 6 metals

Chiral titanium and zirconium complexes of the type [ZrL(CH_2Ph)$_2$] and [TiL(CH_2Ph)$_2$] (L= **B**, **C** in Figure 16) were tested as catalysts in olefin polimerization. Zirconium complexes presented high activities in the polymerization of propylene (2.1×10^3 and 1.5×10^3 $g_{pol}mmol_{cat}^{-1}h^{-1}$, respectively), leading to atatic polypropylene, whereas analogous titanium complexes showed no activity.[47]

Mo, W and V complexes of the type $[MoO_2L]$, $[WO_2L]$, [VOLCl] and $[(VOL)_2(\mu\text{-}O)]$ were evaluated in the catalytic epoxidation of *cis*-cyclooctene using H_2O_2 and TBHP as oxidants and high catalitic activity and conversions, up to 98%, were achieved using the vanadium catalysts.[40]

Vanadium (III) and (V) complexes based on ligands **A**, **B** and **C** were also described (Figure 17). All vanadium(V) complexes were tested in thioanisole sulfoxidation catalysis revealing very high selectivity when H_2O_2 was used as oxidant. However, no enantioselectivity was observed even when the chiral complexes were used as catalyst precursors.[44]

The complexes have a well-defined octahedral structure with trans-phenolate ligands and for most of them the oxo ligand was *trans* to the tripodal nitrogen; only the isopropoxide derivative **L16** was obtained as a mixture of isomers. The oxidation of a V(IV) diamine bis(phenolate) complex in air gave the dimer **L20**, in which oxygen bridges the two metallic centers.

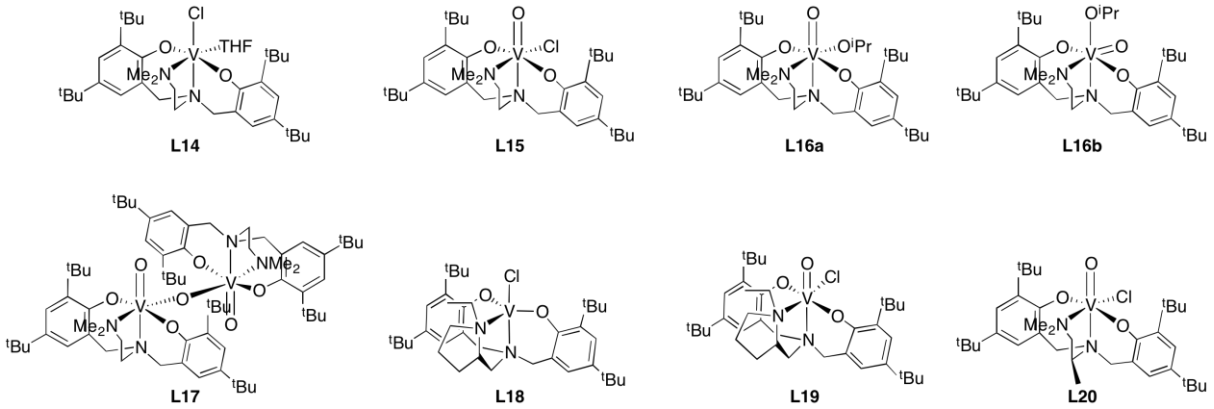

Figure 17: Vanadium (III) and (V) complexes with the diamine bis(phenolate) ligands 1, 2 and 3

Titanium complexes supported by ligand **A** have also been synthetized and studied thoroughly.[46,47] Martins and co-workers reported the synthesis and structure of the paramagnetic Ti^{III} complex of diamine bis(phenolate) **L21**, and studied one-electron transfer processes with a wide range of acceptors species, as schematized in Figure 18.[55]

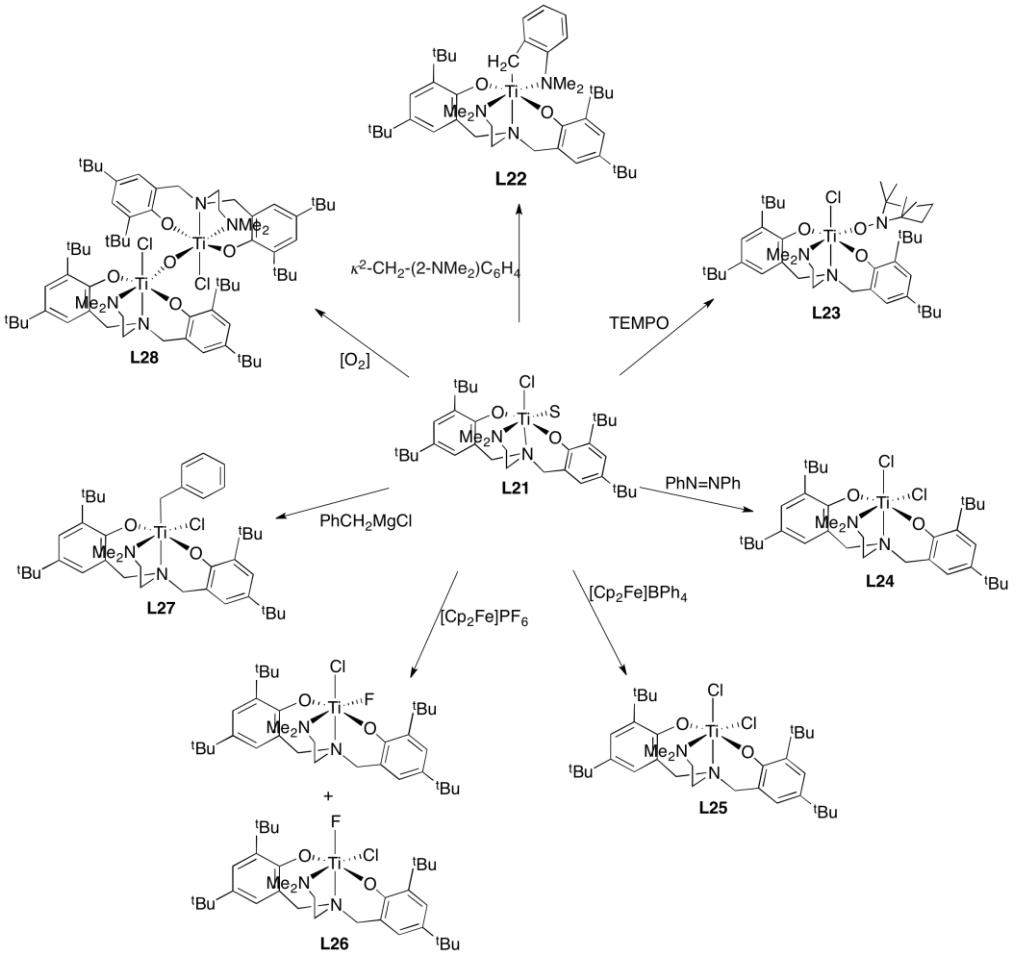

Figure 18: Electron-transfer reactions of the paramagnetic complex L21

1.4 Objectives of the work

The chemistry of early-transition metals with diamine bis(phenolate) ligands has been a focus of interest in our group. One of the goals of this work is the syntheses of titanium complexes using tripodal diamine bis(phenolate) ligands and the assessment of their properties in the pinacol coupling reaction.

The other target of the work is the establishment of new synthetic methods for titanium and vanadium diamine bis(phenolate) complexes.

2 Results and Discussion

2.1 Synthesis of titanium and vanadium diamine bis(phenolate) complexes

The ligand precursors used in this work, 6,6'-(2-(dimethylamino)ethylazanediyl) bis(methylene) bis(2,4-di-tert-butylphenol) (**H_2L^1**, **1**) and (*S*)-6,6'-((1-ethylpyrrolidin-2-yl)methylazanediyl) bis(methylene)-bis(2,4-di-tert-butylphenol) (**H_2L^2**, **2**), were synthetized through a single-step Mannich Condensation Reaction following the procedures reported in the literature, as shown in Figure 19.[26,47]

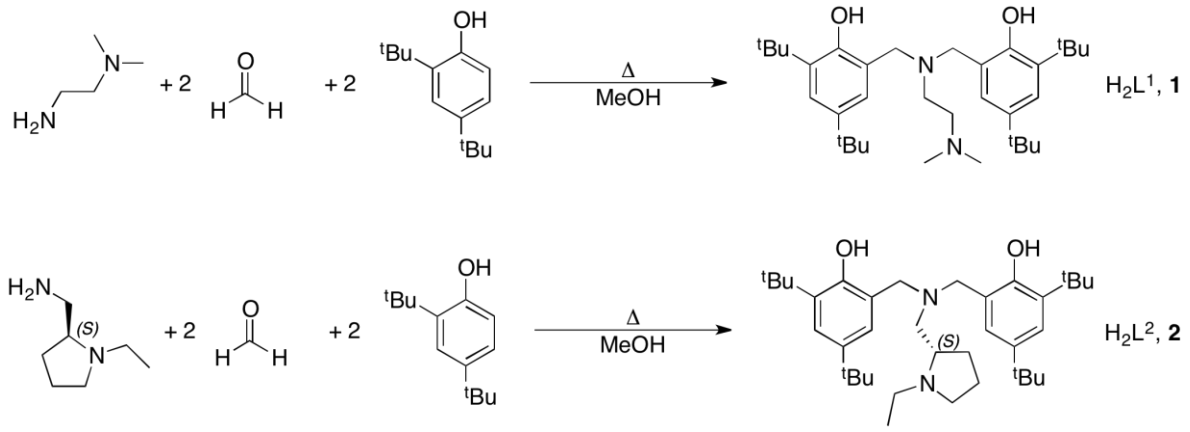

Figure 19: Synthesis of ligand precursors H_2L^1 and H_2L^2.

$VOCl_3$ and $VO(O^iPr)_3$ were used as starting materials for the preparation of chiral oxo-vanadium (V) complexes, as shown in Figure 20.

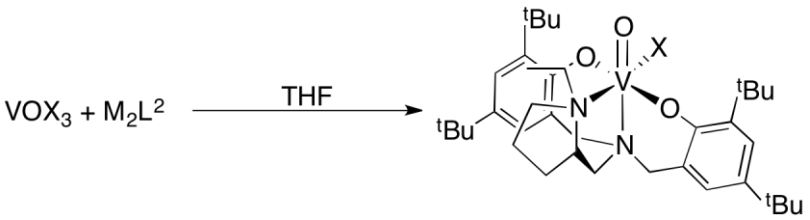

Figure 20: Synthesis of oxovanadium complexes with H_2L^2. (X = Cl; O^iPr; M = Na, H)

The reaction of $VOCl_3$ with the sodium salt **Na_2L^2** gave a dark blue solution that formed immediately after contact of the reagents but it turned dark green after overnight reaction. A dark greenish solid was obtained after workup.

The ^1H NMR spectrum of the product revealed a mixture of species where the major peaks were those of the protonated ligand precursor. Very small peaks, for which no definitive attribution was possible, were also present. Although these may reflect the formation of $[VOL^2Cl]$, suggested by the

dark blue color obtained, the NMR results were inconclusive. Several attempts to crystallize a product from this mixture were tried without success.

An alternative procedure for the synthesis of a V(V) oxocomplex supported by ligand **L^2** was attempted using $[VO(OiPr)_3]$ as starting material. $[V^{V}OL^{2}OiPr]$ (**3**), was obtained as a dark brownish solid with 60% yield from the reaction of $[VO(OiPr)_3]$ with **H_2L^2**. The ^{1}H NMR of the product is shown in Figure 21.

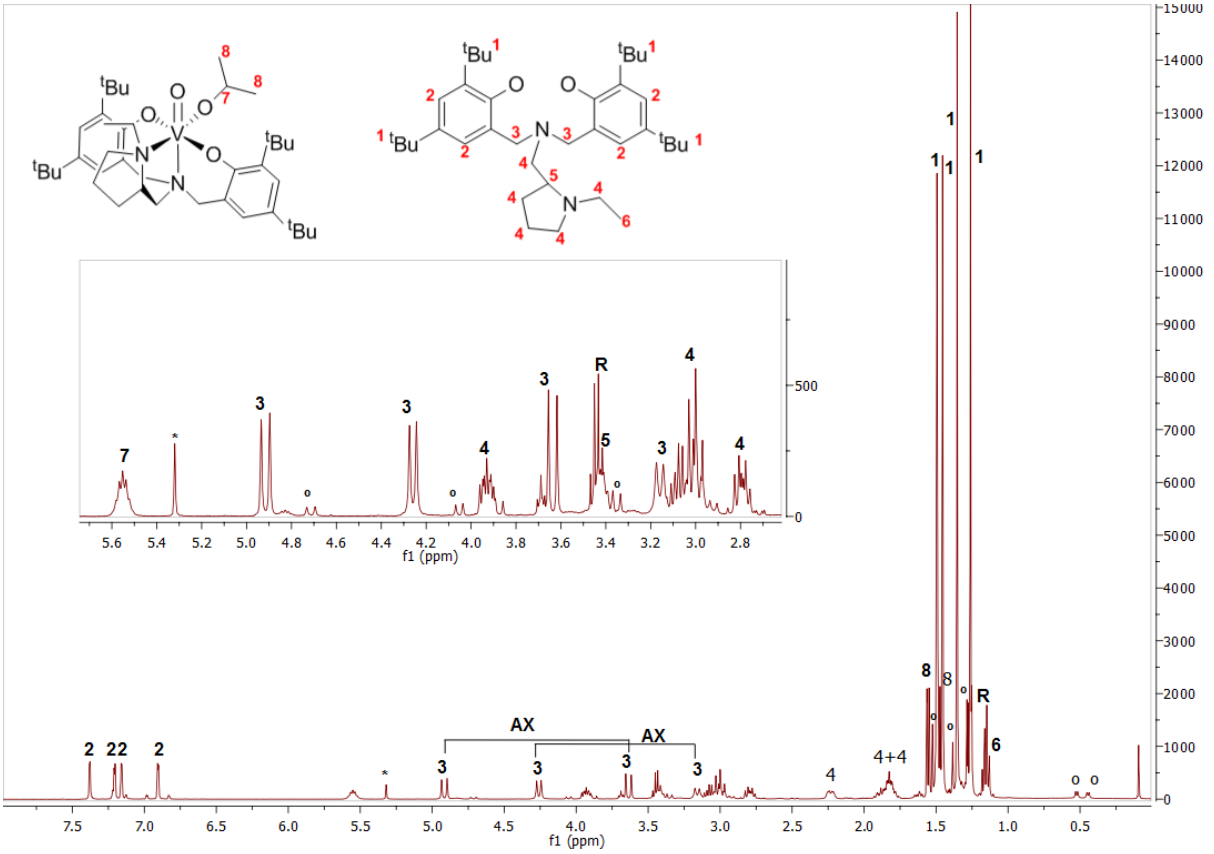

Figure 21: ^{1}H NMR of $[VOL^2(O^iPr)]$, 3. The residual solvent peak (CH_2Cl_2 δ= 5,32 ppm) is marked with a * and the excess HO^iPr peaks are marked with R. Peaks corresponding to a minor isomer are identified with º.

As is to be expected for a rigid asymmetric complex, the NMR shows distinct resonances for all protons. The spectrum also shows a set of peaks (identified with º) of much lower intensity at slightly different chemical shifts and with the same multiplicity, which indicate the presence of a minor isomer. Four isomers of complex **3**, shown in Figure 22**,** are possible**.** The molecules labeled **a** and **b** display *trans*-phenolate moieties whereas the other two isomers, **c** and **d**, show *cis*-phenolate bonding. The latter structures are usually less stable than the former, leading to the assumption that the two isomers that are seen in the ^{1}H NMR spectrum correspond to structures **a** and **b**.

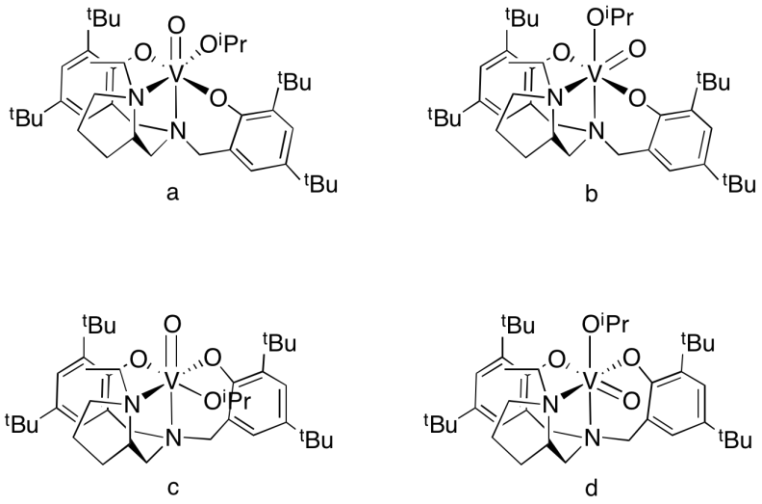

Figure 22: Possible isomers of 3.

Brownish crystals of **3** suitable for X-ray diffraction were grown from a toluene/hexane solution. The compound crystallizes in the monoclinic system, space group $P2_1$, with four molecules in the asymmetric unit. As shown in Figure 23 the four molecules differ mainly in the coordination mode of the diamine side arm. An ORTEP view of one of the molecules, **3*a***, is depicted in Figure 24 and selected structural parameters for **3*a*-3*c*** are listed in Table 2.

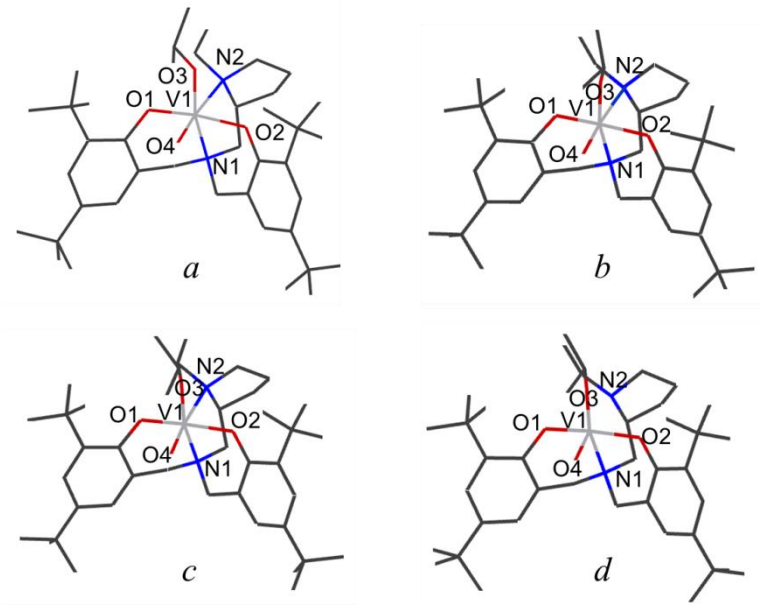

Figure 23: Wireframe diagrams of the four molecules of [VOL^2(O^{i}Pr)] (3*a*-3*d*) present in the asymmetric unit.

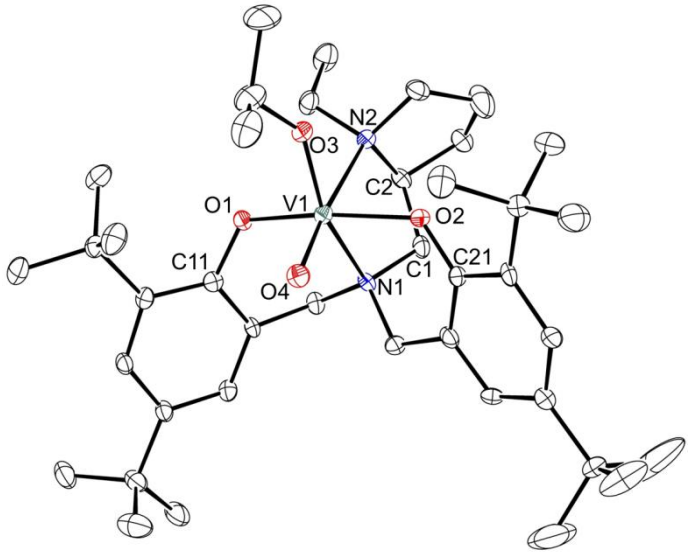

Figure 24: ORTEP-3 diagram of [VOL^2(O^iPr)] (3*a*), using 40 % probability level ellipsoids. Hydrogen atoms are omitted for clarity.

Compound **3** presents distorted octahedral geometry with the equatorial plane defined by atoms O1, O2 and N2 of L2 and the oxo ligand ligand (O4), while the axial positions are occupied by the isopropoxo ligand (O3) and the tripodal nitrogen N1. The crystallized isomer presents the oxo ligand *cis* to the tripodal nitrogen, as was also observed for the analogous alkoxo diamine bis(phenolate) vanadium complex [VOL^1(O^iPr)], synthetized and characterized in previous studies[44]. The ethylpyrrolidine moiety is coordinated to the metal through the nitrogen atom N2. Chiral atoms N2 and C2 have *S* configuration in the four molecules. The V=O and V-$O_{phenolate}$ bond distances are in the expected ranges for such bonds.[54,57,58] The phenolate moieties adopt *trans* configuration bending towards the oxo ligand and define dihedral angles of 109.71(1)º to 121.72(1)º between the aromatic planes.

Table 2: Selected structural parameters for 3*a*-3*d*.

Distances (Å)				
	a	b	c	d
V(1)-N(1)	2.249(3)	2.234(3)	2.231(3)	2.231(3)
V(1)-N(2)	2.460(3)	2.495(3)	2.426(4)	2.472(3)
V(1)-O(1)	1.912(2)	1.902(2)	1.898(2)	1.910(2)
V(1)-O(2)	1.899(2)	1.890(2)	1.909(2)	1.910(2)
V(1)-O(3)	1.774(3)	1.770(3)	1.772(2)	1.761(2)
V(1)-O(4)	1.590(3)	1.596(3)	1.595(3)	1.595(3)
V(1)-eq. plane[a]	0.209(1)	0.222(1)	0.216(1)	0.224(1)

Angles (º)				
O(1)-V(1)-O(2)	161.00(11)	160.21(12)	160.30(12)	160.24(12)
O(1)-V(1)-O(3)	96.16(11)	97.40(11)	97.16(11)	98.20(11)
O(2)-V(1)-O(3)	97.46(11)	94.60(11)	95.29(11)	94.34(11)
O(1)-V(1)-N(1)	83.48(10)	83.51(11)	83.35(11)	83.44(11)
O(2)-V(1)-N(1)	78.65(10)	79.61(11)	79.44(11)	79.37(10)
O(3)-V(1)-N(1)	155.65(12)	158.54(13)	158.19(13)	158.64(12)
O(1)-V(1)-N(2)	83.27(10)	80.13(10)	83.69(11)	80.87(10)
O(2)-V(1)-N(2)	85.75(10)	85.35(11)	82.74(11)	85.22(11)
O(3)-V(1)-N(2)	81.32(11)	84.89(12)	83.00(12)	84.44(11)
N(1)-V(1)-N(2)	74.37(10)	74.11(11)	75.36(11)	74.76(11)
O(1)-V(1)-O(4)	95.04(11)	95.92(12)	95.76(13)	95.47(12)
O(2)-V(1)-O(4)	93.43(12)	95.49(12)	94.93(12)	95.31(13)
O(3)-V(1)-O(4)	107.52(13)	107.17(14)	107.66(13)	107.29(13)
N(1)-V(1)-O(4)	96.79(12)	94.00(13)	93.93(13)	93.68(13)
N(2)-V(1)-O(4)	171.16(12)	167.76(12)	169.28(12)	168.15(12)
θ^b	109.71(1)	122.63(1)	123.24(1)	121.72(1)

[a] *The equatorial plane is defined by atoms O1, O2, N2 and O4.*
[b] *θ is the dihedral angle between the planes containing the phenolate rings.*

The paramagnetic complex $[Ti^{III}L^1Cl(THF)]$ (**4**) was obtained by adding $\mathbf{Na_2L^1}$ (prepared in situ by reacting $\mathbf{H_2L^1}$ with two equivalents of NaH) to a THF solution of the bright blue $TiCl_3(THF)_3$, following a procedure previously developed in the group and shown in Figure 25.[45,46] The reaction mixture quickly turned to a yellowish orange that gave an orange-yellow powder in 38% yield after workup.

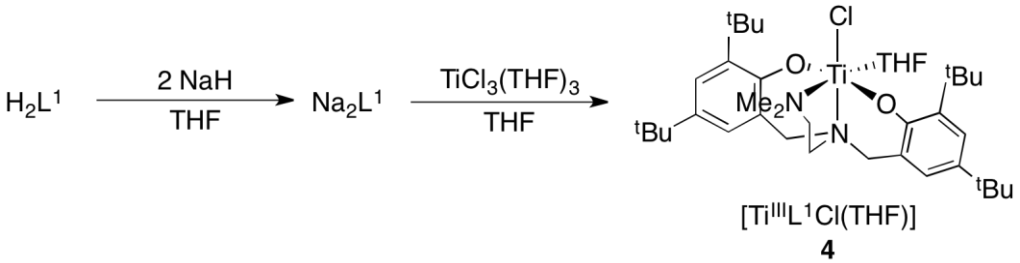

Figure 25: Synthesis and structure of complex 4.

Complex **4** is extremely sensitive to air and moisture, oxidizing to $[Ti^{IV}L^1Cl]_2(\mu\text{-}O)$ (**5**) (Figure 26). The compound was obtained as a dark red solid in 85% yield.

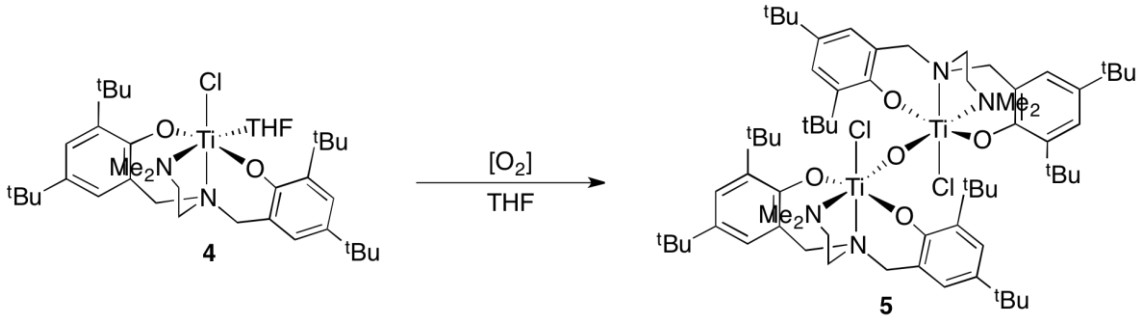

Figure 26: Oxidation of 4 by air to give the oxo-bridged dimer 5

Complex **5** may be converted to the monomeric [$Ti^{IV}L^1(O^iPr)_2$] (**6**) by reaction with isopropanol, in the presence of a base such as triethylamine, through the cleavage of the oxygen bridge. Through this method the isopropoxide may be obtained as a bright yellow solid in 75% yield. Complex **6** may alternatively be prepared in 96% yield by directly adding a solution of commercial $Ti(OiPr)_4$ to the ligand precursor $\mathbf{H_2L^1}$ in diethyl ether. Both these reactions are schematized in Figure 27.

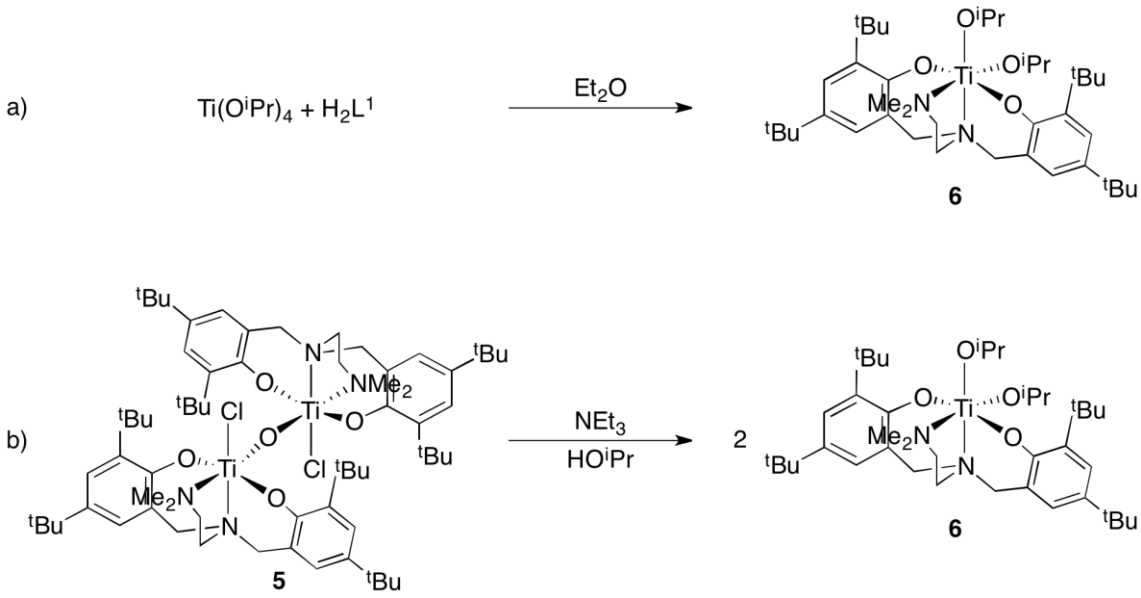

Figure 27: Syntheses of 6 from the dimer 5 (a) and from commercial $Ti(OiPr)_4$ (b)

Compound **6** was reacted with two equivalents of TMSCl in dichloromethane to give [$Ti^{IV}L^1Cl_2$] (**7**) in 89% yield. The synthesis of **7** was also attempted from the reaction of [$TiCl_2(acac)_2$] with $\mathbf{H_2L^1}$ in THF, but it was unsuccessful, giving a mixture of products. Both these reactions are schematized in Figure 28. The NMR data obtained for compound **7** are in agreement with those reported in the literature.[55]

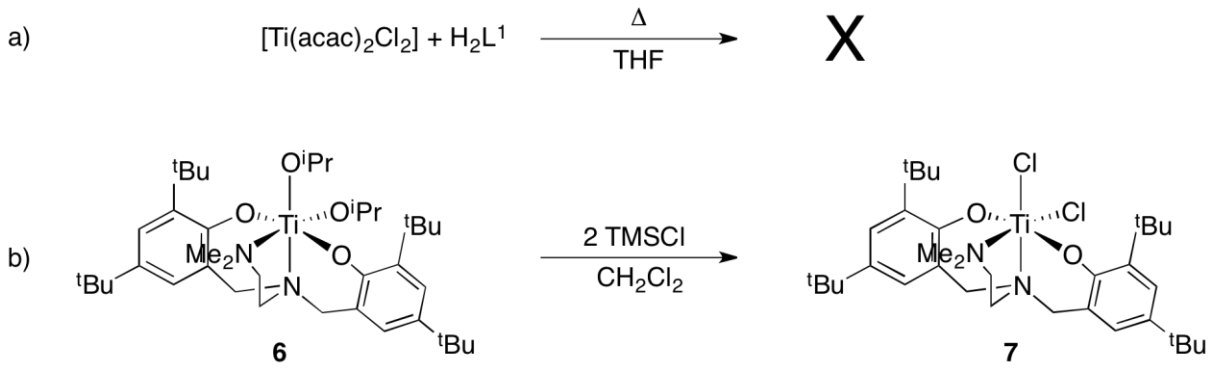

Figure 28: Synthesis of 7 from 6 (a) and reaction of $[Ti(acac)_2Cl_2]$ with H_2L^1 (b)

Orange crystals of **7** suitable for X-ray diffraction were grown from a toluene/hexane double layer solution. The compound crystallizes in the monoclinic system, space group $P2_1/a$, with one molecule in the asymmetric unit. The molecular structure of the compound is depicted in Figure 29 and selected structural parameters are listed in Table 3.

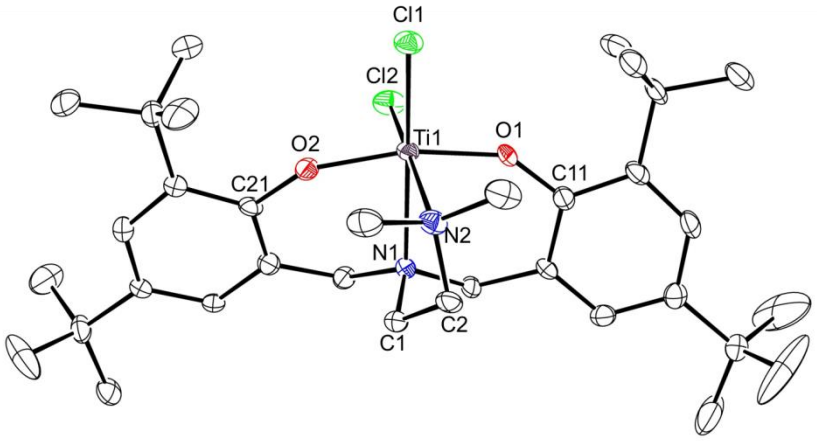

Figure 29: ORTEP-3 diagram of 7, using 40 % probability level ellipsoids. Hydrogen atoms are omitted for clarity.

The titanium coordination geometry is distorted octahedral with the equatorial plane defined by atoms O1, O2 and N2 of **L^1** and the chloride ligand Cl2, while the tripodal nitrogen N1 and the chloride ligand Cl1 occupy the axial positions. The titanium is slightly away from the equatorial plane [0.199(2) Å] towards Cl1. The two phenolate moieties occupy *trans* positions with a dihedral angle of 159.0(2)º between the phenolate ring planes. The sidearm fragment is coordinated to the metal and the tripodal ligand forces the two chloride ligands to adopt mutually *cis* dispositions. The Ti-O and Ti-N distances are within the expected values and compare well with values reported for octahedral titanium(IV) diaminebisphenolate complexes,[26,27,29,35,59] and the Ti-Cl distances also fit values reported for titanium(IV) systems supported by O- and N- based ligands.[60–62]

Table 3: Selected structural parameters for 7

Distances (Å)			
Ti(1)-O(1)	1.831(3)	Ti(1)-N(2)	2.307(4)
Ti(1)-O(2)	1.838(3)	Ti(1)-Cl(1)	2.304(1)
Ti(1)-N(1)	2.275(3)	Ti(1)-Cl(2)	2.307(1)
Ti(1)-eq. plane[a]	0.191(1)		
Angles (º)			
O(1)-Ti(1)-O(2)	166.5(1)	N(1)-Ti(1)-N(2)	78.0(1)
O(1)-Ti(1)-N(1)	85.2(1)	N(1)-Ti(1)-Cl(1)	165.3(1)
O(1)-Ti(1)-N(2)	86.8(1)	N(1)-Ti(1)-Cl(2)	93.0(1)
O(1)-Ti(1)-Cl(1)	97.6(1)	N(2)-Ti(1)-Cl(1)	88.0(1)
O(1)-Ti(1)-Cl(2)	90.0(1)	N(2)-Ti(1)-Cl(2)	170.6(1)
O(2)-Ti(1)-N(1)	81.4(1)	Cl(1)-Ti(1)-Cl(2)	101.4(1)
O(2)-Ti(1)-N(2)	91.3(1)	Ti(1)-O(1)-C(11)	146.0(3)
O(2)-Ti(1)-Cl(1)	95.6(1)	Ti(1)-O(2)-C(21)	144.0(3)
O(2)-Ti(1)-Cl(2)	89.8(1)	θ[b]	176.8(2)

[a] *The equatorial plane is defined by atoms O1, O2, N2 and Cl2.*
[b] *θ is the dihedral angle between the planes containing the phenolate rings.*

2.2 Application of titanium complexes to the Pinacol Coupling Reaction

The procedure used for the pinacol coupling reaction was adapted from the literature.[20] The catalytic study involved optimization of several parameters such as the nature of the catalyst, the catalyst:substrate ratio, the reducing agent, the reaction temperature and the solvent.

Benzaldehyde was used as a starting material for several reasons: it is a cheap reagent that is available with high purity (as opposed to formaldehyde which is usually either polymeric or in aqueous solution) and can be easily dried and de-aerated; it has a single, well-defined reaction site with no other functional groups prone to attack; it is readily soluble in most organic solvents and has a rather high boiling point, allowing for low-pressure drying of the reaction crude during work-up; and it has been successfully used in the pinacol coupling reaction to give 1,2-bis(phenyl)-1,2-ethanediol, a well-defined pinacolate with two chiral centers that has two diastereomers, one of which is chiral (Figure 30).

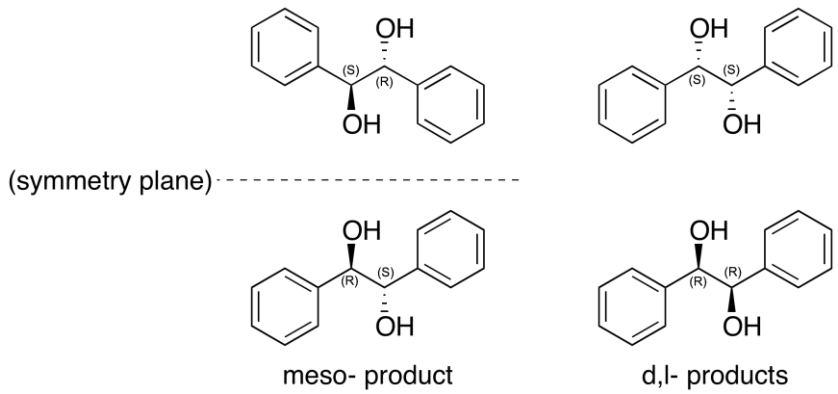

Figure 30: The products of the pinacol coupling of two benzaldehyde molecules: on the left, the *meso*-diastereomer, and on the right the two enantiomers of the *dl*- diastereomer.

In addition to the mentioned advantages, it was found that specific peaks in ^{1}H NMR spectra can be used to identify both the reagent (PhC*H*O, 1H, singlet, 10,03 ppm) and the two diastereomers (PhC*H*OHC*H*OHPh, 2H, singlet, 4,73ppm (*dl*) and 4,83 ppm (*meso*). The integration of the ^{1}H NMR spectra using the benzaldehyde proton as reference allowed quantitative information of conversion, diastereomeric proportion and diastereomeric excess, without the need to fully purify the product. Expressions 1-3 were used for the calculations.

$$Conversion\ (\%) = \frac{\frac{\int dl}{2}+\frac{\int meso}{2}}{\frac{\int dl}{2}+\frac{\int meso}{2}+\int benzaldehyde} \times 100 = \frac{\frac{\int dl}{2}+\frac{\int meso}{2}}{\frac{\int dl}{2}+\frac{\int meso}{2}+1} \times 100 \quad (1)$$

$$Diastereomer\ Excess = \frac{\int dl - \int meso}{\int dl + \int meso} \times 100 \quad (2)$$

$$Diastereomer\ Fraction\ (dl{:}meso) = \frac{\int dl}{\int meso} \quad (3)$$

A preliminary test for the pinacol coupling reaction was made using $[TiL^1Cl]_2(\mu\text{-}O)$, **5** , magnesium flakes as the metallic reducing species and THF as the solvent. The catalyst was used in 7,5% relative to the benzaldehyde, which corresponds to a ratio of 15% Ti:benzaldehyde. The reaction proceeded for 16 hours at room temperature, under nitrogen to avoid side reactions and catalyst degradation by atmospheric oxygen. The purification of the product was attempted by chromatography using a 1:9 mixture of ethyl acetate in hexane but the ^{1}H NMR showed the presence of tert-butyl groups originated by diaminebisphenolate ligand residues. A second column was then tried using hexane as the eluent but it was not possible to obtain pure products because the phenolic ligand fragments are too similar to the pinacol product for a successful separation. Nevertheless, characteristic peaks of reagent and product in the ^{1}H RMN spectrum of the reaction crude (Figure 31) were integrated and used to calculate the reaction conversion as 43% and the diastereomeric excess of 11%.

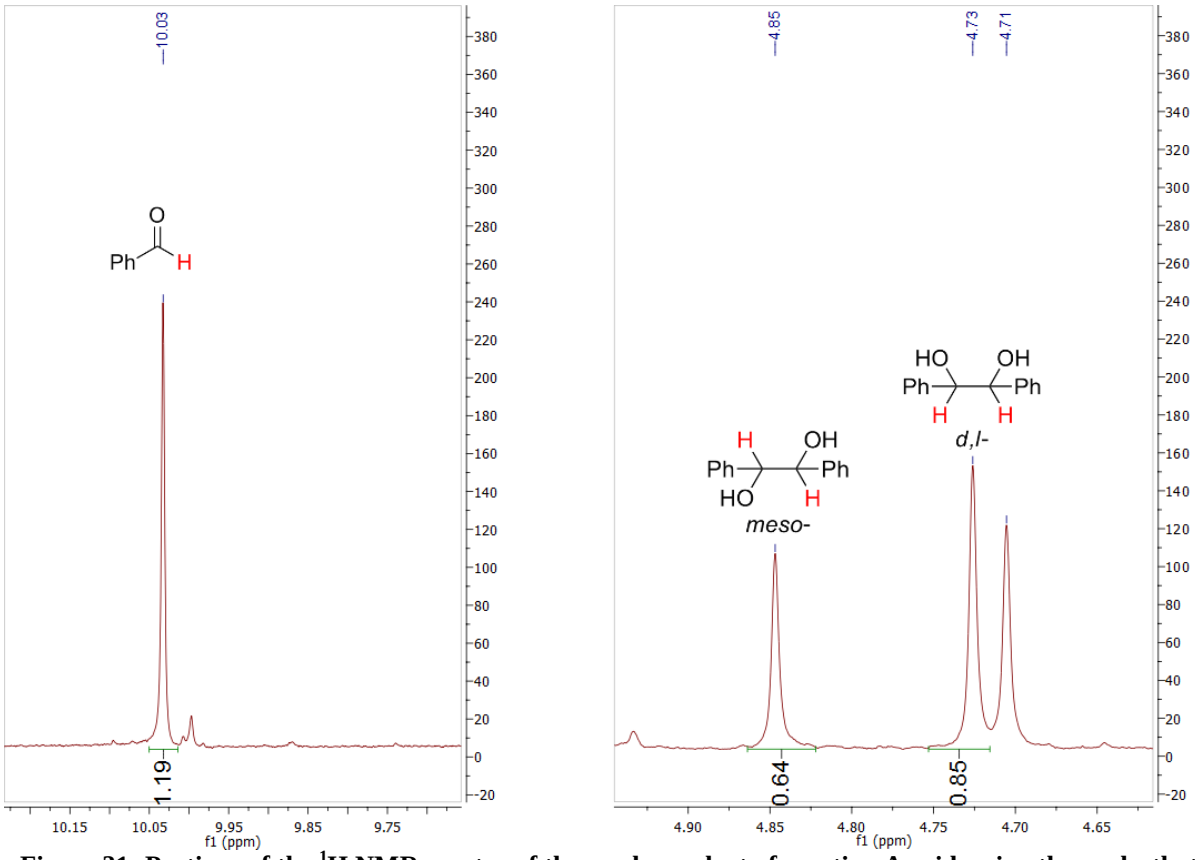

Figure 31: Portions of the ^{1}H NMR spectra of the crude product of reaction A evidencing the peaks that identify the benzaldehyde (s, 10,03 ppm) the *meso*- product (s, 4,85 ppm) and the *dl*- product (s, 4,73 ppm).

Two blank tests were made, one without titanium and the other without Mg/TMSCl. The results, shown in Table 4, clearly confirm that in the absence of either reagent the reaction does not take place.

Table 4: Results of preliminary pinacol coupling tests[a]

ID	Catalyst	%	T(ºC)	Reductant	$\int dl$	$\int meso$	Conversion	Diastereomeric Excess
A	$[TiL^1Cl]_2(\mu\text{-}O)$	15%	20ºC	Mg/TMSCl	0,85	0,64	43%	14,1%
B	$[TiL^1Cl]_2(\mu\text{-}O)$	15%	20ºC	Blank Test	0,01	0,00	1%	73,9%
C1	Blank Test	-	20ºC	Mg/TMSCl	0,06	0,06	6%	0,0%

[a]*The conversion and diastereomeric excess were obtained from the ^{1}H NMR spectra of the product mixture after work-up. All the NMR spectra are in the Appendix, identified by the reaction ID*

Complex $[TiL^1Cl_2]$ (**7**) was also tested as catalyst expecting that this complex might be easier to reduce and therefore more reactive. Indeed, when 5% of **7** was tested in the same conditions, the mixture changed from dark orange to greenish yellow, which is a typical color indicative of the presence of Ti^{III} species, minutes after the addition of magnesium flakes and TMSCl. After addition of benzaldehyde the mixture returned back to orange. The conversion of benzaldheyde was 15% and the diastereomeric excess is far superior, at 26% (**C1**, Table 5) It was therefore concluded that the $[TiL^1Cl_2]$ complex is a more active catalyst than dimer the $[TiL^1Cl]_2(\mu\text{-}O)$, as expected.

Table 5: Summary of the results obtained with several reducing metals and the respective blank tests.[a]

ID	Catalyst	%	TºC	Reductant	$\int dl$	$\int meso$	Conversion	Diastereomeric Excess
C2	$[TiL^1Cl_2]$	5%	20ºC	Mg/TMSCl	0,22	0,13	15%	26%
D1	Blank Test	-	20ºC	Mn/TMSCl	0,19	0,05	11%	58%
D2	$[TiL^1Cl_2]$	5%	20ºC	Mn/TMSCl	6,17	3,04	82%	34%
E1	Blank Test	-	20ºC	Zn/TMSCl	5,88	6,42	86%	-4%
E2	$[TiL^1Cl_2]$	5%	20ºC	Zn/TMSCl	8,38	6,11	88%	16%
F1	Blank Test	-	20ºC	Sn/TMSCl	0,09	0	4%	100%
F2	$[TiL^1Cl_2]$	5%	20ºC	Sn/TMSCl	0	0	0%	0%

The most efficient reducing species for the activation of Ti^{IV} was assessed by comparison of reactions that used magnesium, zinc, tin and manganese. For each metal, a blank reaction was performed. The results are summarized in Table 5.

Zinc was found to be the most active metal but its role in the reaction is not only as a reducing agent because the reaction takes place even in the absence of the titanium catalyst. The comparison of the ^{1}H NMR spectra of the samples taken before and after work-up (see **Appendix**, Figure 43 - Figure 46), reveal that it is during the work-up that the product is formed. This is coherent with the results found in the literature, that show that Zinc is *per se* a catalyst for the pinacol coupling reaction in acidic conditions. [63] The unique peak that appears around δ = 4,74 ppm in the NMR spectrum can

be assigned either to the *dl*- product or to a byproduct such as benzoic acid. It should be noted that Magnesium has also been reported to have similar catalytic activity in the pinacol coupling reaction, but that was not observed in this study. [63,64]

Apart from Zinc, none of the metals tested are able to promote the reaction in the absence of the titanium precursor and Tin revealed inappropriate for reduction of Ti. The best results were obtained with Manganese powder.

The influence of the amount of catalyst was tested within the range of 1% to 20% in relation to the benzaldehyde. In Table 6 it can be seen that the reaction occurs even with 1% catalyst but the activity increases greatly with the amount of catalyst. With 7.5% catalyst, a local maximum is reached (92% conversion, **G3**), making this the most efficient (conversion to amount of catalyst used) proportion, although higher proportions of catalyst give better conversions in absolute terms. The diastereomeric excess, on the other hand, doesn't have a direct correlation with proportion, changing with no apparent reason and reaching its maximum at 15% of catalyst proportion (**G5**).

Table 6: Summary of the results obtained with several different catalyst proportions.[a]

ID	Catalyst	%	TºC	Reductant	$\int dl$	$\int meso$	Conversion	Diastereomeric Excess
G1	$[TiL^1Cl_2]$	1,0%	20ºC	Mn/TMSCl	0,63	0,39	34%	23,5%
G2	$[TiL^1Cl_2]$	2,5%	20ºC	Mn/TMSCl	5,65	2,55	80%	38%
G3	$[TiL^1Cl_2]$	7,5%	20ºC	Mn/TMSCl	16,68	7,73	92%	37%
G4	$[TiL^1Cl_2]$	10%	20ºC	Mn/TMSCl	11,99	7,26	91%	25%
G5	$[TiL^1Cl_2]$	15%	20ºC	Mn/TMSCl	23,62	8,38	94%	48%
G6	$[TiL^1Cl_2]$	20%	20ºC	Mn/TMSCl	69,15	39,04	98%	28%

The other major factor that can influence the reaction is temperature. Indeed, varying the temperature influences both the yield and selectivity. The reaction was tested at 0ºC and 55ºC temperatures using two catalyst proportions: the most efficient, 7,5% catalyst, and the most stereoselective, 15% catalyst (Table 7).

It was found that both the conversion and the stereoselectivity greatly increase with temperature: at 55ºC the reaction can be considered complete at both proportions (**I1** and **I2**), and the 15% proportion (**I2**) gave a 71% diastereomeric excess (d.e.); on the other hand, at 0ºC only 50% conversion and 31% d.e. was attained for the 15% proportion (**H2**). This is particularly interesting because it differs from the results found in the literature, according to which the lower temperature greatly increases the stereoselectivity and even the yield when using both titanocene- and Schiff ligand-based titanium catalysts.[13,15,20,23] Considering these results, two additional tests were carried: a blank at 55ºC (**J**), which yielded a modest conversion with inverted diastereoselectivity, and a

medium-temperature reaction at 45ºC with 7,5% catalyst (**K**), which gave slightly lower conversion and diastereomeric excess than the 55ºC reaction.

Table 7: Summary of the results obtained at several different temperatures and respective blank tests.[a]

ID	Catalyst	%	TºC	Solvent	$\int dl$	$\int meso$	Conversion	Diastereomeric Excess
H1	$[TiL^1Cl_2]$	7.5%	0ºC	THF	0.94	0.68	44.8%	16 %
H2	$[TiL^1Cl_2]$	15.0%	0ºC	THF	1.3	0.68	49.7%	31%
I1	$[TiL^1Cl_2]$	7.5%	55ºC	THF	658.56	131.85	99.7%	67%
I2	$[TiL^1Cl_2]$	15.0%	55ºC	THF	571.61	97.52	99.7%	71%
J	Blank Test	-	55ºC	THF	0.16	0.47	24.0%	-49%
K	$[TiL^1Cl_2]$	7,5%	40ºC	THF	41.14	10.77	96.3%	58.5%
L	$[TiL^1Cl_2]$	7,5%	55ºC	Toluene	3.69	2.97	76.9%	11%

A final test was made to check whether the solvent had a significant effect on the reaction. A reaction was carried in toluene at 55ºC (Table 7**, L**) led to a conversion of 77% and a diastereomeric excess of only 11%. This indicates that the more polar environment of THF is a key factor in the reaction mechanism, increasing not only the yield but also the selectivity. Considering that THF is a coordinating solvent, it may force a specific conformation of a reaction intermediate.

The comparison of complex **7** with other catalysts found in the literature (Table 8) shows that it has a very good activity and may have potential for future applications in the pinacol coupling reaction. The major drawback of the system is the diastereoselectivity, which is slightly lower than for other catalysts, particularly those with chiral ligands. This shows that the achiral $\mathbf{L^1}$ ligand does not control the reaction center's geometry as much as, for example, chiral Schiff bases.

Table 8: Comparison of the best results obtained with selected data of Ti catalysed pinacol coupling reactions

Catalyst[a]	%	T(ºC)	Reductant	Yield	Diastereomeric Excess
Cp_2TiCl_2,[16]	10%	25ºC	Mn/TMSCl	73.0%	86%
$TiL(a)Cl_2$,[21]	10%	-10ºC	Zn/TMSCl	94.0%	96%
$TiL(b)Cl_2$,[20]	15%	0ºC	Mn/TMSCl	95.0%	86%
$TiL(c)Cl_2$,[23]	10%	25ºC	Zn/TMSCl	99.0%	66%
$[TiL^1Cl_2]$	7.5%	55ºC	Mn/TMSCl	99.7%	67%

[a] *Ligands (a) to (d) shown in Figure 9*

A mixture of **6** and zinc powder in THF led to the reduction of Ti(IV) to Ti(III). The EPR spectra of that sample taken before and immediately after the addition of benzaldehyde shown in Figure 32 that clearly indicates the existence of paramagnetic species before and after the addition of benzaldehyde. The complexity of the spectra reveals the presence of more than one Ti(III) species in both cases, which may correspond to the formation of conformational isomers of the Ti(III) species, or to different complexes. Immediately after the addition of benzaldehyde some of the signals disappear.

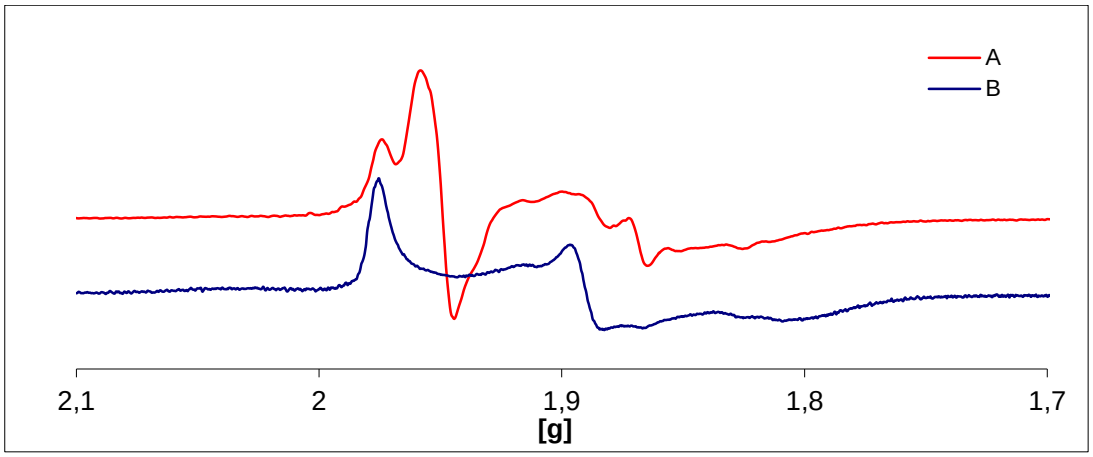

Figure 32: EPR spectra of the pinacol coupling reaction. A: mixture of $[TiL^1Cl]_2(\mu\text{-}O)$, TMSCl and Zinc powder. B: mixture of $[TiL^1Cl]_2(\mu\text{-}O)$, TMSCl, zinc powder and benzaldehyde.

A stoichiometric reaction between complex $[TiL^1Cl(THF)]$ (**5)** and benzaldehyde was carried out in THF at room temperature (NMR tube scale). This reaction was characterized by ^1H NMR in $CDCl_3$ (Figure 33) revealing the formation of the pinacol product with 72% conversion. It is interesting to note that the stoichiometric reaction gives no diastereomeric excess, unlike the catalytic reactions. This result may indicative that the role of the reducing metal species is not only the reduction of the Ti(IV) to Ti(III) by electron transfer, but it might participate in the reaction selectivity, possibly by forming metallic aggregates similar to those described in Figure 7.

This result indicates that $[Ti^{III}L^1Cl]$ is able to catalyze the reaction. A tentative proposal for the catalytic sequence, based on this result and on literature information, is shown in Figure 34. Previous studies have shown that the THF ligand in $[Ti^{III}L^1Cl(THF)]$ is labile.[46] Its dissociation gives $[TiL^1Cl]$, which is likely the active species that coordinates and reduces the aldehyde by electron-transfer from the Ti center to the carbonyl carbon. The coupling of two radicals, which possibly involves two $[TiL^1(Cl)(OCHPh)]$ moieties, eventually displaying chloride or phenolate bridging ligands to Mn, may lead to the release of the product in presence of TMSCl. A Ti(IV) dichloride complex may then be formed. In catalytic conditions, the reduction of Ti(IV) to Ti(III) is achieved through electron transfer from Mn.

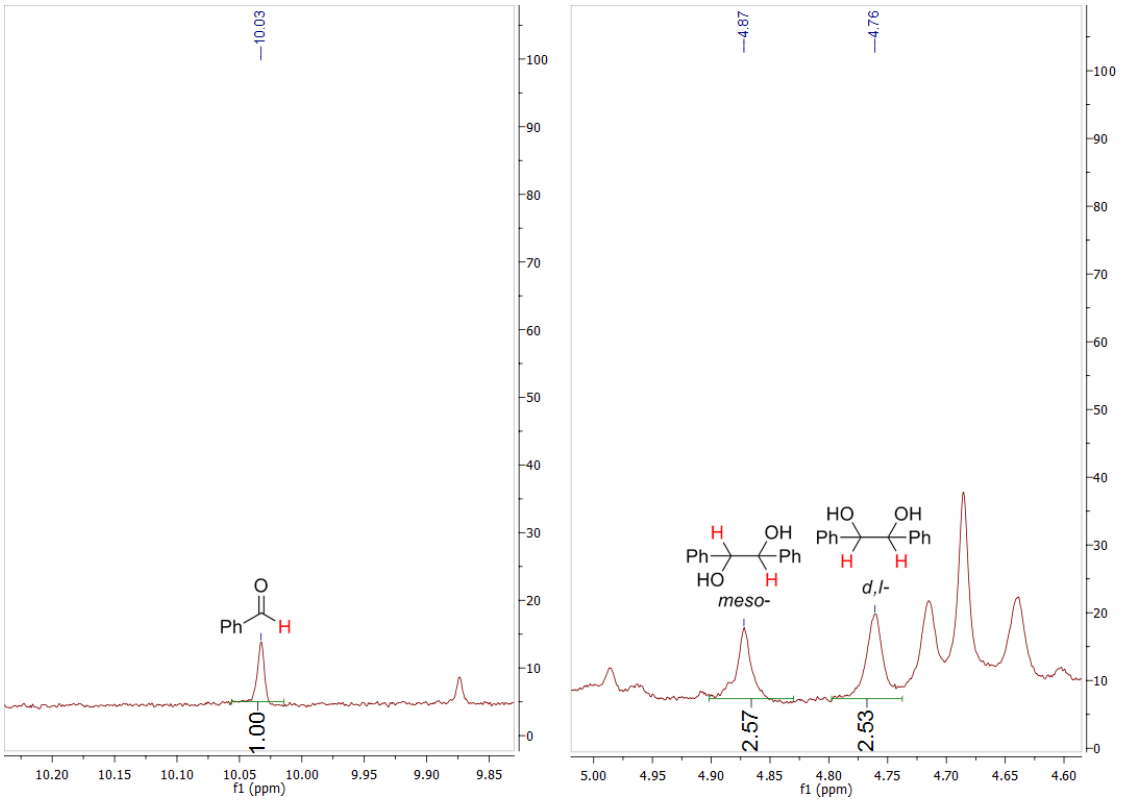

Figure 33: Portions of the ^{1}H NMR spectra of the reaction products for the stoichiometric reaction between complex 5 and benzaldehyde. The labeled peaks identify the benzaldehyde and pinacolate products.

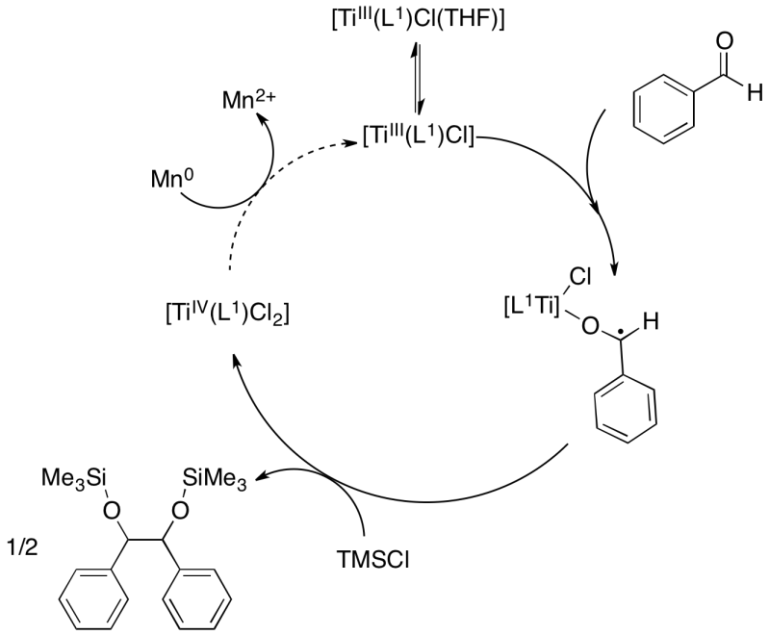

Figure 34: Tentative catalytic sequence for the [TiL^{1}Cl$_2$] catalysed pinacol coupling

3 Conclusions

The ligand precursors **H_2L^1** and **H_2L^2** were successfully synthetized. The synthesis of the novel complex [VOL^2(OiPr)] (**3**) and its molecular structure were achieved. The syntheses of titanium complexes **4** to **7** were also obtained and a new synthetic method for the synthesis of [$TiL^1(OiPr)_2$] (**6**) from commercially available $Ti(OiPr)_4$ was described.

Titanium complexes **5** and **7** were tested as catalysts for the pinacol coupling of benzaldehyde, and several experimental factors were optimized. It was concluded that the best system is [TiL^1Cl_2] with Mn/TMSCl as reductant in THF at 55ºC. Both 7,5% and 15% [Ti]:benzaldehyde proportions gave complete conversion in these conditions and the diastereomeric excesses obtained varied only slightly (67% to 71%, respectively). In the future, it would be interesting to test chiral ligands of the same kind in an effort to obtain better diastereomeric excesses and ultimately enantioselectivity. It would also be important to test benzaldehydes with both electron-donating and electron-withdrawing substituents, in order to gain insight on the electronic effects influencing the reaction.

EPR and NMR experiments were run in order to get information about the catalytic reactions. The EPR spectra showed the presence of Ti(III) species in the reaction medium, some of which are quenched by addition of benzaldehyde. Furthermore, the stoichiometric reaction of [TiL^1Cl(THF)] with benzaldehyde showed no diastereoselectivity, which may indicate that the reductant metal plays a role in the catalysis mechanism despite its reducing function. The interaction between Ti and the reducing metals is likely to occur in solution, and this interaction is important in determining the diastereoselectivity.

4 Experimental Section

4.1 General Considerations

All preparations and subsequent manipulations of air/moisture sensitive compounds were performed under a nitrogen atmosphere using standard Schlenk line and glovebox techniques. THF, toluene, n-hexane, CH_2Cl_2 and Et_2O were dried by standard methods (sodium/benzophenone for THF, toluene and Et_2O; calcium hydride for n-hexane and CH_2Cl_2) and distilled prior to use. Benzaldehyde was washed with a 5% aqueous solution of Na_2CO_3, dried with CaCl, distilled under vacuum and kept under inert N_2 atmosphere.

NMR samples of air/moisture sensitive compounds were prepared in a glovebox under inert atmosphere using NMR tubes equipped with J-Young stopcocks. The C_6D_6 used for NMR samples was dried over Na and distilled under reduced pressure.

Unless stated otherwise, all reagents were purchased from commercial suppliers (e. g. Aldrich, Acrös, Fluka) and used as received.

1D NMR (^1H, ^{13}C-{^1H}, 13C-{1H} APT) and 2D NMR (COSY, NOESY, HSQC) spectra were recorded on Bruker Advance II+ 300 and 400 MHz (UltraShield Magnet), at ambient temperature. ^1H and ^{13}C chemical shifts (δ) are expressed in ppm relative to Me_4Si. Coupling constants (J) are given in Hz and multiplicities are presented as: br (broad), s (singlet), d (doublet), dd (double doublet), t (triplet), q (quartet), sept (septet) and m (multiplet).

Crystals suitable for single-crystal X-ray analysis were grown as described in the synthetic procedures. Crystallographic data were collected at *Instituto Superior Técnico* by Dr. Sónia Barroso. Crystals of air/moisture sensitive compounds were selected inside the glovebox, covered with polyfluoroether oil and mounted on a nylon loop. The data were collected using graphite monochromated Mo-K_α radiation (λ = 0.71073 Å) on a Bruker AXS-KAPPA APEX II diffractometer equipped with an Oxford Cryosystem open-flow nitrogen cryostat. Cell parameters were retrieved using Bruker SMART software and refined using Bruker SAINT on all observed reflections. Absorption corrections were applied using SADABS.[65] The structures were solved and refined using direct methods with programs SIR2004 or SHELXS-97.[66–68] All programs are included in the package of programs WINGX-Version 1.80.01 SHELXL.[69,70] All non-hydrogen atoms were refined anisotropically and the hydrogen atoms were inserted in idealized positions and allowed to refine riding on the parent carbon atom. The molecular diagrams were drawn with ORTEP-3 for Windows, included in the software package.[71] Selected crystallographic experimental data and structure refinement parameters are presented in Table 9.

Table 9: Selected crystallographic experimental data and structure refinement parameters for 3 and 7.

	7	3
Empirical formula	$TiC_{34}H_{54}Cl_2N_2O_2$	$VC_{40}H_{65}N_2O_4$
Formula weight	641.59	688.88
Temperature (K)	150(2)	150(2)
Crystal system	Monoclinic	Monoclinic
Space group	$P2_1/c$	$P2_1$
V(Å^3)	3567.3(4)	7823.8(7)
a(Å)	16.6997(11)	15.5180(11)
b(Å)	15.6387(10)	23.5210(10)
c(Å)	15.1741(10)	21.8270(10)
α(°)	90	90
β(°)	115.821(2)	100.875(2)
γ(°)	90	90
Z, ρ_{calc} (gcm^{-3})	4, 1.195	8, 1.170
μ(mm^{-1})	0.420	0.293
Crystal size	0.04×0.18×0.18	0.20×0.20×0.30
Crystal colour	orange	brown
Crystal shape	plate	block
Refl. collected	15403	48641
Unique refl. [R(int)]	6299 [0.0811]	24929 [0.0490]
R1 [I>2σ(I)]	0.0608	0.0495
wR2 [I>2σ(I)]	0.1292	0.0967
GooF	0.936	1.000
Flack's param.		-0.003(12)

4.2 Synthetic Procedures

Synthesis of 6,6'-(2-(dimethylamino)ethylazanediyl)bis(methylene)bis(2,4-di-tert-butylphenol), H_2L^1, 1.[26]

A solution of 2,4-di-tert-butylphenol (5.00 g, 24.2 mmol), N,N-dimethylethylenediamine (1.40 mL, 12.3 mmol), and 36% aqueous formaldehyde (2.50 mL, 33.6 mmol) in methanol (10 mL) was stirred at room temperature for 3 days. The mixture was cooled to -4 ºC overnight and a precipitate formed. The solution was filtered off and the solid was thoroughly washed with ice-cold methanol to give a white powder. Yield: 3.72 g, 58%. The compound was further purified by recrystallization from methanol.

^{1}H NMR (300 MHz, $CDCl_3$, ppm): 9.81 (br, 2H, O*H*), 7.19 (d, $^4J_{HH}$ = 2.1 Hz, 2H, o- C*H*-Ar), 6.87 (d, $^4J_{HH}$ = 2.0 Hz, 2H, p-C*H*-Ar), 3.60 (br, 4H, NCH_2Ar), 2.59 (s, 4H, NCH_2CH_2N), 2.31 (s, 6H, N(CH_3)$_2$), 1.39 (s, 18H, C(CH_3)$_3$), 1.27 (s, 18H, C(CH_3)$_3$).

Synthesis of (*S*)-6,6'-((1-ethylpyrrolidin-2-yl)methylazanediyl)bis(methylene)- bis(2,4-di-tert-butylphenol), H_2L^2, 2.[47]

A solution of 2,4-di-tert-butylphenol (4.13 g, 20.0 mmol), (*S*)-ethylpyrrolidine (1.35 mL, 12.3 mmol), and 36% aqueous formaldehyde (1.65 mL, 22.0 mmol) in methanol (10 mL) was stirred at room temperature for 3 days. The mixture was cooled to -4 ºC overnight leading to the formation of a sticky precipitate. The supernatant solution was decanted and the solid was redissolved in MeOH. Upon cooling the compound precipitate out of solution. The solid was separated by filtration and washed thoroughly with ice-cold methanol to give an off-white solid. Yield: 1.70 g, 30%. The compound was further purified by recrystallization from methanol.

^{1}H NMR (300 MHz, CDCl3, ppm): 9.69 (br, 2H, O*H*), 7.20 (d, $^4J_{HH}$ = 2.2 Hz, 2H, C*H*-Ar), 6.87 (d, $^4J_{HH}$ = 2.2 Hz, 2H, C*H*-Ar), 3.87 (d, $^2J_{HH}$ = 13.3 Hz, 2H, ArCH_2N), 3.43 (d, 2H, $^2J_{HH}$ = 13.2 Hz, ArCH_2N), 3.35 (m, 1H, CH_2), 3.04 (m, 1H, CH_2CH$_3$), 2.66 (m, 2H, CH_2 + C*H*), 2.48 (m, 1H, NCH_2), 2.25 (m, 2H, CH_2CH3 + CH$_2$), 1.90 (m, 1H, CH_2), 1.68 (m, 2H, CH_2), 1.48 (m, 1H, CH_2), 1.39 (s, 18H, C(CH_3)$_3$), 1.27 (s, 18H, C(CH_3)$_3$), 1.20 (t, $^3J_{HH}$ = 7.2 Hz, 3H, CH$_2$CH_3).

Reaction of H_2L^2 with $VOCl_3$.

A solution of **H_2L^2** (0.57 g, 1.0 mmol) in THF was slowly added to NaH (0.056 g, 2.2 mmol) and the mixture was stirred for 2 h at 50ºC in inert atmosphere. The colorless solution was cooled to room temperature and $VOCl_3$ (0.095 ml, 1.0 mmol) was slowly added to it. The dark blue reaction mixture was stirred overnight and then evaporated under reduced pressure to give a greenish solid (0.329 g).

Synthesis of [$VOL^2(O^iPr)$], 3.

A solution of **H_2L^2** (0.57 g, 1.0 mmol) in 5 ml THF was prepared under inert atmosphere, and VO(OiPr)$_3$ (0.24 ml, 1.0 mmol) was slowly added to it. The mixture was stirred overnight, and then the

solvent was evaporated under reduced pressure. The resulting dark brownish product was extracted in diethyl ether and again evaporated and dried under reduced pressure (η=60%).

Dark brown crystals suitable for X-ray diffraction were obtained from a toluene/hexane mixture at -4ºC.

^{1}H NMR (300 MHz, CDCl3, ppm): 7.38 (d, $^{4}J_{HH}$ = 2.4 Hz, 1H, C*H*-Ar), 7.21 (d, $^{4}J_{HH}$ = 2.5 Hz, 1H, C*H*-Ar), 7.16 (d, $^{4}J_{HH}$ = 2.4 Hz, 1H, C*H*-Ar), 6.91 (d, $^{4}J_{HH}$ = 2.31H, C*H*-Ar), 4.91 (d, $^{2}J_{HH}$ = 15.3 Hz, 1H, ArC*H*HN), 4.26 (d, 1H, $^{2}J_{HH}$ = 12.3 Hz, ArC*H*HN), 3.93 (m, 1H, CH_2), 3.64 (d, $^{2}J_{HH}$ = 15.3 Hz, 1H, ArC*H*HN), 3.42 (m, 1H, NC*H*$(CH_2)_2$), 3.16 (d, 1H, $^{2}J_{HH}$ = 12.2 Hz, ArC*H*HN), 3.00 (m, 1H, CH_2CH_3), 2.81 (m, 2H, CH_2), 2.24 (m, 1H, CH_2), 1.83 (m, 4H, CH_2 + CH_2), 1.39 (d, $^{2}J_{HH}$= 6.1, 3H, OC(C$H_3)_3$), 1.49 (s, 9H, C(C$H_3)_3$), 1.47 (d, 3H, OC(C$H_3)_3$) 1.45 (s, 9H, C(C$H_3)_3$), 1.35 (s, 9H, C(C$H_3)_3$), 1.26 (s, 9H, C(C$H_3)_3$), 1.13 (m, 3H, CH_2CH_3).

EA calculated for $C_{40}H_{65}N_2O_4V{\cdot}0.5(C_7H_8)$: C, 64.83; H, 8.63; N, 3.48. Found: C, 64.59; H, 8.78; N, 3.64.

Synthesis of [TiL^{1}Cl(THF)], 4.[46]

A solution of **H_2L^1** (1.05 g, 2.0 mmol) in THF was added to NaH (0.11 g, 4.4 mmol) and the mixture was stirred for 2 h at 50ºC. The colorless solution obtained was allowed to cool down to room temperature, filtered through celite and added to a suspension of $TiCl_3(THF)_3$ (0.74 g, 2.0 mmol) in THF at -80ºC. The mixture was allowed to reach room temperature slowly and stirred overnight. The yellow/orange solution obtained was evaporated to dryness and the residue was extracted in Et_2O and filtered. Evaporation of the solution led to a microcrystalline yellow/orange solid, which was filtered from the orange solution. Yield: 0,52 g, 38%.

Synthesis of [TiL^{1}Cl]$_2$(μ-O), 5.[55]

A solution of **4** (0,52 g, 0,8 mmol) in THF was exposed to air, through a $CaCl_2$ drying tube, for 12 h. The red/orange solution obtained was evaporated to dryness, and the residue was extracted with Et_2O and filtered. Evaporation of the Et_2O solution to dryness led to an orange crystalline solid. Yield: 0,40 g, 85%.

^{1}H NMR (300 MHz, C_6D_6, ppm): 7.47 (s, 4H, p-C*H*-Ar), 7.11 (s, 4H, o-C*H*-Ar), 5.77 (d, 4H, $^{2}J_{HH}$ = 13.7 Hz, NCH_2Ar), 3.30 (d, 4H, $^{2}J_{HH}$ = 13.8 Hz, NCH_2Ar), 2.25 (m, 4H, CH_2), 1.90 (s, 12H, N(C$H_3)_2$), 1.46 (m, 4H, CH_2), 1.44 (s, 36H, C(C$H_3)_3$), 1.36 (s, 36H, C(C$H_3)_3$).

Synthesis of [TiL^1(OiPr)$_2$], 6.

Method 1: From [TiL^{1}Cl]$_2$(μ-O).

Triethylamine (0.22 mL, 1.6 mmol) was added to a solution of **5** (0,5 g, 0.4 mmol) in isopropanol and the mixture was stirred for 48 h. The orange-yellow solution obtained was evaporated to dryness, and the residue was extracted in Et_2O and filtered. Evaporation of the Et_2O solution under vacuum led to an orange powder.

Method 2: From Ti(O^iPr)$_4$.

A solution of Ti(O^iPr)$_4$ 1M in Toluene was prepared and added (3 ml, 3.0 mmol) to a THF solution of **H_2L^1** (1,574 g, 3.0 mmol). The mixture was stirred for 2 hours and the yellow solution obtained was evaporated and dried under reduced pressure. The product was then extracted in toluene and again evaporated to dryness. Yield: 1,86 g, 96%.

^{1}H NMR (300 MHz, C_6D_6, ppm): 7.58 (d, 2H, $^4J_{HH}$ = 2.3 Hz, p-C*H*-Ar), 7.06 (d, 2H, $^4J_{HH}$ = 2.1 Hz, o-C*H*-Ar), 5.23 (sept, $^3J_{HH}$ = 5.9 Hz, 1H, C*H*(CH_3)$_2$), 4.81 (sept, $^3J_{HH}$ = 5.9 Hz, 1H, C*H*(CH_3)$_2$), 4.24 (d, 2H, $^2J_{HH}$ = 13.1 Hz , NC*H*$_2$Ar), 3.12 (d, 2H, $^2J_{HH}$ = 13.1 Hz, NC*H*$_2$Ar), 2.28 (m, 2H, NC*H*$_2$$CH_2NMe_2$), 2.09 (s, 6H, N(C*H*$_3$)$_2$), 1.81 (m, 2H, NCH_2C*H*$_2$$NMe_2$), 1.76 (s, 18H, C(C*H*$_3$)$_3$), 1.50 (d, $^3J_{HH}$ = 6.0 Hz, 6H, CH(C*H*$_3$)$_2$), 1.43 (s, 18H, C(C*H*$_3$)$_3$), 0.98 (d, $^3J_{HH}$ = 6.0 Hz, 6H, CH(C*H*$_3$)$_2$).

Synthesis of [TiL^1Cl_2], 7.[55]

To a solution of **6** (1,86 g, 2.9 mmol) in CH_2Cl_2, TMSCl in great excess (0,84 ml, 6,6 mmol) was slowly added. The mixture was stirred overnight and the dark orange solution obtain evaporated to dryness. The product was then extracted in Toluene and evaporated to dryness under vacuum to give a reddish-orange powder. Yield: 1,60 g, 89%. Dark orange crystals suitable for X-ray diffraction were obtained from toluene at -4ºC.

^{1}H NMR (300 MHz, C_6D_6, ppm): 7.59 (d, 2H, $^4J_{HH}$ = 2.3 Hz, p-C*H*-Ar), 6.97 (d, 2H, $^4J_{HH}$ = 2.3 Hz, o-C*H*-Ar), 4.35 (d, $^2J_{HH}$ = 13.8 Hz, 2H, NC*H*$_2$Ar), 2.79 (d, $^2J_{HH}$ = 13.3 Hz, 2H, NC*H*$_2$Ar), 2.14 (m, 2H, C*H*$_2$), 1.94 (s, 6H, N(C*H*$_3$)$_2$), 1.80 (s, 18H, C(C*H*$_3$)$_3$), 1.61 (m, 2H, C*H*$_2$), 1.39 (s, 36H, C(C*H*$_3$)$_3$).

EA calculated for $C_{34}H_{54}Cl_2N_2O_2Ti \cdot 0.5(C_7H_8)$: C, 65.51; H, 8.50; N, 4.07. Found: C, 65.47; H, 8.67; N, 3.83.

General Procedure for the catalytic pinacol coupling reactions.

A solution of the [Ti^{IV}] complex (in adequate proportion) in THF was prepared in a vial inside the glovebox. The metallic reductant (6.0 mmol) and TMSCl (0,28 ml, 3.0 mmol) were sequentially added. The mixture was stirred for 10 minutes and benzaldehyde (0,20 ml, 2.0 mmol) was added. The vial was sealed and brought outside the glovebox, where the reaction stirred overnight at the appropriate temperature. After 16 hours of reaction, the vial was opened to air and the reaction quenched with 5 ml of an aqueous 5% Na_2CO_3 solution. The mixture was filtered and extracted with 3x15 ml of ethyl acetate, which was then evaporated at reduced pressure. The crude obtain was stirred with 5 ml of a HCl solution 1M in THF for 2 hours at room temperature, diluted with 10 ml distilled water and, again, extracted in 3x15 ml ethyl acetate and evaporated to dryness under vacuum. An NMR sample of the product was taken in $CDCl_3$.

Preparation of sample for EPR spectra

To a small deareated vial with Zinc powder (0,390 g, 6.0 mmol) a solution of 5% [TiL^1Cl]$_2$(μ-O) in 4 ml THF was added. TMSCl (0,28 ml, 3.0 mmol) was then added and, after 5 minutes stirring, the

first aliquot was taken. Benzaldehyde (0,20 ml, 2.0 mmol) was then added and the second aliquot immediately taken. The aliquots were frozen until the EPR spectra were taken.

Reaction of 4 with benzaldehyde.

A solution of benzaldehyde 1:100 in THF was prepared in the glovebox, and 0,2 ml (0,02 mmol) of that solution were added to crystalline **4** (15 mg, 0,02 mmol) in the same solvent in a J-Young NMR tube. The mixture was left to react for two days inside the glovebox, after which the solvent was evaporated under vacuum and the products redissolved in $CDCl_3$.

Bibliography

1. Nair V, Mathew J, *Chem. Soc. Rev.* **1997** (26), 127–132.

2. Reetz MT, *Top. Curr. Chem.* **1982** (106), 1–54.

3. Rossi B, Prosperini S, Pastori N, Clerici A, Punta C, *Molecules*. **2012** (17), 14700–32.

4. Ramón DJ, Yus M, *Chemical reviews*. **2006** (106), 2126–208.

5. Liu Y, Schwartz J, *J. Org. Chem.* **1994** (4), 940–942.

6. Liu Y, Schwartz J, *Tetrahedron*. **1995** (51), 4471–4482.

7. Barden M, Schwartz J, *J. Org. Chem.* **1995** (16), 5963–5965.

8. Dosa P, Kronish I, McCallum J, *J. Org. Chem.* **1996** (3263), 4886–4887.

9. Spencer RP, Schwartz J, *Tetrahedron*. **2000** (56), 2103–2112.

10. RajanBabu T, Nugent W, *J. Am. Chem. Soc*. **1994** (7), 986–997.

11. Gansäuer A, Narayan S, *Adv. Synth. Catal.* **2002**, 465–475.

12. Bensari a, Renaud JL, Riant O, *Org. Lett.* **2001** (3), 3863–5.

13. McMurry J, *Chem. Rev.* **1989**, 1513–1524.

14. McMurry JE, Fleming MP, *J. Am. Chem. Soc.* **1974** (96), 4708–4709.

15. Ephritikhine M, *Chem. Commun.* **1998**, 2549–2554.

16. Dunlap MSM, Nicholas KKM, *Synth. Commun.* **1999** (29), 1097–1106.

17. Dunlap MS, Nicholas KM, *J. Organomet. Chem.* **2001** (630), 125–131.

18. Tian Q, Jiang C, Li Y, You T, *J. Mol. Catal.* **2004** (219), 315–317.

19. Bandini M, Cozzi PG, Morganti S, Umani-Ronchi A, *Tetrahedron Lett.* **1999** (40), 1997–2000.

20. Li Y-G, Tian Q-S, Zhao J, Feng Y, Li M-J, You T-P, *Tetrahedron, Asymmetry*. **2004** (15), 1707–1710.

21. Chatterjee A, Bennur T, Joshi N, *J. Org. Chem*. **2003**, 5668–5671.

22. Chatterjee A, Joshi NN, *Tetrahedron*. **2006** (62), 12137–12158.

23. Wen J, Zhao J, You T, *J. Mol. Catal. A Chem.* **2006** (245), 278–280.

24. Li Y, Jiang C, Zhao J, *Chinese J. of Chem*. **2004** (4), 950–952.

25. Bujnowski K, Adamczyk A, Synoradzki L, *Org. Prep. Proc. Int.* **2007** (39), 417.

26. Tshuva EY, Versano M, Goldberg I, Kol M, Weitman H, Goldschmidt Z, *Inorg. Chem. Commun.* **1999** (2), 371–373.

27. Tshuva EY, Goldberg I, Kol M, Goldschmidt Z, *Inorg. Chem.* **2001** (40), 4263–70.

28. Peri D, Manna CM, Shavit M, Tshuva EY, *Eur. J. Inorg. Chem.* **2011** (31), 4896–4900.

29. Groysman S, Goldberg I, Kol M, Genizi E, Goldschmidt Z, *Inorganica Chim. Acta*. **2003** (345), 137–144.

30. Woodgate PD, Horner GM, Maynard NP, Rickard CEF, *J. Organomet. Chem.* **1999** (592), 180.

31. Lyle RR, Walsh DA., *J. Organomet. Chem.* **1974** (67), 363-367.

32. Chirachanchai S, Laobuthee A, Phongtamburg S, Siripatanasarakit W, Ishida H., *J. Appl. Polym. Sci.* **2000** (77), 2561.

33. Morimura S, *Heterocycles*. **1980** (14), 1331-1332.

34. Neuvonen K, Pihlaja K., *Acta Chem. Scand.* **1993** (47), 695.

35. Boyd C, Toupance T, Tyrrell B, *Organometallics*. **2005** (5), 309–330.

36. Tshuva EY, Goldberg I, Kol M, *Organometallics*. **2001** (20), 3017–3028.

37. Tshuva EY, Groysman S, Goldberg I, Kol M, *Organometallics*. **2002** (21), 662–670.

38. Liu X, Shang X, Tang T, et al., *Organometallics*. **2007** (26), 2747.

39. Willans CE, Sinenkov MA, Fukin GK, Sheridan K, Lynam JM, Trifonov AA, Kerton FM, *Dalt. Trans.* **2008**, 3592–3598.

40. Madeira F, Barroso S, Namorado S, Reis PM, Royo B, Martins AM, *Inorganica Chim. Acta*. **2011**, 383, 152-156.

41. Groysman S, Goldberg I, Goldschmidt Z, Kol M, *Inorg. Chem.* **2005** (44), 5073–80.

42. Mba M, Prins LJ, Zonta C, et al., *Dalton Trans.* **2010** (39), 7384–92.

43. Mba M, Prins LJ, Licini G, Chimiche S, Marzolo V, *Org. Lett.* **2007** (9), 21–24.

44. Barroso S, Adão P, Madeira F, Duarte MT, Pessoa JC, Martins AM, *Inorg. Chem.* **2010** (49), 7452–7463.

45. Barroso S. PhD Dissertation, "Diaminebisphenolate Titanium, Zirconium and Vanadium Complexes, Syntheses, Reactivity and Applications", *Instituto Superior Técnico*, **2010**.

46. Barroso S, Cui J, Carretas JM, Cruz A, Santos IC, Duarte MT, Telo JP, Marques N, Martins AM, *Organometallics*. **2009** (28), 3449–3458.

47. Barroso S, Adão P, Duarte MT, Meetsma A, Pessoa JC, Bouwkamp MW, Martins AM, *Eur. J. Inorg. Chem.* **2011** (27), 4277–4290.

48. Barroso S, Abreu AM, Araújo AC, Coelho AM, Maulide N, Martins AM, *Synlett*. **2010** (16), 2425–2428.

49. Peri D, Meker S, Manna CM, Tshuva EY, *Inorg. Chem.* **2011** (50), 1030–8.

50. Tshuva EY, Goldberg I, Kol M, Weitman H, Goldschmidt Z, *Chem. Commun.* **2000** (5), 379–380.

51. Tshuva EY, Goldberg I, Kol M, Goldschmidt Z, *Chem. Commun.* **2001** (20), 2120-2121.

52. Toupance T, Dubberley SR, Rees NH, Tyrrell BR, Mountford P, *Organometallics*. **2002** (21), 1367–1382.

53. Wolff F, Lorber C, Choukroun R, Donnadieu B, *Eur. J. Inorg. Chem.* **2004** (14), 2861-2867.

54. Lorber C, Wolff F, Choukroun R, Vendier L, *Eur. J. Inorg. Chem.* **2005** (14), 2850-2859.

55. Barroso S, Madeira F, Calhorda MJ, Duarte MT, Martins AM, *Inorg. Chem.* **2013** (52), 9427-9439.

56. Madeira F, Barroso S, Namorado S, Reis PM, Royo B, Martins AM, *Inorg. Chim. Acta*. **2012** (383), 152-157.

57. Wolff F, Lorber C, Choukroun R, Donnadieu B, *Inorg. Chem.* **2003** (42), 7839-7845.

58. Groysman S, Goldberg I, Kol M, Genizi E, Goldschmidt Z, *Inorg. Chim. Acta*. **2003** (345), 137-144.

59. Sarazin Y, Howard RH, Hughes DL, Humphrey SM, Bochmann M, *Dalt. Trans.* **2006** (2), 340-350.

60. Clarkson GJ, Gibson VC, Goh PKY, Hammond ML, Knight PD, Scott P, Smit TM, White AJP, Williams DJ, *Dalt. Trans.* **2006** (46), 5484-5491.

61. Blackmore KJ, Lal N, Ziller JW, Heyduk AF, *Eur. J. Inorg. Chem.* **2009** (6), 735-743.

62. Saito J, Mitani M, Matsui S, Matsui S, Makio H, Nakano T, Tanaka H, Kashiwa N, Fujita T, *Macromol. Chem. Phys.* **2002** (203), 59-65.

63. Barden M, Schwartz J, *J. Am. Chem. Soc.* **1996** (3), 5484–5485.

64. Zhang W-C, Li C-J, *J. Org. Chem.* **1999** (64), 3230–3236.

65. Sheldrick GM. "SADABS, Program for Empirical Absorption Correction." *University of Göttingen, Germany,* **1996**.

66. Burla MC, Caliandro R, Camalli M, Carrozzini B, Cascarano GL, De Caro L, Giacovazzo C, Polidori G, Spagna R, *J. Appl. Cryst.* **2005** (38), 381-388.

67. Sheldrick GM., *Acta Cryst.* **1990** (A46), 467.

68. Sheldrick GM., *Acta Crystallogr.* **2008** (A64), 122.

69. Farrugia LJ., *J. Appl.Crystallogr.* **1999** (32), 837-838.

70. Sheldrick GM. "SHELXL-97 – Programs for Crystal Structure Analysis." *Göttingen, Germany*. **1998**, Release 97–2.

71. Farrugia LJ, *J. Appl. Crystallogr.* **1997** (30), 565.

Appendix

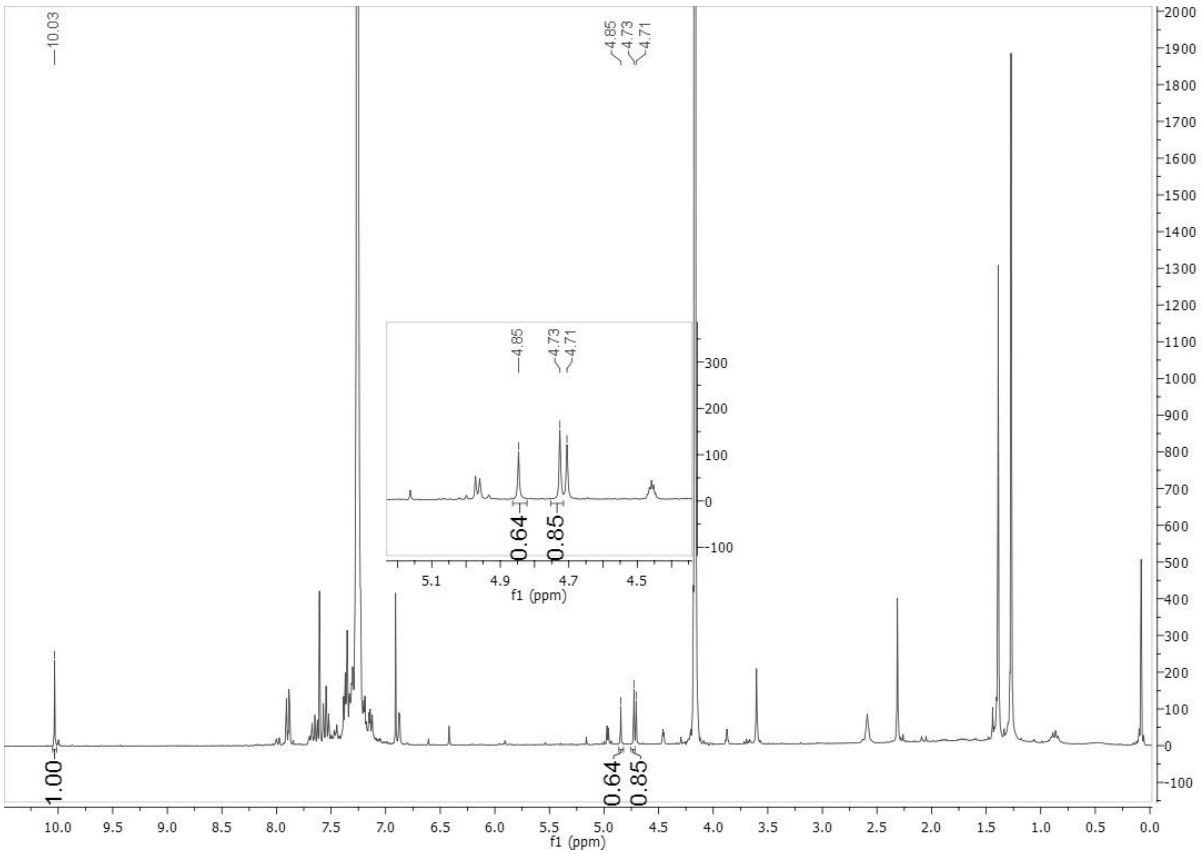

Figure 35: ^{1}H NMR Spectra of the crude products of reaction A after work-up. The labelled peaks identify the benzaldehyde (s, 10,03 ppm) the *meso*- product (s, 4,85 ppm) and the *dl*- product (s, 4,73 ppm). The peak marked with * is the solvent (CDCl3, 7,26 ppm) and the peak marked with º is the ferrocene internal standard (4,17 ppm)

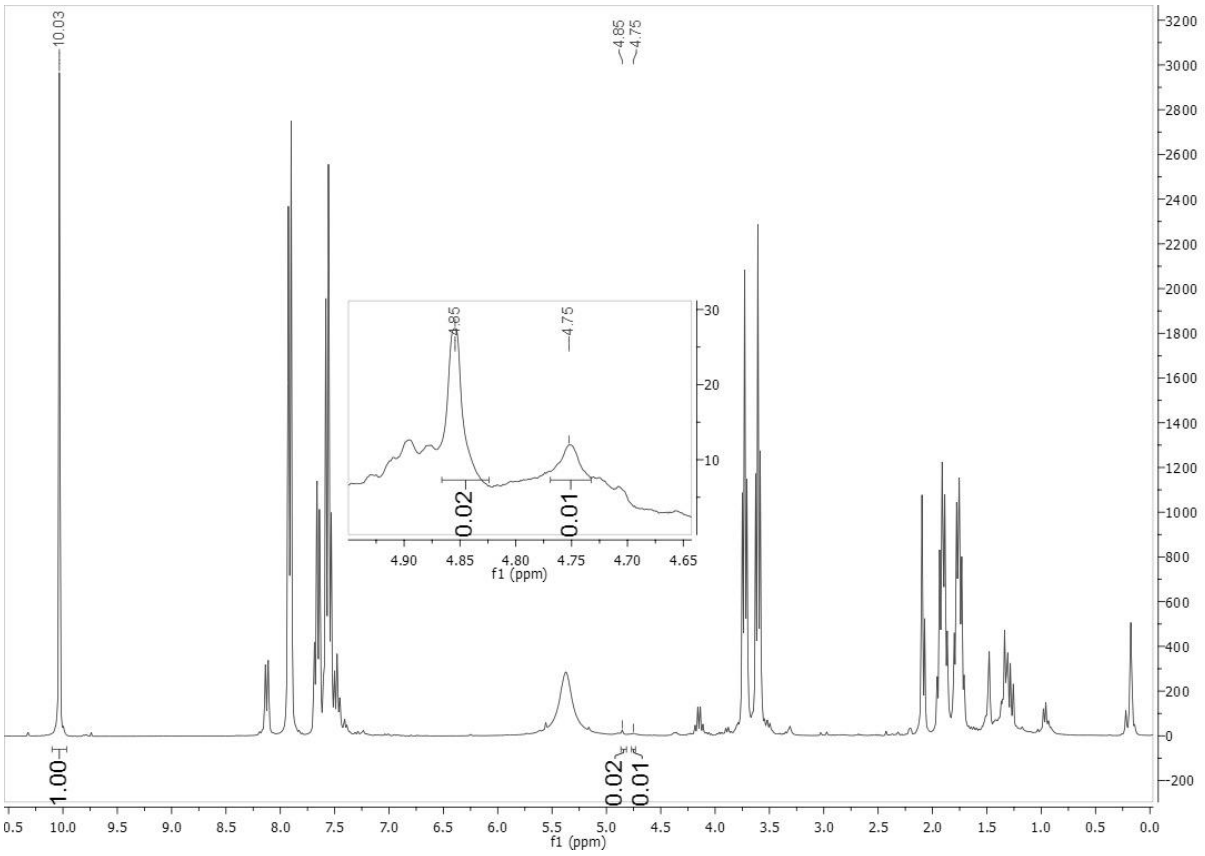

Figure 36: ^{1}H NMR Spectra of the crude products of reaction B after work-up. The labelled peaks identify the benzaldehyde (s, 10,03 ppm) the *meso*- product (s, 4,85 ppm) and the *dl*- product (s, 4,75 ppm)

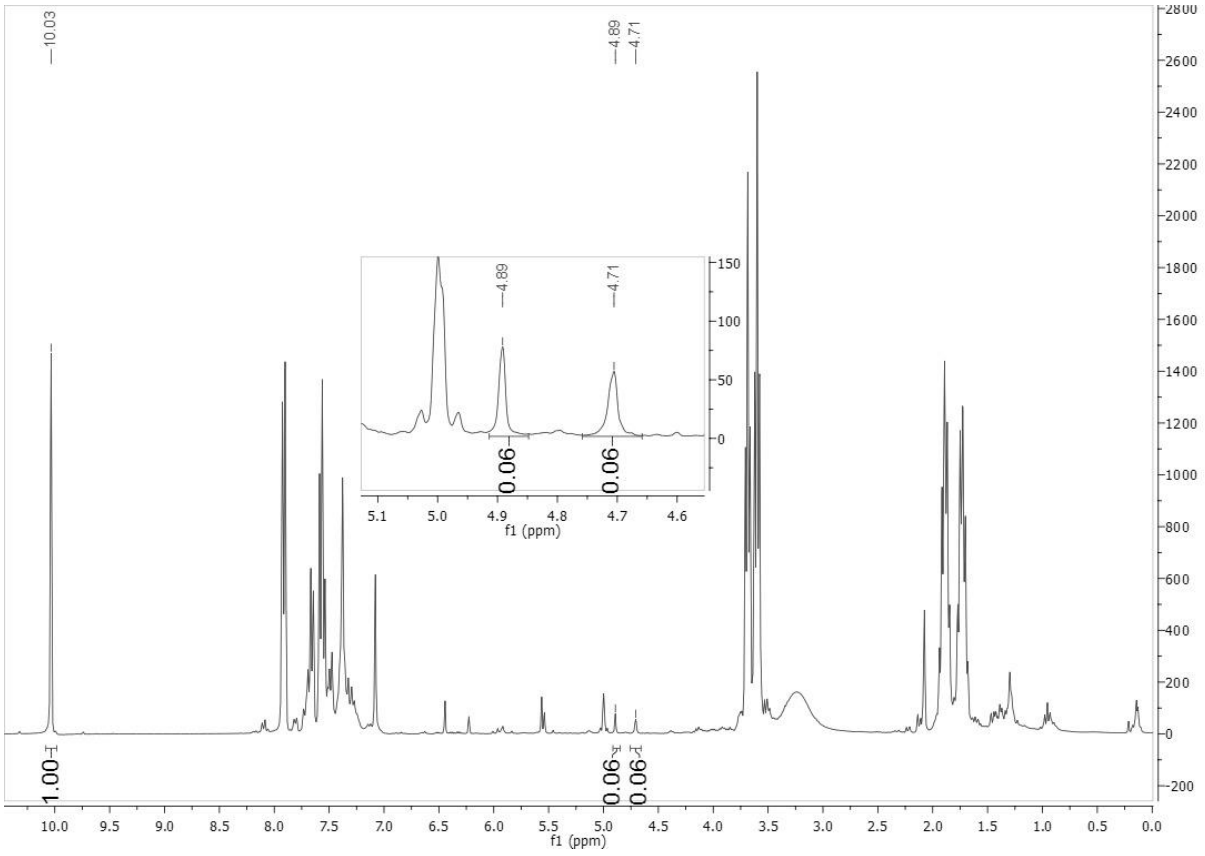

Figure 37: ^{1}H NMR Spectra of the crude products of reaction C1 after work-up. The labelled peaks identify the benzaldehyde (s, 10,03 ppm) the *meso*- product (s, 4,89 ppm) and the *dl*- product (s, 4,71 ppm)

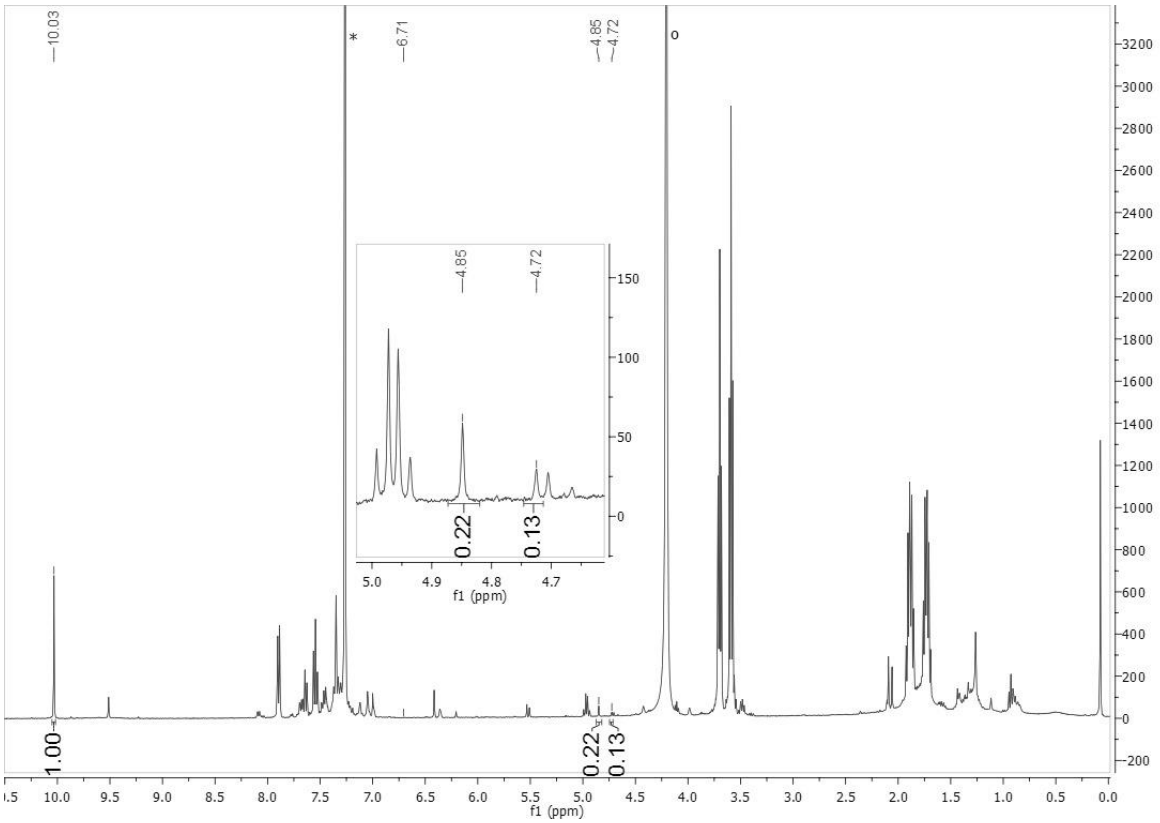

Figure 38: ^{1}H NMR Spectra of the crude products of reaction C2 after work-up. The labelled peaks identify the benzaldehyde (s, 10,03 ppm) the *meso*- product (s, 4,85 ppm) and the *dl*- product (s, 4,72 ppm). The peak marked with * is the solvent (CDCl3, 7,26 ppm) and the peak marked with º is the ferrocene internal standard (4,20 ppm)

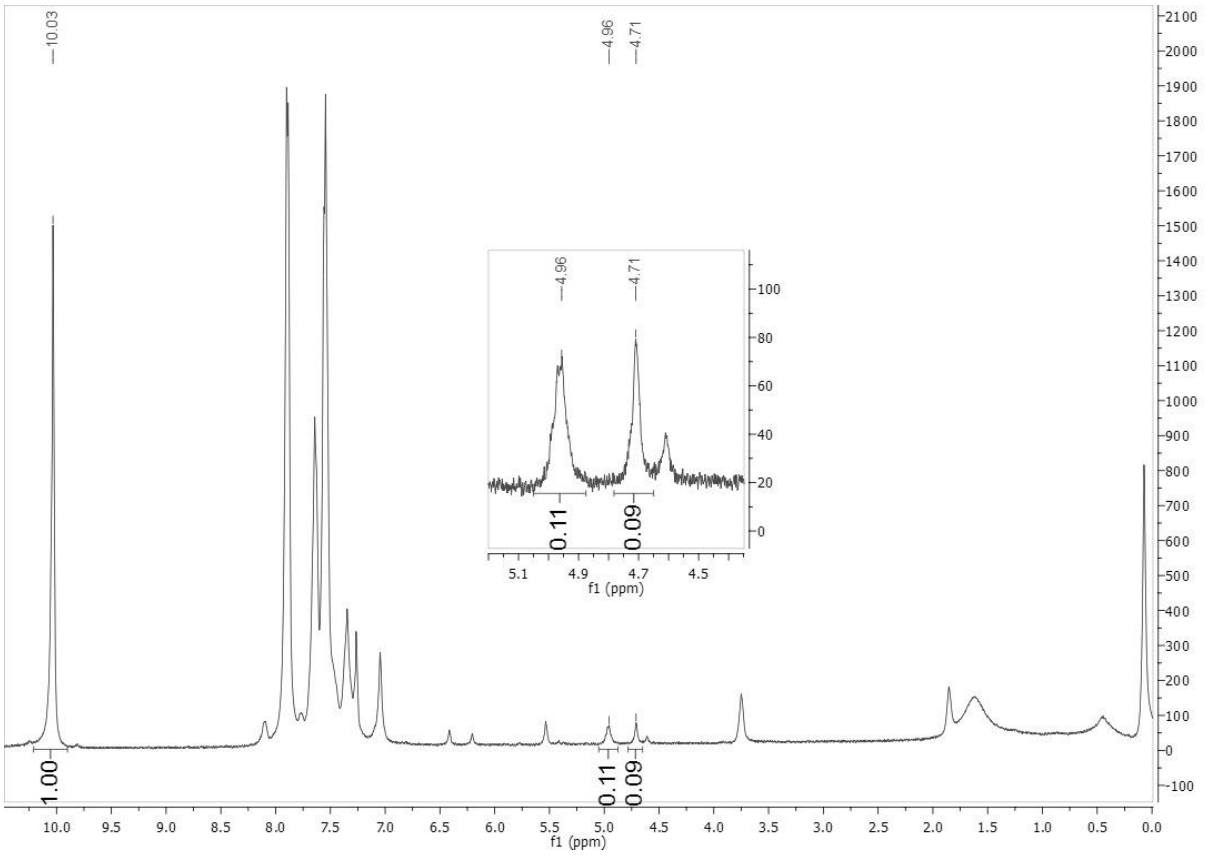

Figure 39: ^{1}H NMR Spectra of the crude products of reaction D1 before work-up. The labelled peaks identify the benzaldehyde (s, 10,03 ppm) the *meso*- product (s, 4,96 ppm) and the *dl*- product (s, 4,71 ppm).

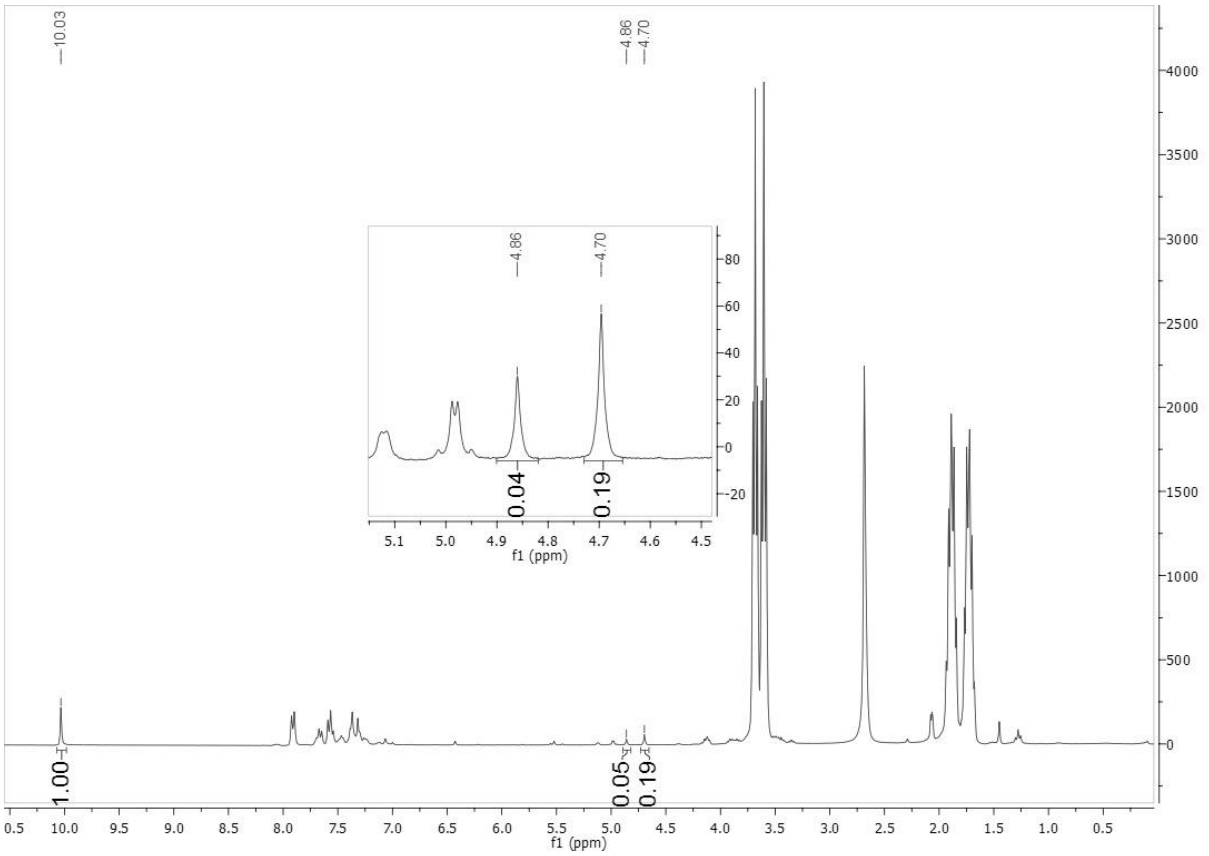

Figure 40: ^{1}H NMR Spectra of the crude products of reaction D1 after work-up. The labelled peaks identify the benzaldehyde (s, 10,03 ppm) the *meso*- product (s, 4,86 ppm) and the *dl*- product (s, 4,70 ppm).

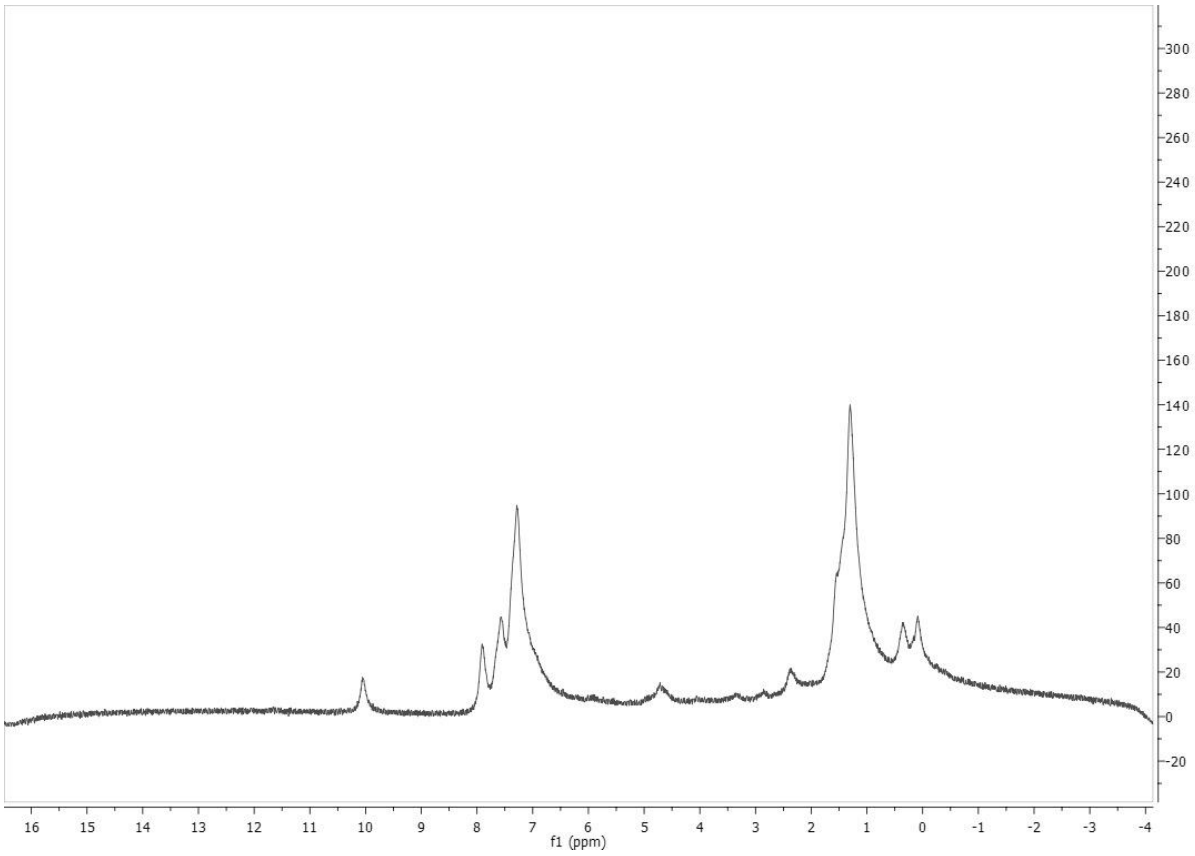

Figure 41: ^{1}H NMR Spectra of the crude products of reaction D2 before work-up. The shape of this spectrum shows the existence of paramagnetic [Mn^{X+}] species.

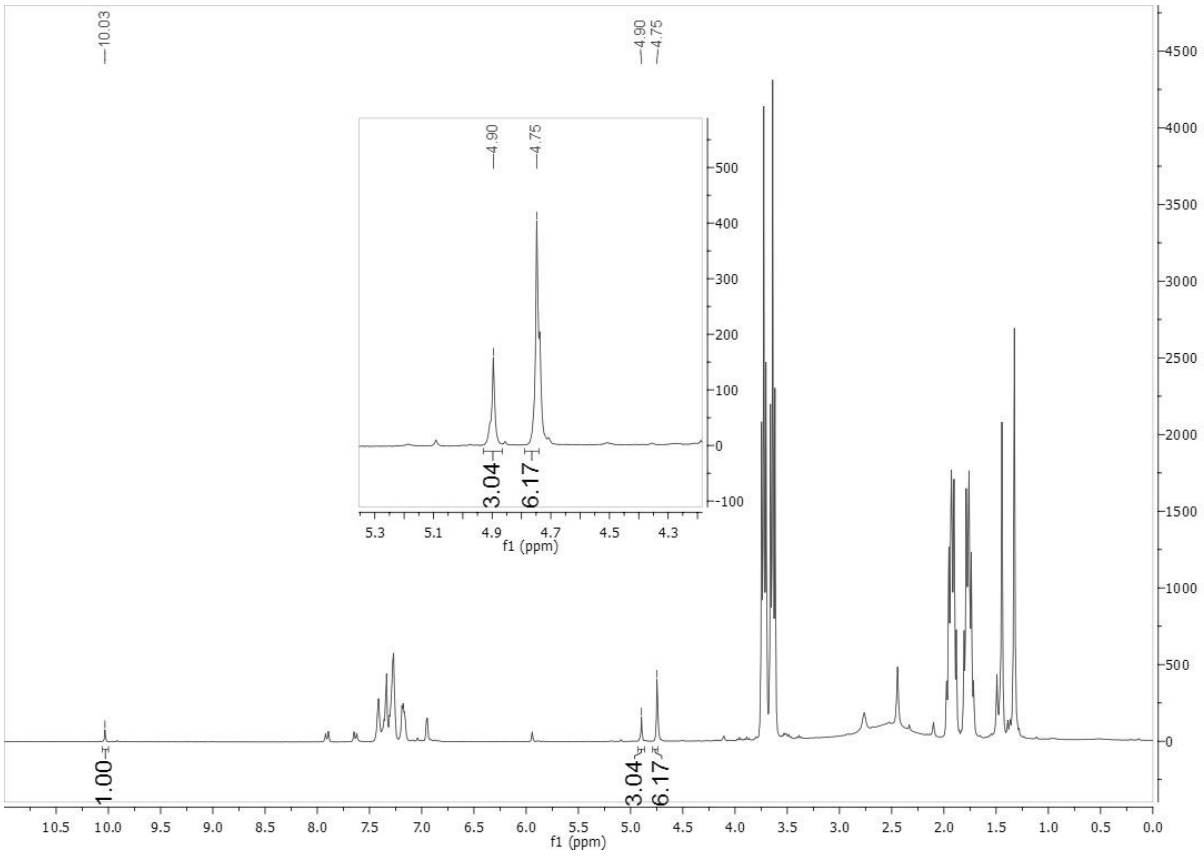

Figure 42: ^{1}H NMR Spectra of the crude products of reaction D2 after work-up. The labelled peaks identify the benzaldehyde (s, 10,03 ppm) the *meso*- product (s, 4,90 ppm) and the *dl*- product (s, 4,75 ppm).

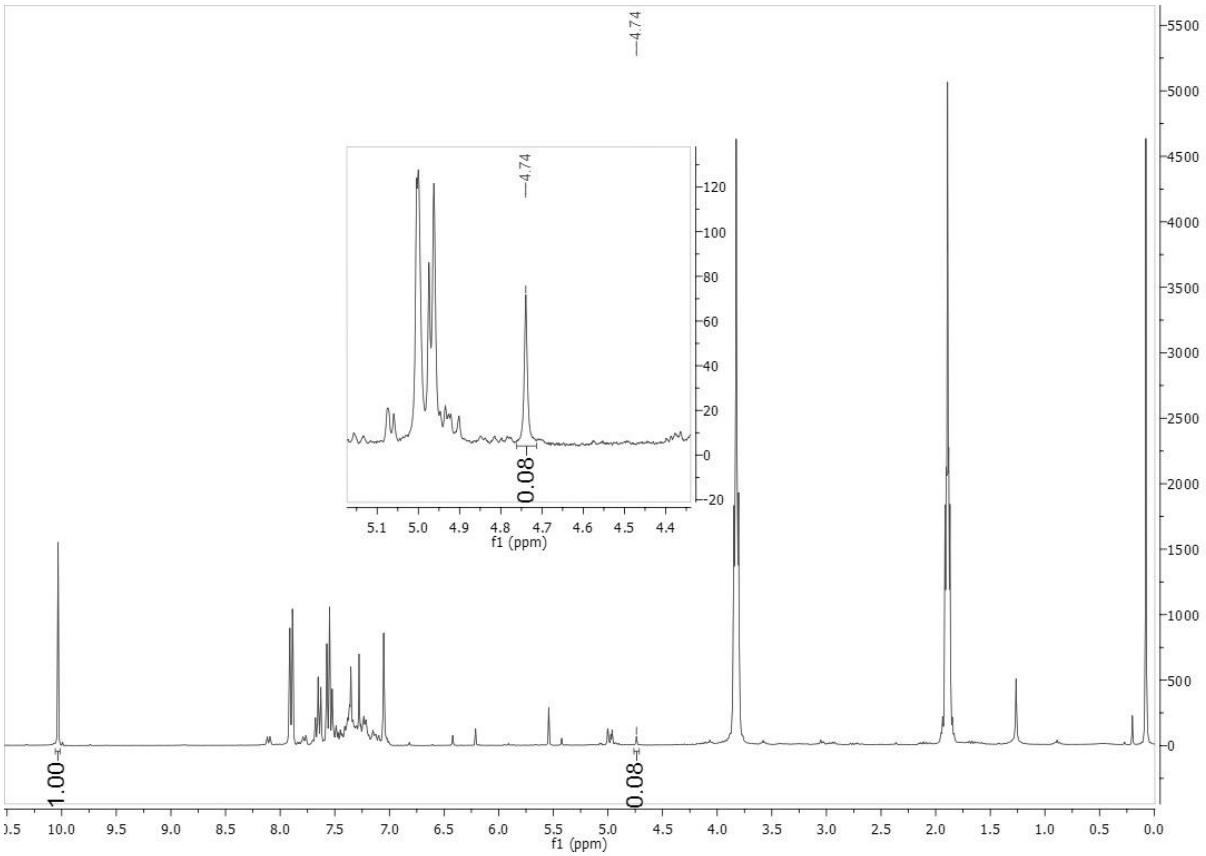

Figure 43: ^{1}H NMR Spectra of the crude products of reaction E1 before work-up. The labelled peaks identify the benzaldehyde (s, 10,03 ppm) and the product obtained (s, 4,74 ppm).

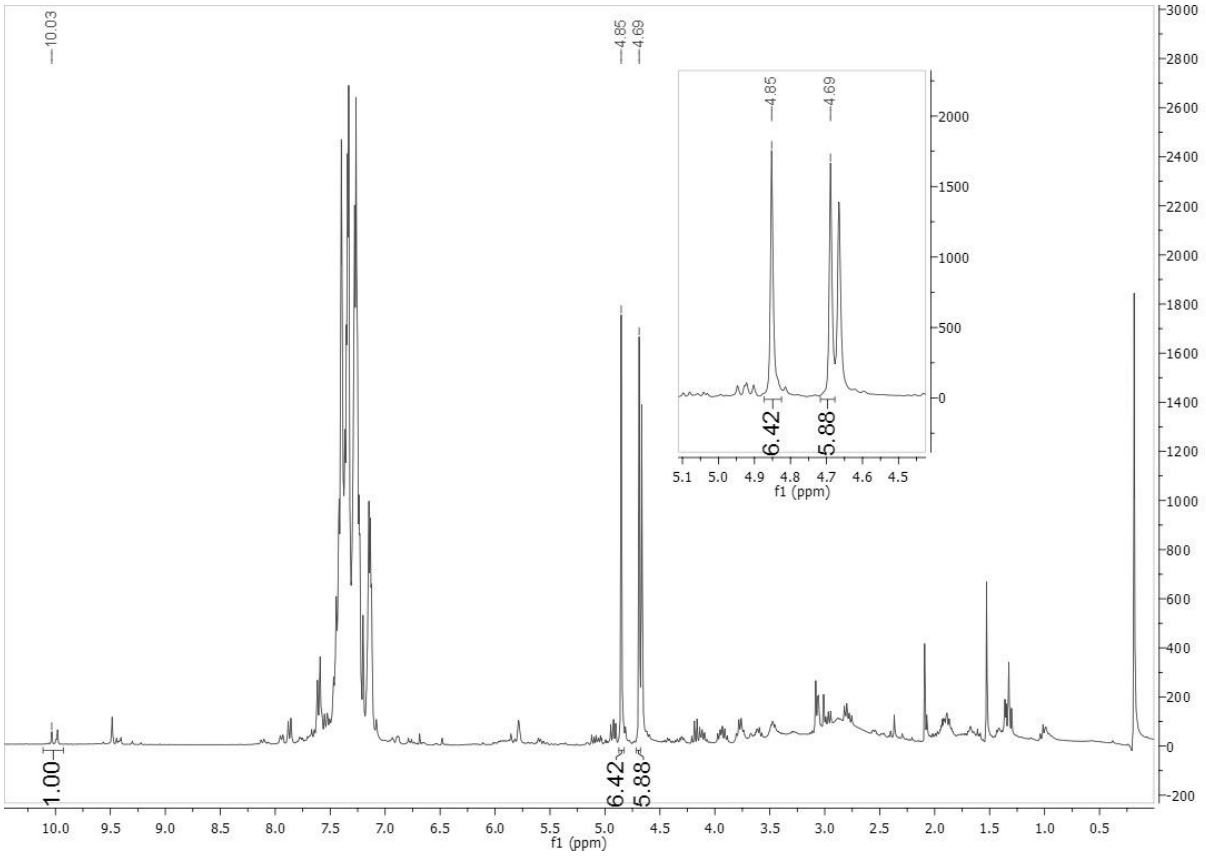

Figure 44: ^{1}H NMR Spectra of the crude products of reaction E1 after work-up. The labelled peaks identify the benzaldehyde (s, 10,03 ppm) the *meso*- product (s, 4,85 ppm) and the *dl*- product (s, 4,69 ppm).

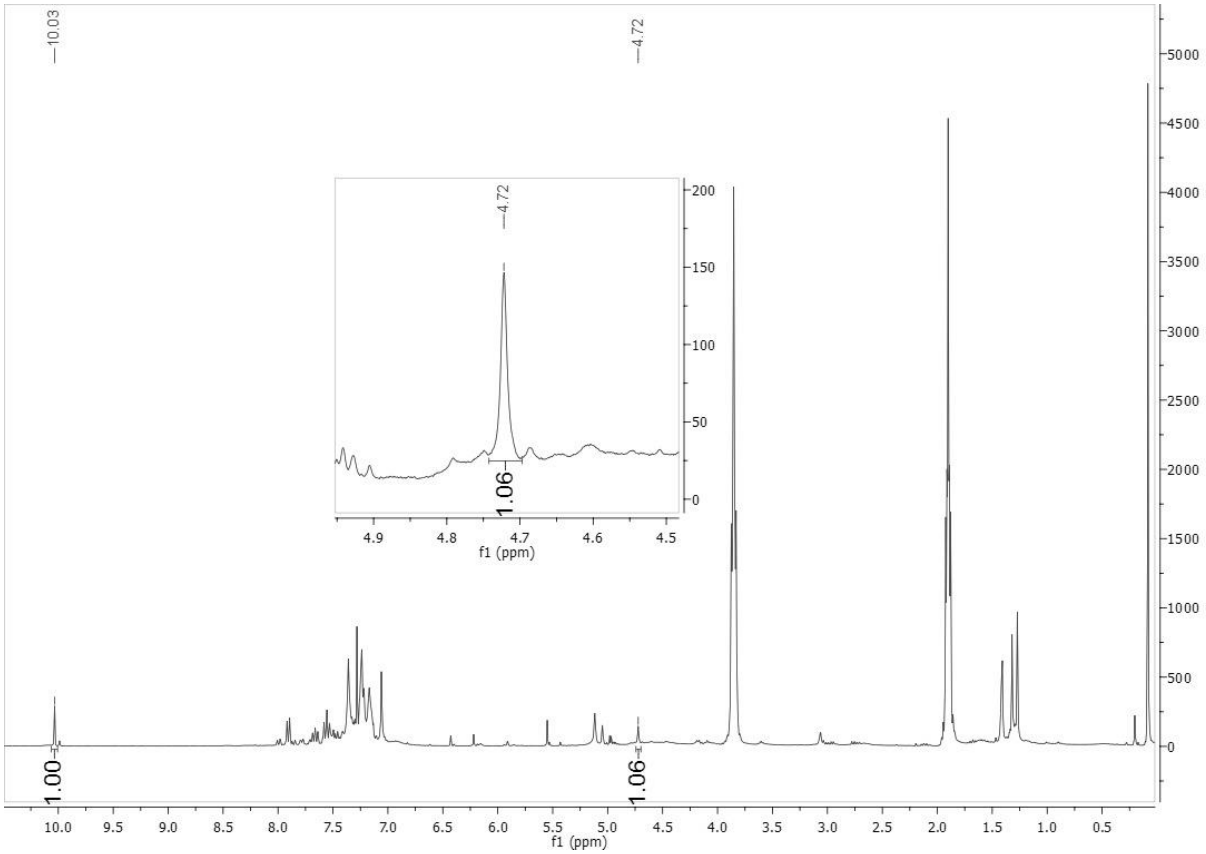

Figure 45: ^{1}H NMR Spectra of the crude products of reaction E2 before work-up. The labelled peaks identify the benzaldehyde (s, 10,03 ppm) and the product obtained (s, 4,72 ppm).

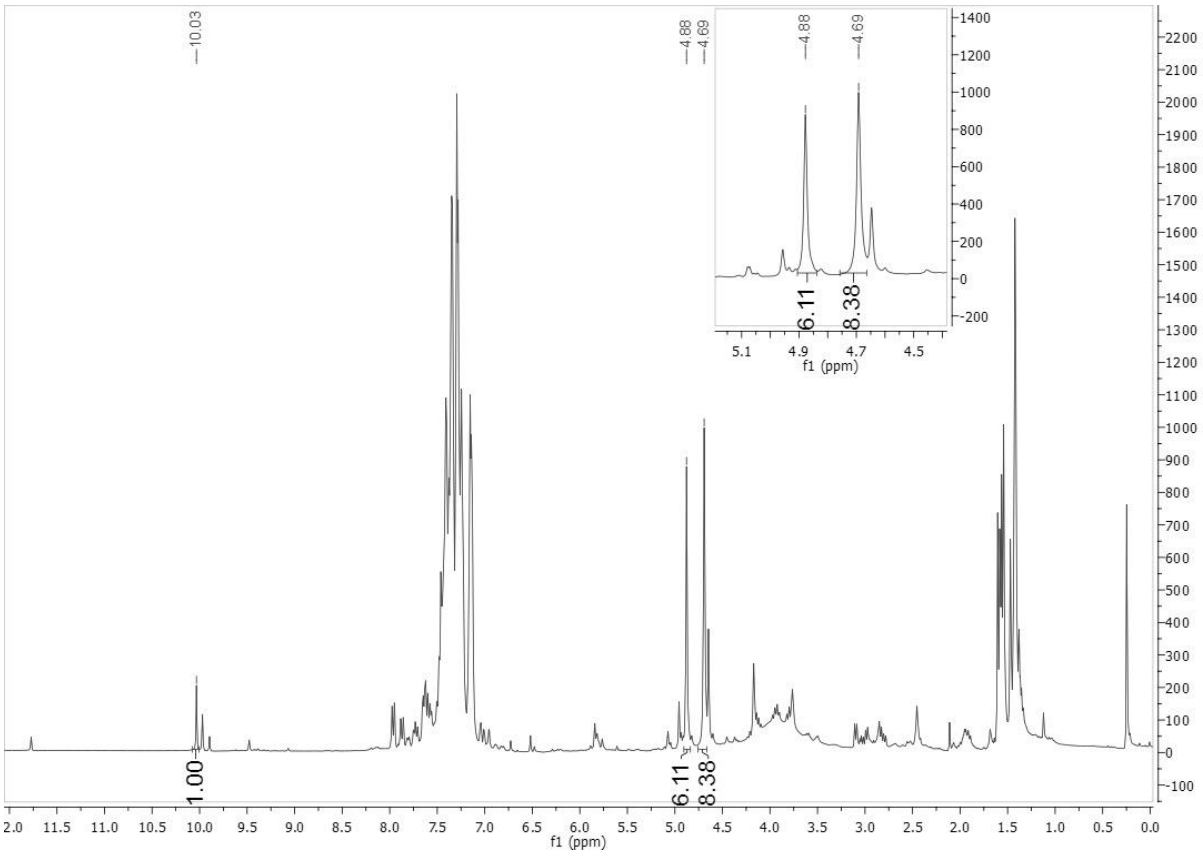

Figure 46: ^{1}H NMR Spectra of the crude products of reaction E2 after work-up. The labelled peaks identify the benzaldehyde (s, 10,03 ppm) the *meso*- product (s, 4,88 ppm) and the *dl*- product (s, 4,69 ppm).

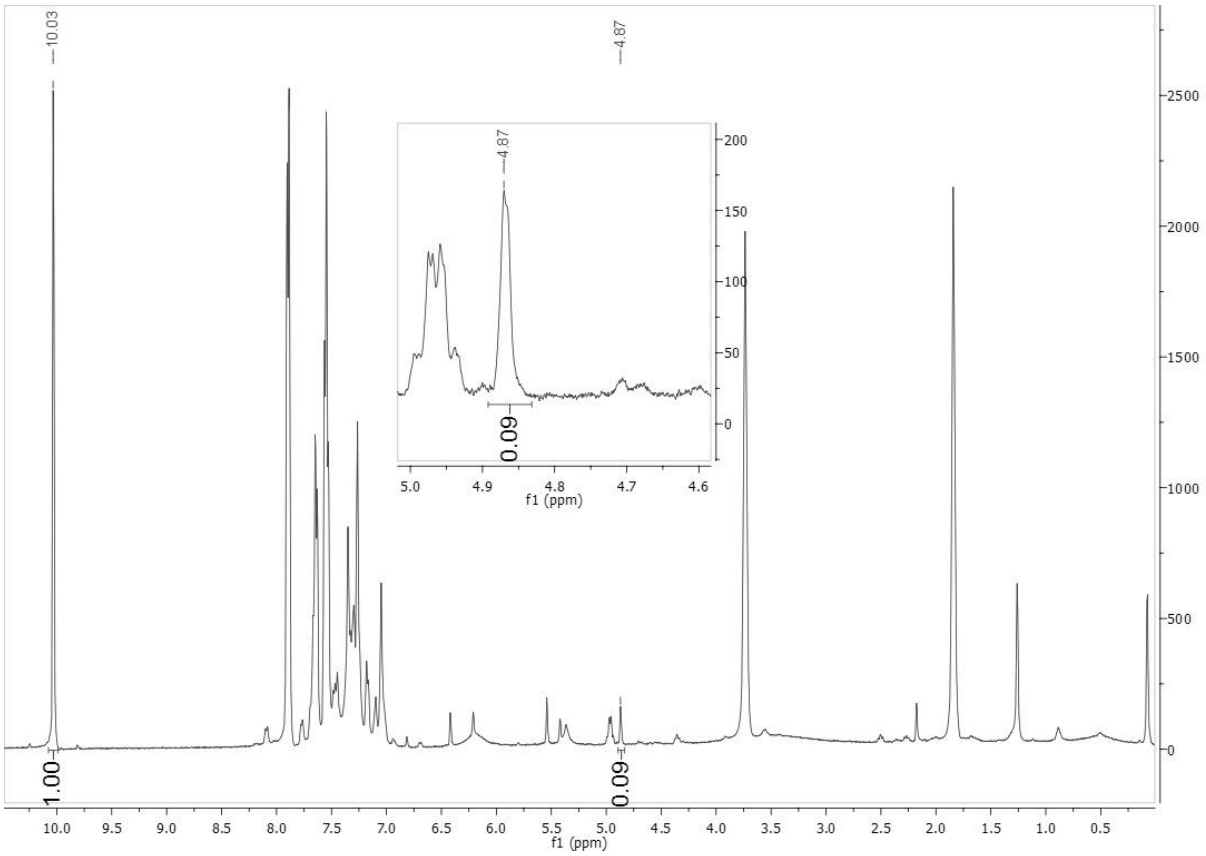

Figure 47: ^{1}H NMR Spectra of the crude products of reaction F1 before work-up. The labelled peaks identify the benzaldehyde (s, 10,03 ppm) and the product obtained (s, 4,87 ppm)

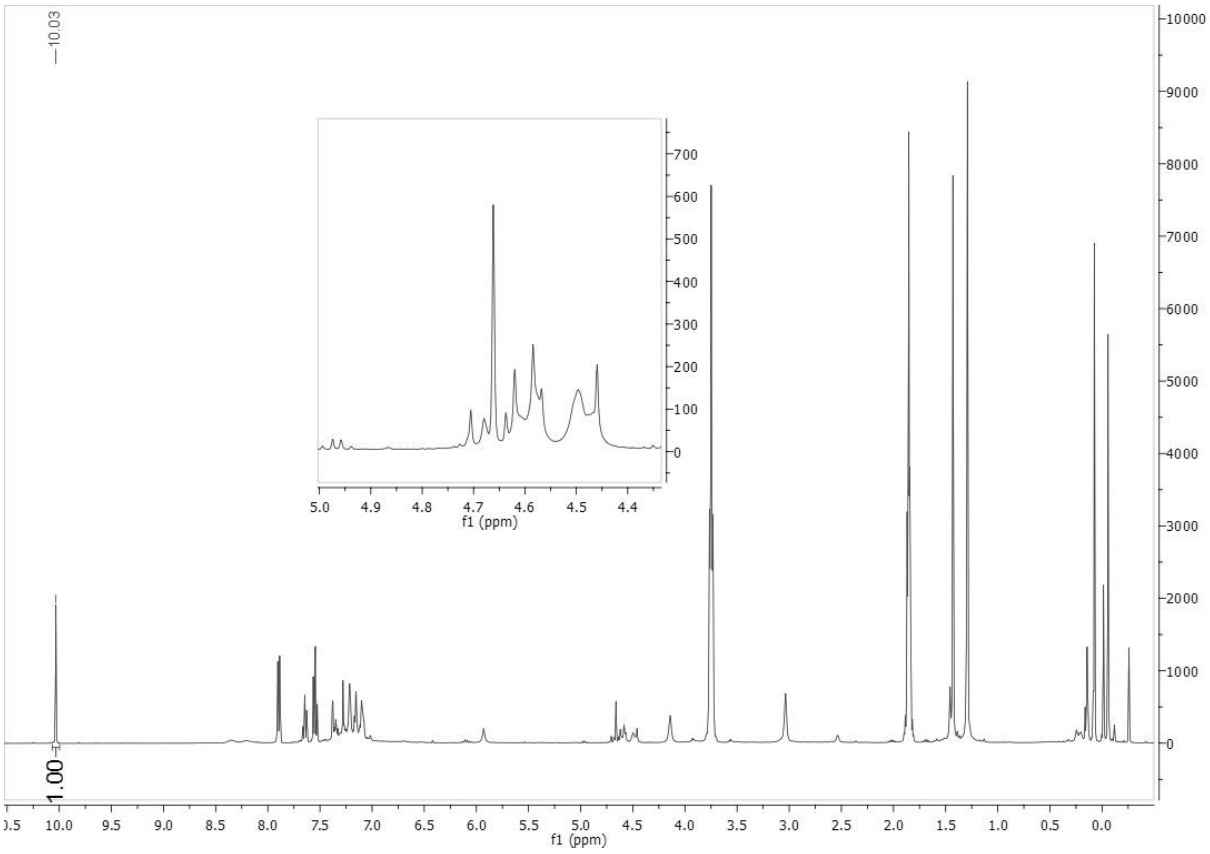

Figure 48: ^{1}H NMR Spectra of the crude products of reaction F2 before work-up. The labelled peak identify the benzaldehyde (s, 10,03 ppm); the product peaks are absent.

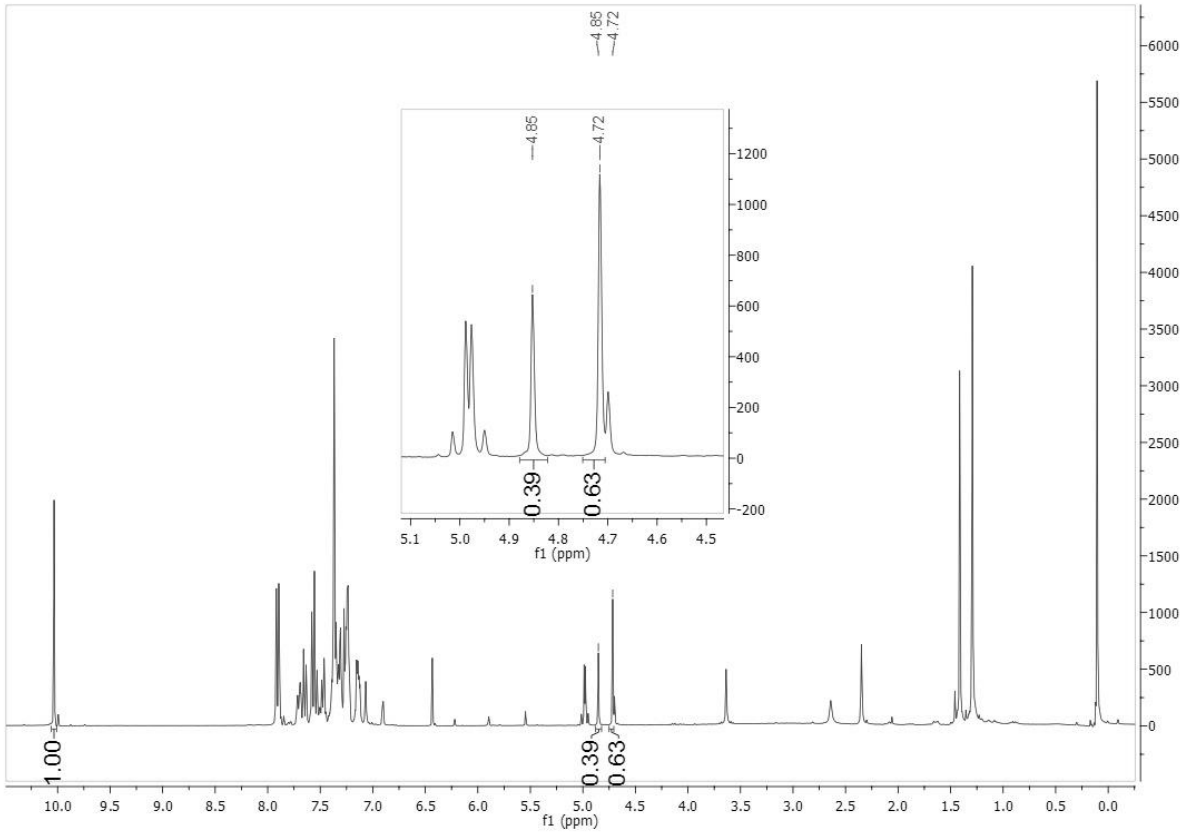

Figure 49: ^{1}H NMR Spectra of the crude products of reaction G1 after work-up. The labelled peaks identify the benzaldehyde (s, 10,03 ppm) the *meso*- product (s, 4,85 ppm) and the *dl*- product (s, 4,72 ppm).

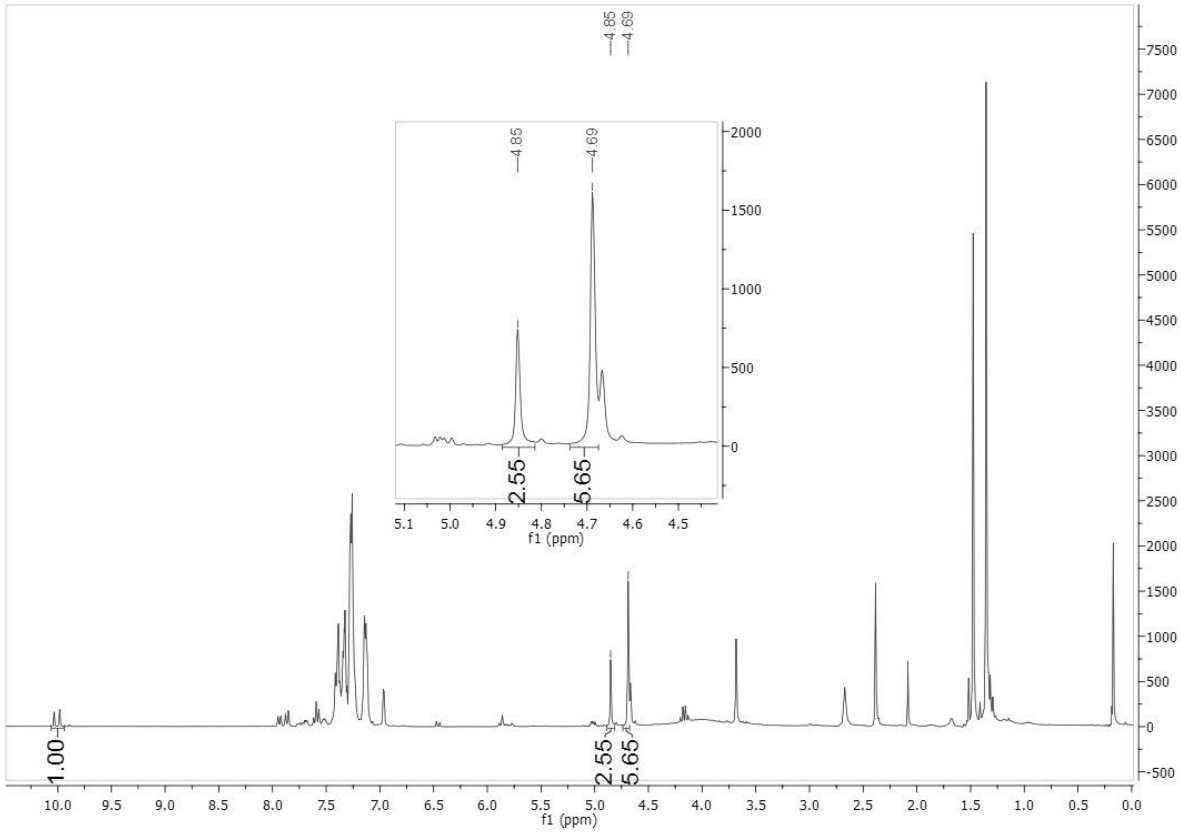

Figure 50: ^{1}H NMR Spectra of the crude products of reaction G2 after work-up. The labelled peaks identify the benzaldehyde (s, 10,03 ppm) the *meso*- product (s, 4,85 ppm) and the *dl*- product (s, 4,69 ppm).

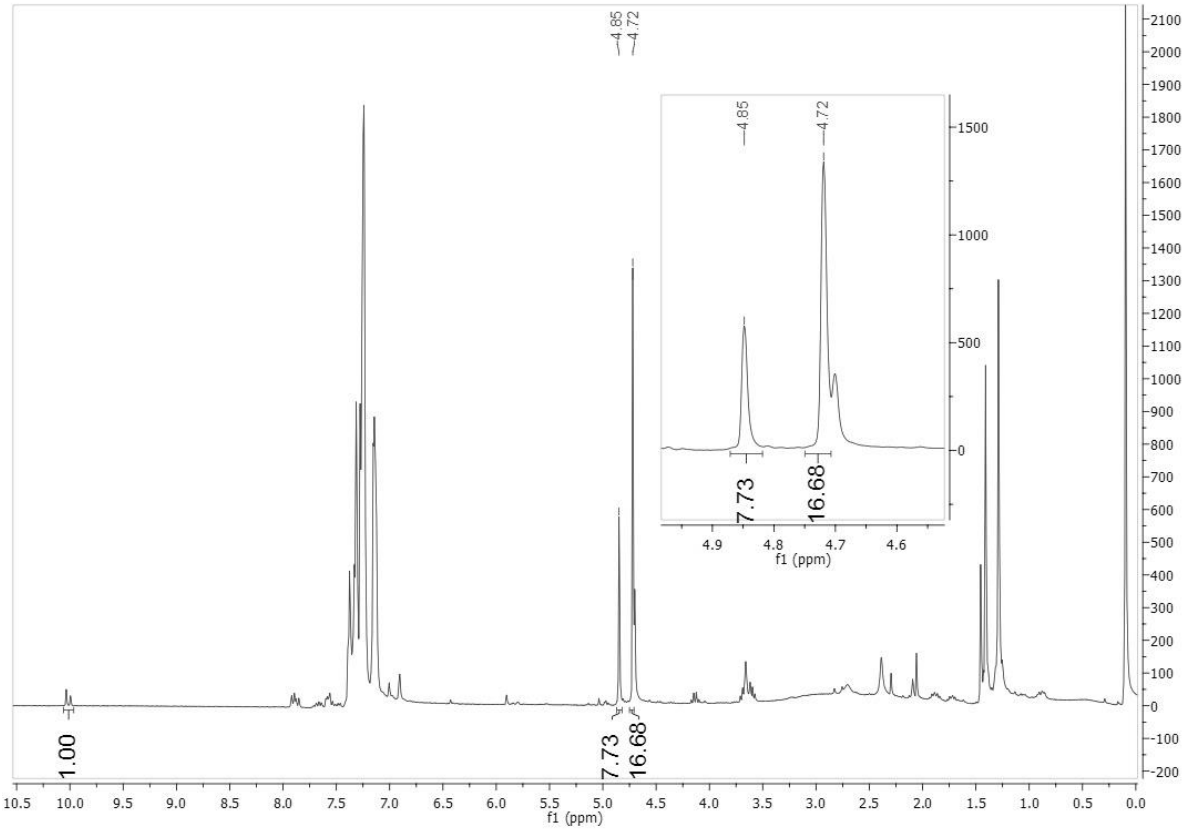

Figure 51: ^{1}H NMR Spectra of the crude products of reaction G3 after work-up. The labelled peaks identify the benzaldehyde (s, 10,03 ppm) the *meso*- product (s, 4,85 ppm) and the *dl*- product (s, 4,72 ppm).

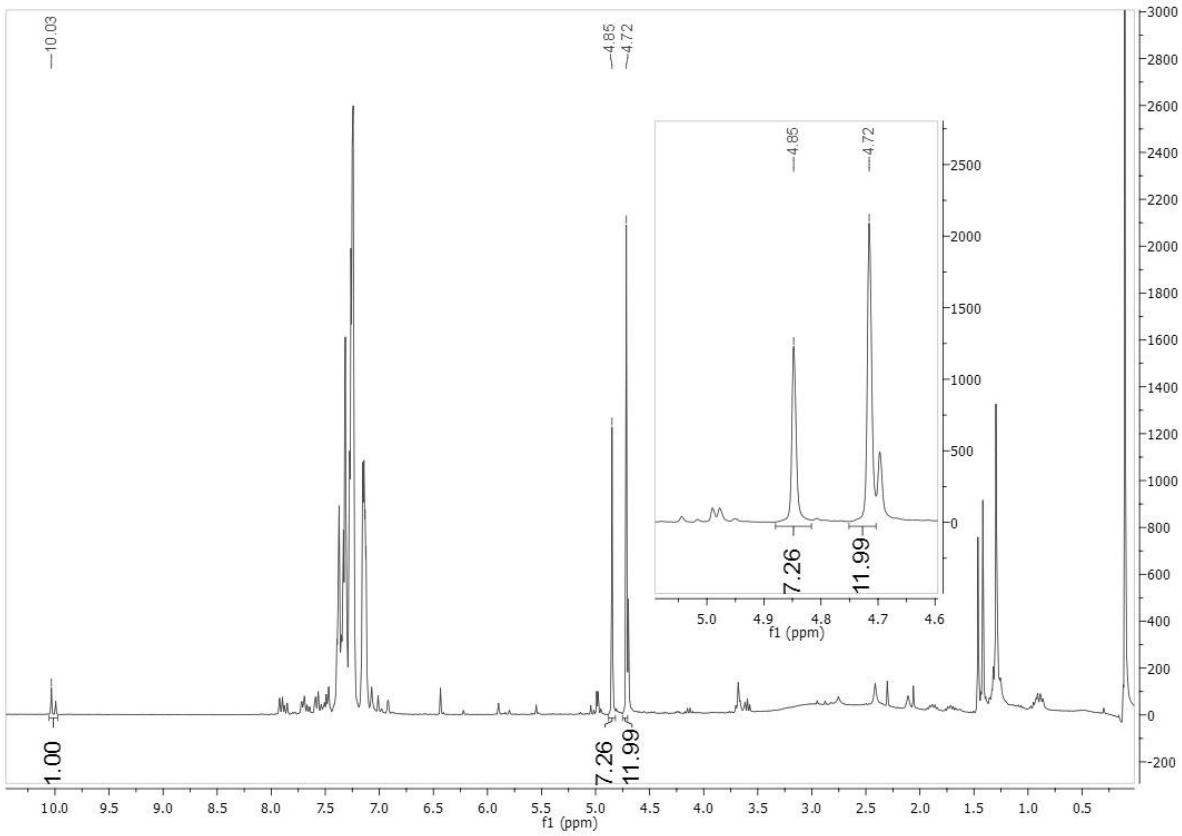

Figure 52: ^{1}H NMR Spectra of the crude products of reaction G4 after work-up. The labelled peaks identify the benzaldehyde (s, 10,03 ppm) the *meso*- product (s, 4,85 ppm) and the *dl*- product (s, 4,72 ppm).

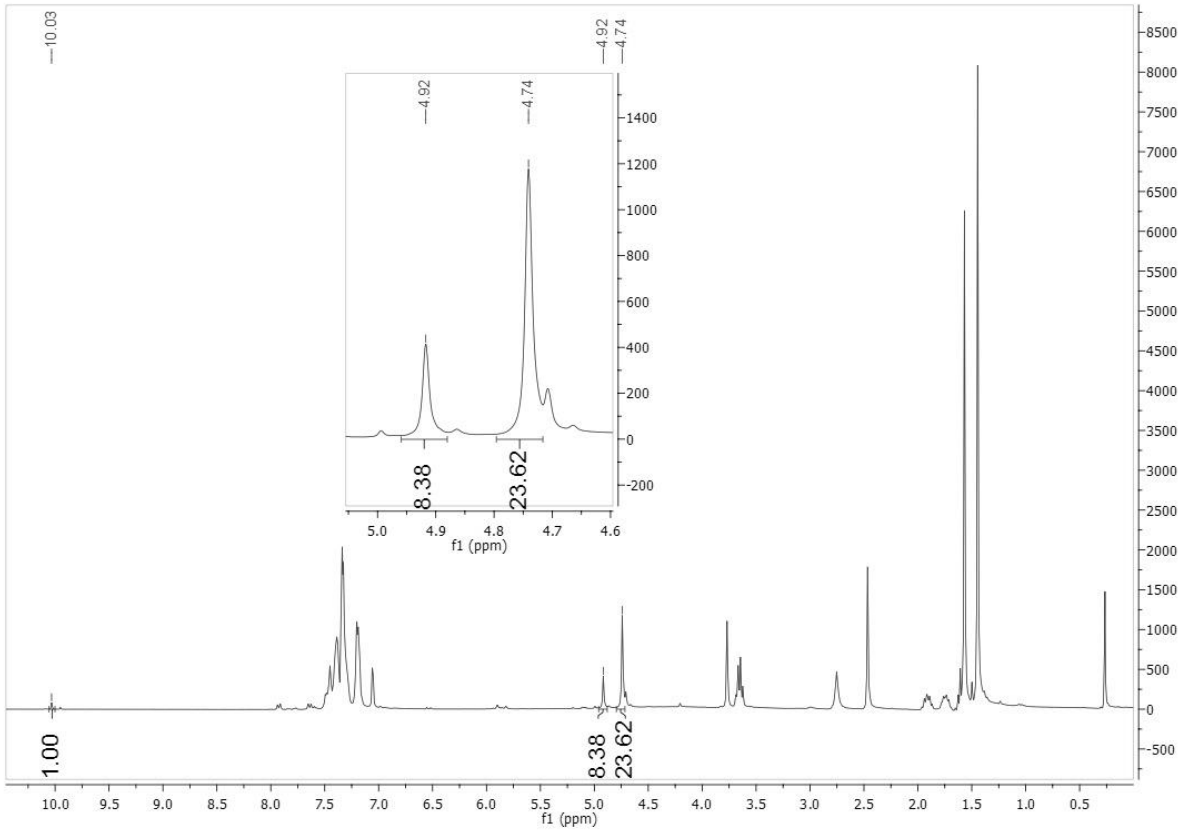

Figure 53: ^{1}H NMR Spectra of the crude products of reaction G5 after work-up. The labelled peaks identify the benzaldehyde (s, 10,03 ppm) the *meso*- product (s, 4,92 ppm) and the *dl*- product (s, 4,74 ppm).

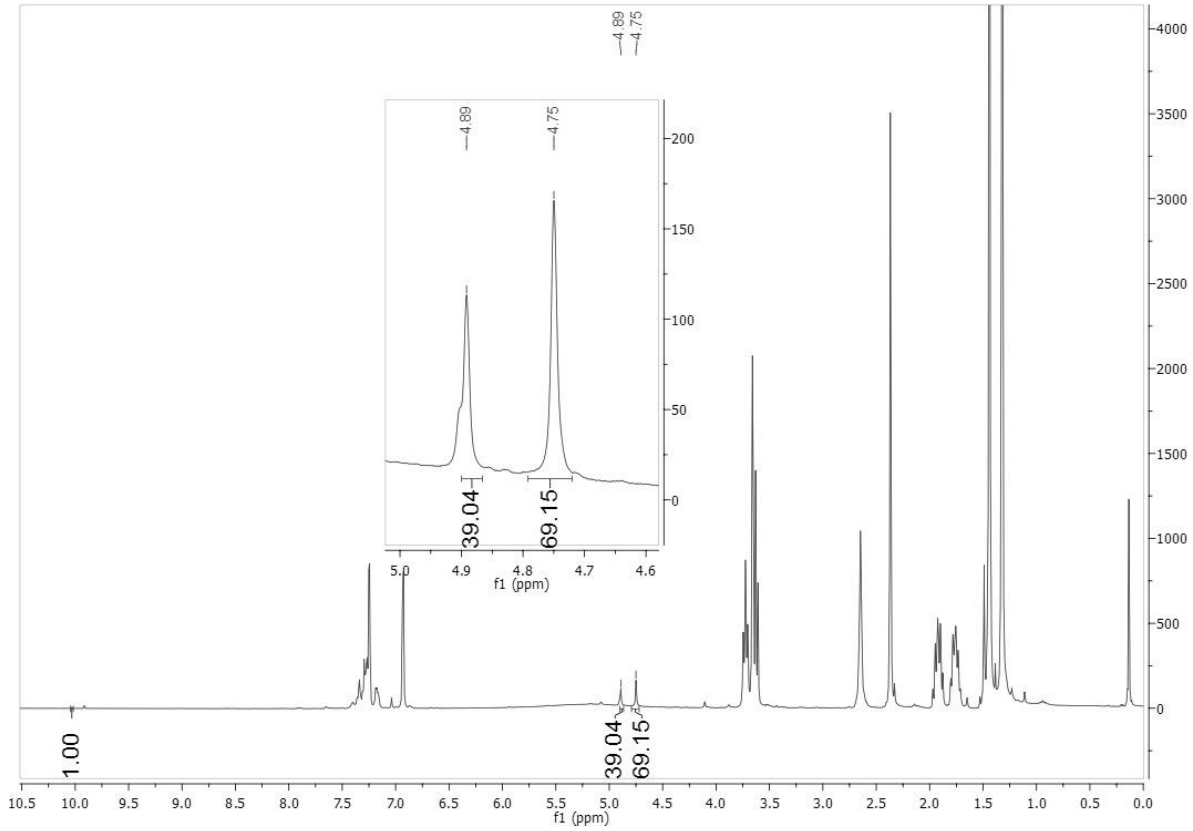

Figure 54: ^{1}H NMR Spectra of the crude products of reaction G6 after work-up. The labelled peaks identify the benzaldehyde (s, 10,03 ppm) the *meso*- product (s, 4,89 ppm) and the *dl*- product (s, 4,75 ppm).

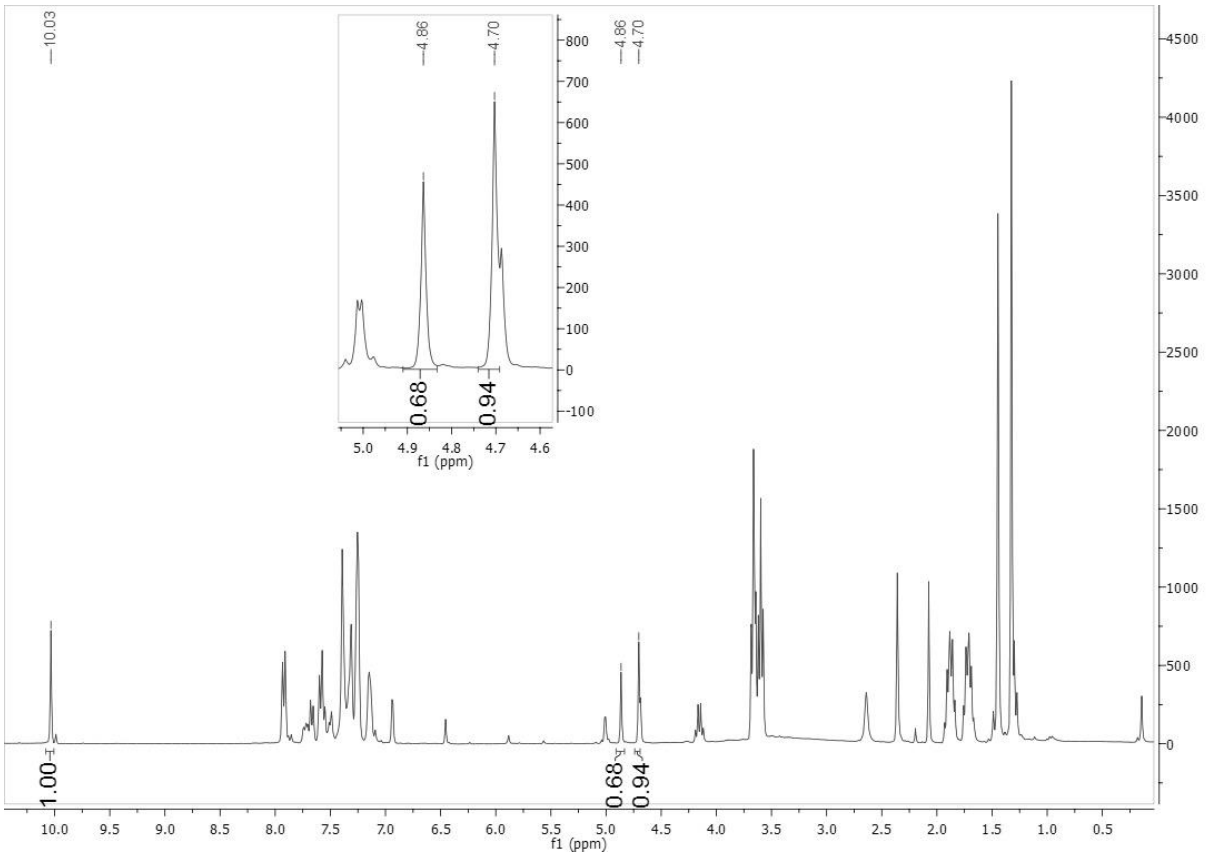

Figure 55: ^{1}H NMR Spectra of the crude products of reaction H1 after work-up. The labelled peaks identify the benzaldehyde (s, 10,03 ppm) the *meso*- product (s, 4,86 ppm) and the *dl*- product (s, 4,70 ppm).

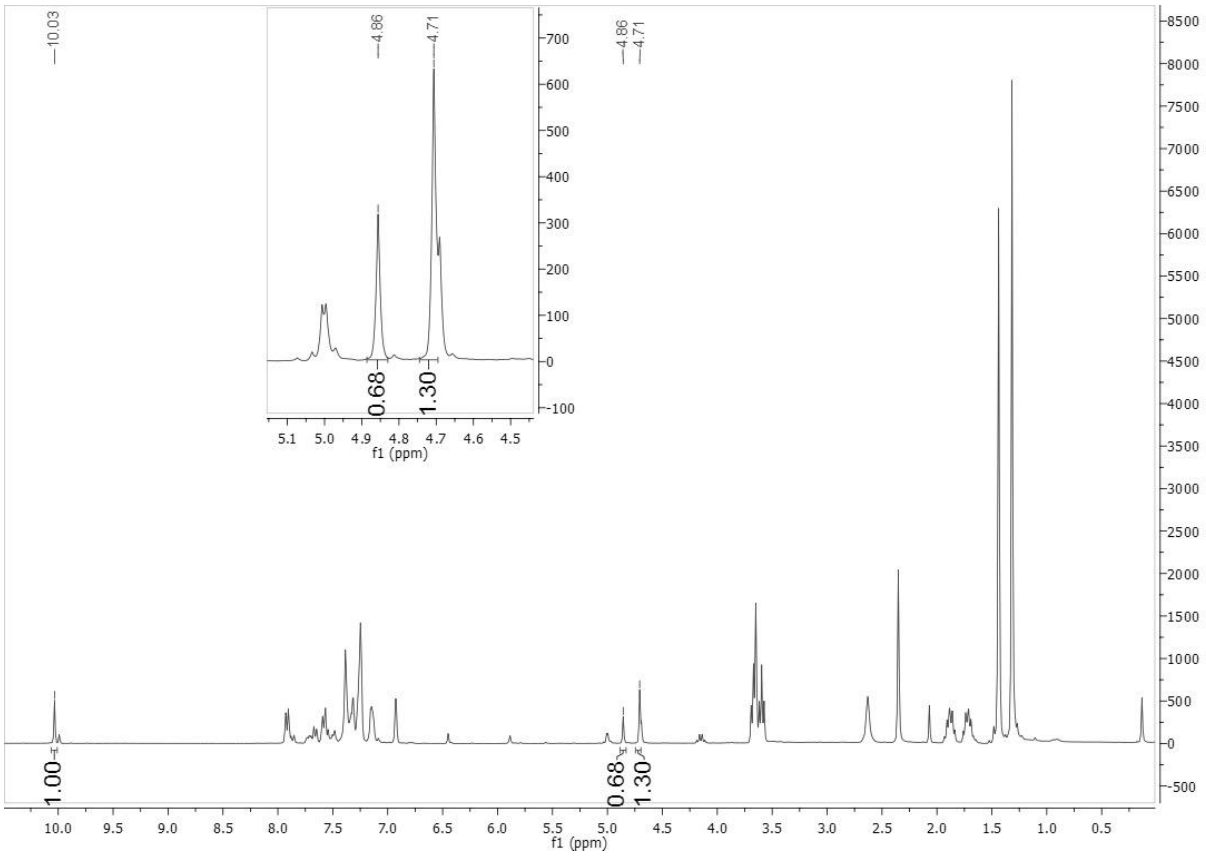

Figure 56: ^{1}H NMR Spectra of the crude products of reaction H2 after work-up. The labelled peaks identify the benzaldehyde (s, 10,03 ppm) the *meso*- product (s, 4,86 ppm) and the *dl*- product (s, 4,71 ppm).

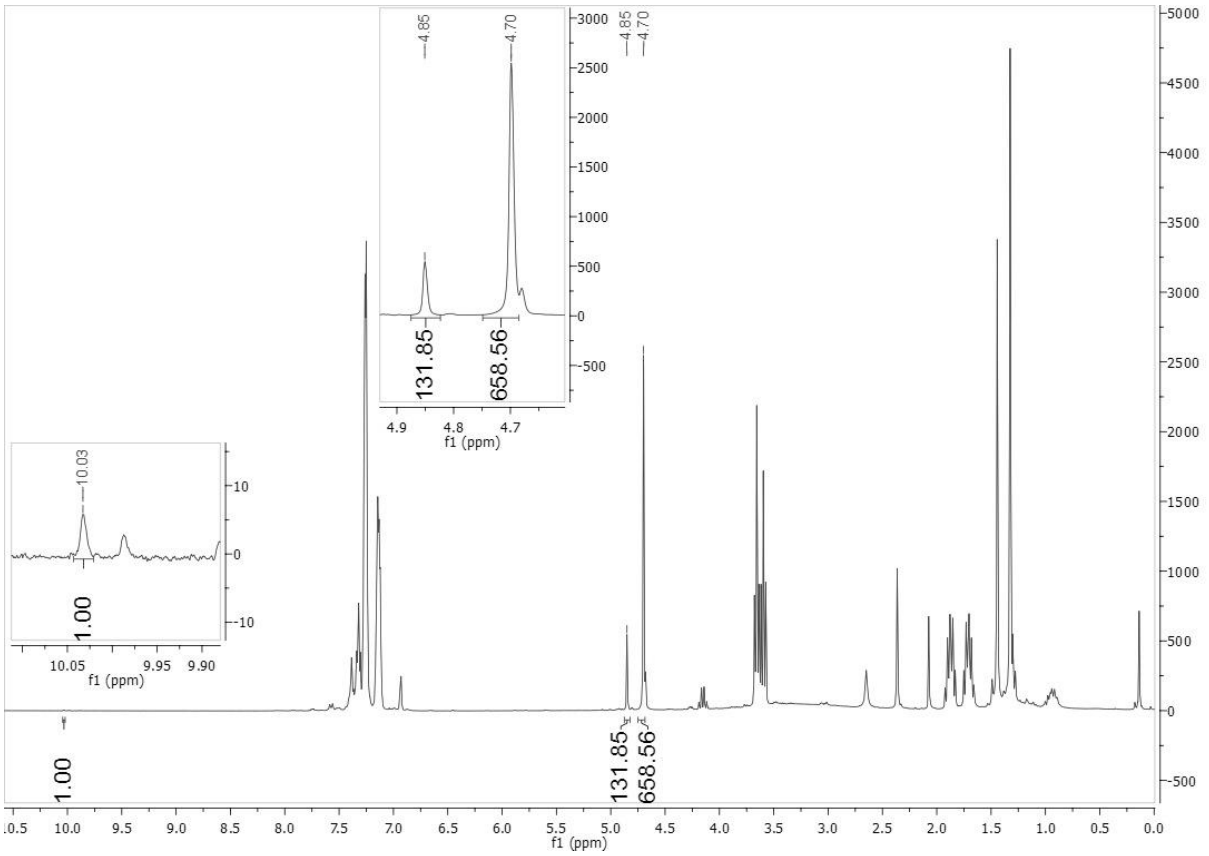

Figure 57: ^{1}H NMR Spectra of the crude products of reaction I1 after work-up. The labelled peaks identify the benzaldehyde (s, 10,03 ppm) the *meso*- product (s, 4,85 ppm) and the *dl*- product (s, 4,70 ppm).

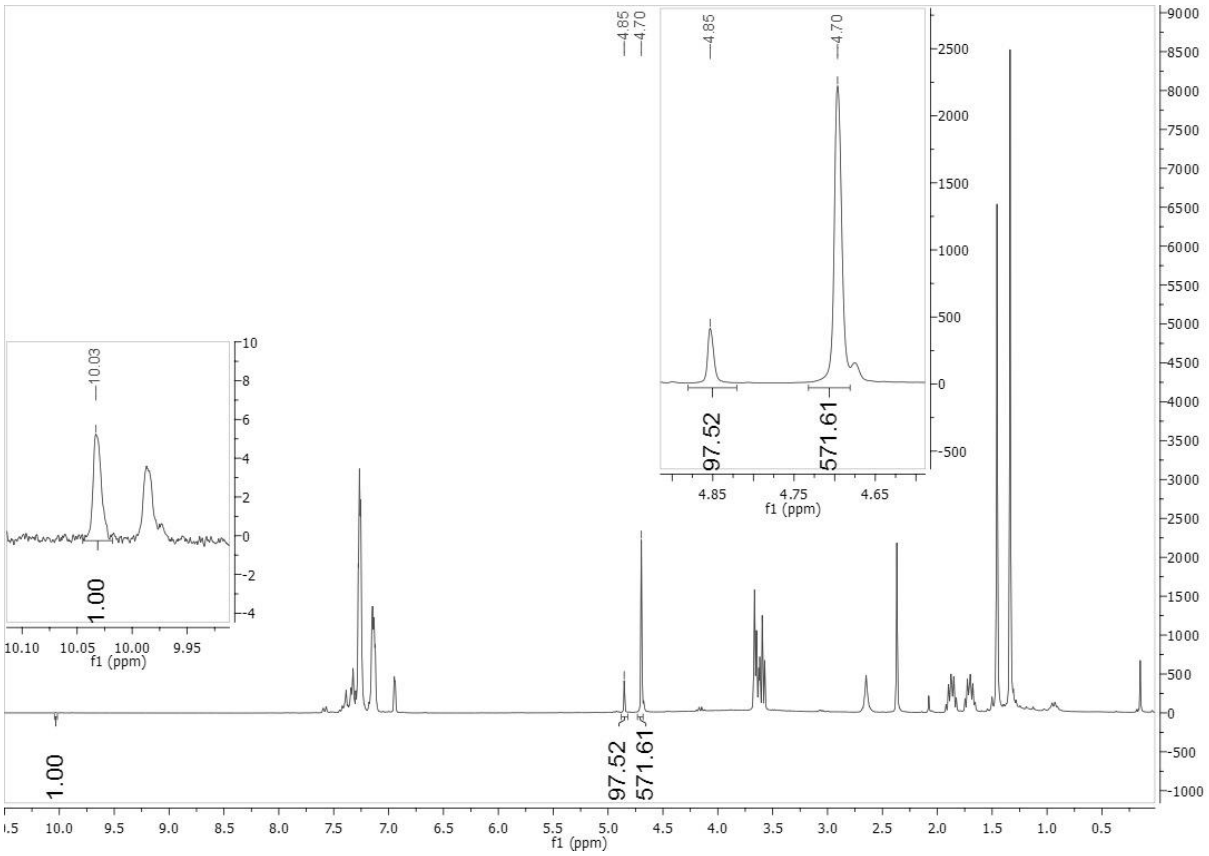

Figure 58: ^{1}H NMR Spectra of the crude products of reaction I2 after work-up. The labelled peaks identify the benzaldehyde (s, 10,03 ppm) the *meso*- product (s, 4,85 ppm) and the *dl*- product (s, 4,70 ppm).

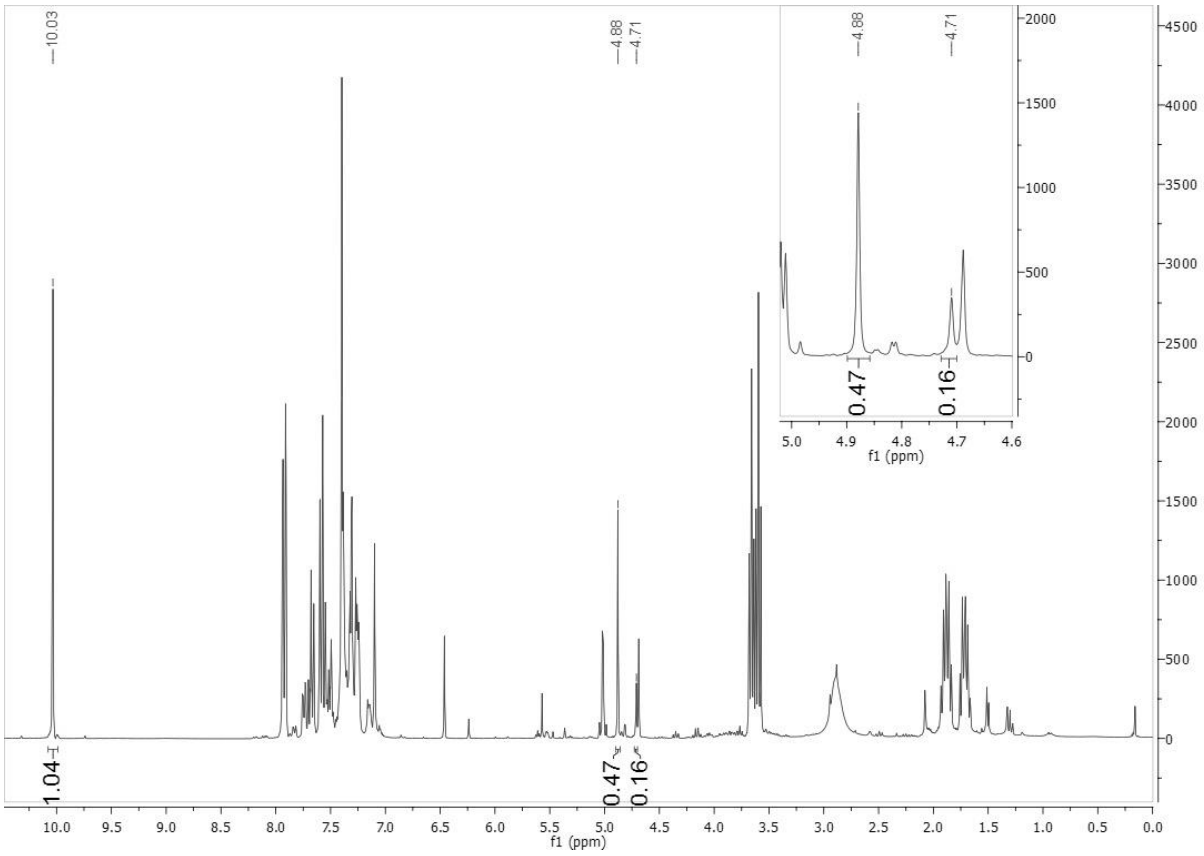

Figure 59: ^{1}H NMR Spectra of the crude products of reaction J after work-up. The labelled peaks identify the benzaldehyde (s, 10,03 ppm) the *meso*- product (s, 4,88 ppm) and the *dl*- product (s, 4,71 ppm).

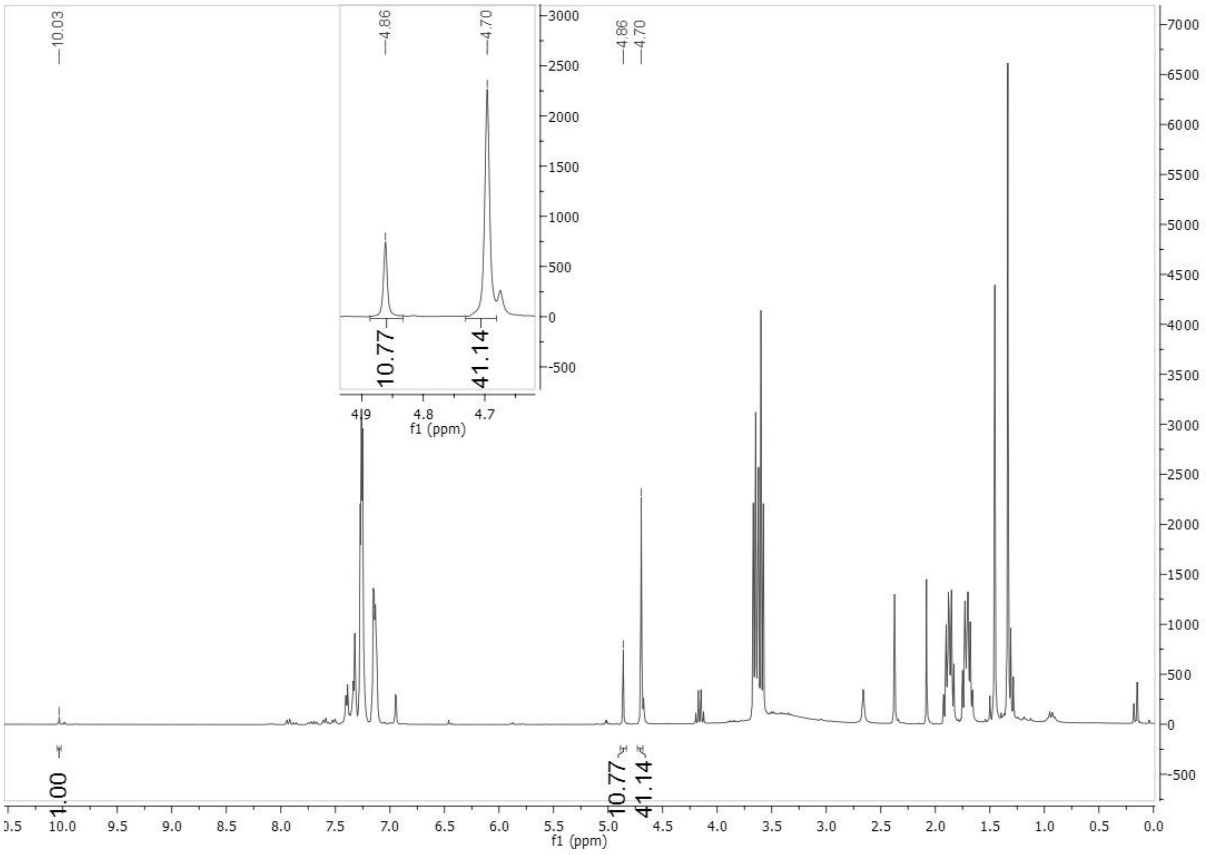

Figure 60: ^{1}H NMR Spectra of the crude products of reaction K after work-up. The labelled peaks identify the benzaldehyde (s, 10,03 ppm) the *meso*- product (s, 4,86 ppm) and the *dl*- product (s, 4,70 ppm).

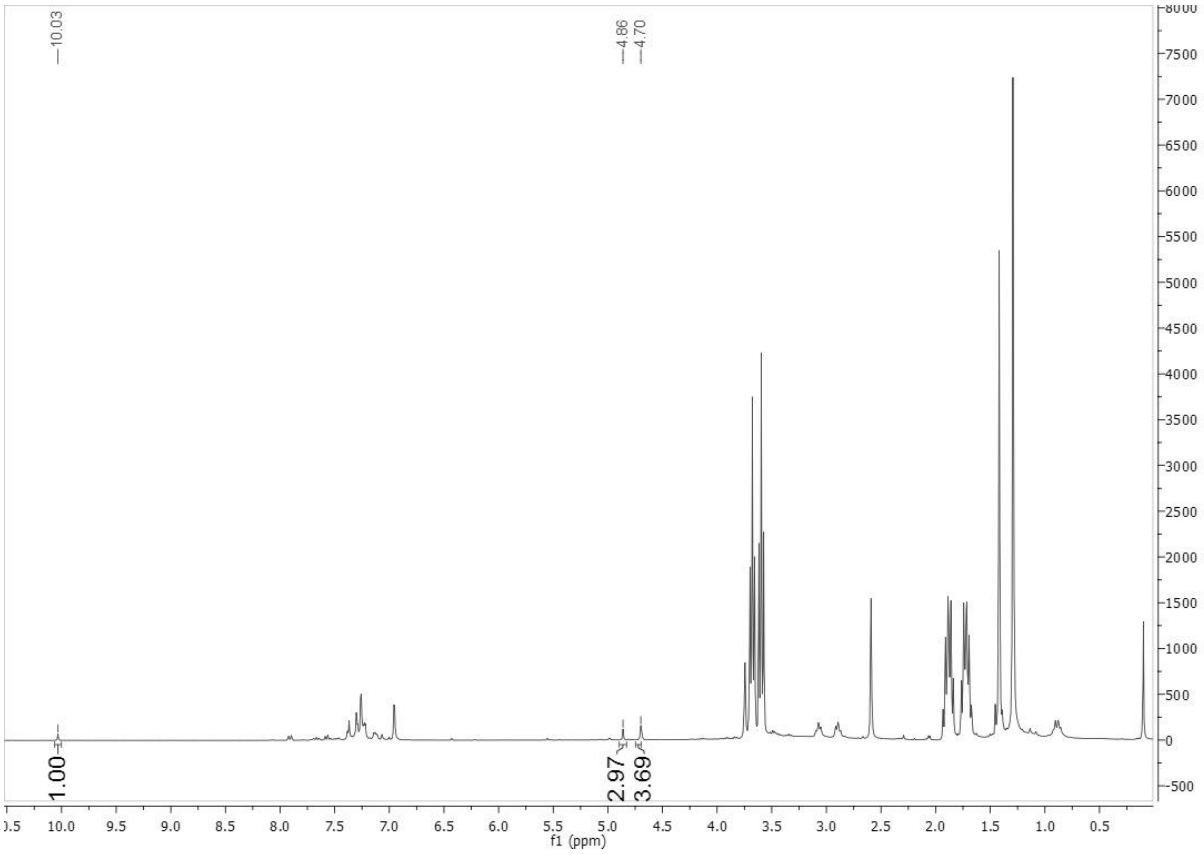

Figure 61: ^{1}H NMR Spectra of the crude products of reaction L after work-up. The labelled peaks identify the benzaldehyde (s, 10,03 ppm) the *meso*- product (s, 4,86 ppm) and the *dl*- product (s, 4,70 ppm).